CHARACTERIZING NOVEL CIRCADIAN CLOCK FUNCTIONS FOR *Drosophila* PHOSPHATASES AND NON-CLOCK FUNCTIONS FOR CIRCADIAN PHOTORECEPTORS

A Dissertation

by

PARUL AGRAWAL

Submitted to the Office of Graduate and Professional Studies of
Texas A&M University
in partial fulfillment of the requirements for the degree of

DOCTOR OF PHILOSOPHY

Chair of Committee,	Paul E. Hardin
Committee Members,	Deborah Bell-Pedersen
	Vlad M. Panin
	Mark J. Zoran
Head of Department,	Thomas D. McKnight

August 2016

Major Subject: Biology

ABSTRACT

Circadian (~24 h) clocks regulate daily cycles in gene expression to control overt rhythms in physiology, metabolism and behavior. In *Drosophila*, a transcriptional feedback loop activated by CLOCK-CYCLE (CLK-CYC) complexes, repressed by PERIOD-TIMELESS (PER-TIM) complexes, and synchronized to light:dark cycles primarily by CRYPTOCHROME (CRY), keeps circadian time. The timing of activation and repression is regulated post-translationally, in part through rhythmic phosphorylation of CLK, PER, and TIM. Although kinases that control CLK, PER, and TIM levels, activity, and/or subcellular localization have been identified, less is known about phosphatases that control clock protein dephosphorylation. Using genetic, behavioral and molecular analyses, I identified protein phosphatases that function within the *Drosophila* circadian clock. Moreover, I took advantage of behavioral, molecular, and electrophysiological analyses to characterize CRY expression and function in peripheral tissues of *Drosophila melanogaster*.

To identify phosphatases, clock cell-specific RNAi knockdowns of all annotated phosphatases in *Drosophila* were screened for altered activity rhythms. I identified 22 such phosphatases that either lengthened or shortened circadian period by ≥ 1 h or were significantly arrhythmic. The efficacy and specificity of RNAis was validated by testing RNAis that targeted other regions of the mRNA, transposon inserts, and either existing or CRISPR-generated loss of function mutants for defects in activity rhythms. One phosphatase identified, Leukocyte-Antigen-Related (LAR), regulates the development of

neuronal circuit underlying the communication between clock neurons in the fly brain. This work, along with the analysis of another 15 candidates that remain after validation, will reveal novel features of the circadian timekeeping mechanism in *Drosophila* that may be conserved in all animals including humans.

Furthermore, using a GFP-tagged-*cry* transgene, I show that CRY is expressed in *Drosophila* peripheral tissues and promotes light-dependent TIM degradation. Electrophysiological recordings from larval salivary glands which lack a circadian clock and are non-excitable, demonstrated that CRY regulates cell membrane physiology in collaboration with K^+ channels. These findings for the first time define the expression profile of CRY in *Drosophila* peripheral tissues, and reveal that CRY functions in a light-independent and K^+ channel-dependent manner to alter membrane function in peripheral tissues devoid of a canonical circadian clock.

DEDICATION

This work is dedicated to my parents for making me who I am,

and my brother, Vivek, whose constant support, strength and love have

motivated me to achieve my dream.

ACKNOWLEDGEMENTS

I am thankful to many people who have in one way or the other supported me through my graduate work. First and foremost, I wish to express my thanks to my advisor, Dr. Paul E. Hardin. It was his expertise, understanding, and guidance that made it possible for me to work on such different, yet interesting topics. This journey would not have been possible without his support. I would like to thank my committee members, Dr. Mark J. Zoran, Dr. Deborah Bell-Pedersen, and Dr. Vlad M. Panin, for their valuable suggestions throughout the course of this research. I would like to express my gratitude to Dr. Mark J. Zoran, for working with me on one of my projects, using his lab equipment and skills, fun discussions and encouragement, without which I wouldn't be where I am today.

I am grateful to the past and current members of our lab, Dr. Guruswamy Mahesh, Dr. Abhishek Chatterjee, Dr. Jerry Houl, Dr. Wangjie Yu, Paul Kim, Kushan Gunawardhana, Courtney Caster, Jian Zhou, Tianxin Liu and Stephanie Durkacz for training and supporting me through these years of my graduate school. I am thankful for their help and friendship. I am also grateful to all my friends and colleagues from the Center of Biological Clocks for help with my experiments and making this a memorable experience.

I would also like to thank my family and friends all around the world who have always supported me. Thanks to old friends from India, some who accompanied me to

the US, new friends from and outside the Department, and all my cousins whose love made this day possible.

I need to thank my flies, *Drosophila melanogaster*, and the funding resources, NIH and the Department of Biology for helping me complete my graduate work.

Finally, thanks to my mother, father, and brother for supporting me in my decision to pursue further studies. They taught me to keep working hard no matter what. They believed in me and encouraged me to keep doing better despite numerous pitfalls. I really am indebted to them for their love and support.

TABLE OF CONTENTS

Page

LIST OF FIGURES

Page

LIST OF TABLES

CHAPTER I

INTRODUCTION

Biological clocks, a ubiquitous theme in multiple organisms

Circadian rhythms are a fundamental property of prokaryotic and eukaryotic microbes, plants and animals that impose a ~24 h temporal organization on their physiology, metabolism and behavior. These rhythms are not passively driven by environmental cycles, but are controlled by endogenous circadian (~24 h) clocks that keep time in the absence of environmental cues. However, daily environmental cues such as light and temperature reset these clocks to a precise 24 h period, thereby synchronizing clocks in different cells and tissues. Circadian clocks are essentially ubiquitous, and presumably confer a selective advantage by anticipating environmental transitions such as light:dark (LD) cycles. Importantly, the clock is known to control numerous physiological and molecular processes (e.g., the sleep-wake cycle, melatonin secretion, body core temperature, and the cell cycle) in organisms ranging from bacteria and fungi to humans. Consequently, there is growing evidence that clock deficiencies are associated with abnormal sleep-wake cycles (e.g., Familial Advanced Sleep Phase Syndrome), epilepsy, cerebrovascular diseases, movement disorders, multiple sclerosis and headaches (Turek et al., 2001; Laposky et al., 2008). Disorders caused by a dysfunctional clock emphasize the clinical importance of understanding the molecular organization of the circadian system.

A transcriptional feedback loop underlies the circadian oscillator

A highly conserved feature of circadian clocks is that they are composed of cell-autonomous transcriptional feedback loops that use positive and negative elements to regulate cyclical gene expression (Dunlap et al., 1999). In *Drosophila melanogaster*, the core circadian feedback loop is composed of the positively acting basic-helix-loop-helix (bHLH) PER-ARNT-SIM (PAS) partners CLOCK (CLK) and CYCLE (CYC), which bind to E-box enhancer elements and activate transcription of *period* (*per*) and *timeless* (*tim*) in a time-dependent manner, along with other key clock and downstream effector genes (Fig. 1; Hardin, 2005). In the late afternoon/early evening, PER and TIM begin to accumulate in the cytoplasm and eventually interact to form a complex that enters the nucleus in the middle of the night (Lee et al., and Zeng et al., 1996; Price et al., 1998), an event accompanied by rapid decrease in the levels of *per* and *tim* transcripts (Hardin et al., 1990; Sehgal et al., 1995). Accumulating levels of PER and TIM proteins inhibit CLK-CYC activity, and once PER and TIM are degraded, the next round of CLK-CYC activation begins (Hardin, 2011). A similar circuit whereby a heterodimer composed of CLOCK and BMAL1 (vertebrate homolog of CYC) activating expression of auto-inhibitors (*Per1-3* and *Cry1-2*), is conserved in mammals including humans (Hardin and Panda, 2013; Partch et al., 2014).

A second interlocked transcriptional feedback loop operates in the fruit fly that also contributes to circadian timing. Two CLK-CYC-dependent transcription factors, VRILLE (VRI) and PAR Domain Protein 1 (PDP1), mediate this second transcriptional feedback loop (Fig. 1; Glossop et al., 1999 and 2003; Cyran et al., 2003). The dynamic

interplay of these two loops is thought to be important for maintaining high amplitude transcriptional rhythms, which are important for driving behavioral and physiological rhythms. Additional feedback loops also exists in mammals, one driven by orthologs of VRI (e.g., E4BP4) and PDP1 (e.g., DBP/TEF/HLF) and another driven by ROR and REV-ERB nuclear receptor paralogs (Ueda et al., 2001; Preitner et al., 2002; Bell-Pedersen et al., 2005).

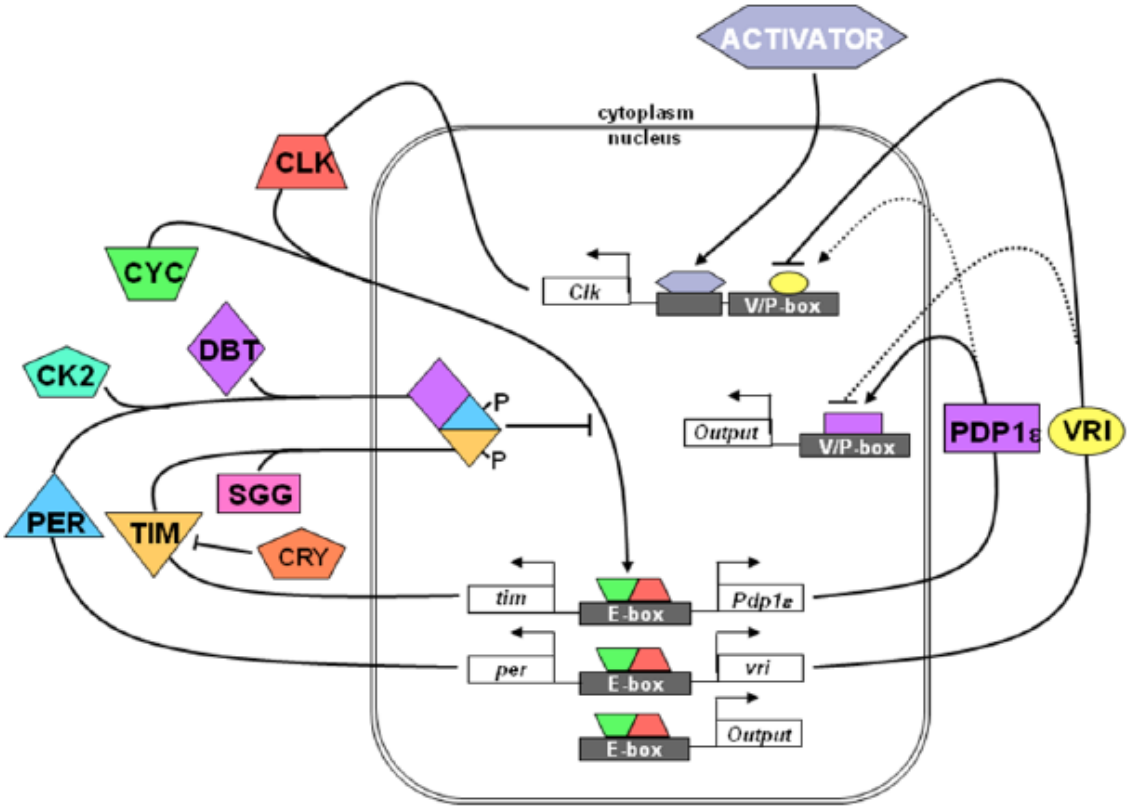

Figure 1: Model of the transcriptional feedback loops that keep circadian time in *Drosophila*. All gene, regulatory element, and protein names are as defined in the text. Double line, nuclear envelope; solid arrows, transcription activation; blocked line, repression; dashed line, possible activation or repression; and P, phosphorylation. (Adapted from Benito et al., 2007).

Regulation of circadian transcription in *Drosophila*

There is a plethora of evidence suggesting that self-sustaining ~24 h oscillatory mechanisms are dependent on integrating multiple regulatory pathways, such as temporal changes in the posttranslational regulation of core clock proteins. These regulatory mechanisms are thought to modulate the stability, activity, and subcellular localization of clock components that determine the timing of their action in the daily cycle (Kloss et al., 1998). Multiple levels of posttranslational controls are built into these systems, presumably to delay the molecular feedback cycles so that they take a full 24 h and maintain robust amplitude of cycling from the transcription of clock components all the way to physiological outputs. In addition, these controls for example, phosphorylation of clock proteins, provide mechanisms through which the clock can be reset by environmental inputs (Mizoguchi et al., 2006).

Cyclic post-translational modifications (PTMs) of clock proteins are also important for molecular clock oscillations that control the timing of circadian transcription in higher eukaryotes (Bae and Edery, 2006; Gallego and Virshup, 2007; Weber et al., 2011). The precise regulation of clock protein accumulation, sub-cellular trafficking, activation, inactivation, and finally degradation involves a cascade of specific co-factor and chromatin interactions, as well as modifications by phosphorylation, acetylation, SUMOylation, glycosylation and ubiquitylation. CLK and PER in flies are reversibly modified by O-GlcNAcylation to regulate their transcriptional activities (Kaasik et al., 2013). BMAL1 is SUMOylated, a modification that destabilizes the circadian activator complex (Cardone et al., 2005; Lee et al., 2008). In addition to

SUMOylation and phosphorylation, mammalian CLK is shown to harbor acetyl-transferase activity (Doi et al., 2006). Acetylation of BMAL1 by mammalian CLK is important for inhibition of circadian transcription (Hirayama et al., 2007). Moreover, activation and repression of circadian transcription are shown to be associated with circadian cycles of histone acetylation and methylation of clock controlled promoter regions (Etchegaray et al., 2003; Ripperger and Schibler, 2006; Taylor and Hardin, 2008; Katada and Sassone-Corsi, 2010). As expected, altering specific phosphorylation sites on clock proteins (Kivimae et al., 2008; Chiu et al., 2008; Mahesh et al., and Lee et al., 2014) and clock protein kinases and phosphatases (Price et al., 1998; Martinek et al., 2001; Lin et al., 2002; Akten et al., 2003; Sathyanarayanan et al., 2004; Fang et al., 2007) causes disruption of the molecular oscillations and changes in the period of free running rhythms. These observations demonstrate that specific PTMs of clock proteins carry timing information for circadian oscillations, where phosphorylation is the most extensively characterized PTM that regulates circadian rhythms.

In the absence of rhythmic transcription, PER and TIM protein levels can still oscillate and drive behavioral rhythms in some flies, albeit weakly (Yang and Sehgal, 2001). This suggests that posttranslational regulation i.e. cyclic phosphorylation of PER and TIM plays an important role in the timekeeping mechanism of the *Drosophila* clock. Regulation of the subcellular localization, stability, interactions and activity of clock components like PER in *Drosophila* and FREQUENCY in *Neurospora* by reversible phosphorylation has been well characterized (Mizoguchi et al., 2006). Moreover, phosphorylation of a key mammalian circadian protein, PER2, precisely controls the

period and phase of circadian oscillations by supporting normal nuclear PER2 accumulation (Maier et al., 2009). Many of the circadian rhythm sleep disorder (CRSD) relevant variations reported to date, affect the phosphorylation status of the clock proteins (Ebisawa et al., 2001), emphasizing the important contribution of phosphorylation of clock proteins to physical and mental health.

In *Drosophila*, the DOUBLE-TIME (DBT) and NEMO (NMO) mediated hyperphosphorylation of CLK is thought to be balanced by protein phosphatase activity, resulting in a dynamic equilibrium between hypo- and hyperphosphorylated CLK variants (Yu et al., 2009 and 2010). This balance between phosphorylation and dephosphorylation presumably stabilizes the levels of CLK, which is thought to be the limiting component in the *Drosophila* transcriptional feedback circuitry (Bae et al., 2002). Hence, an understanding of the role of protein phosphorylation status is essential for understanding circadian timekeeping mechanisms. The phosphorylation of CLK by PER-CRY-CK1 complexes in mammals is also suggested to repress transcription by removal of CLOCK-BMAL1 from E-boxes or by blocking of CLOCK-BMAL1 transactivation (Reppert and Weaver, 2002). Given that core clock proteins are conserved in animals and are regulated by PTMs in different eukaryotic clock systems, what we learn about clock protein phosphorylation in *Drosophila* will likely be relevant to clock function in mammals.

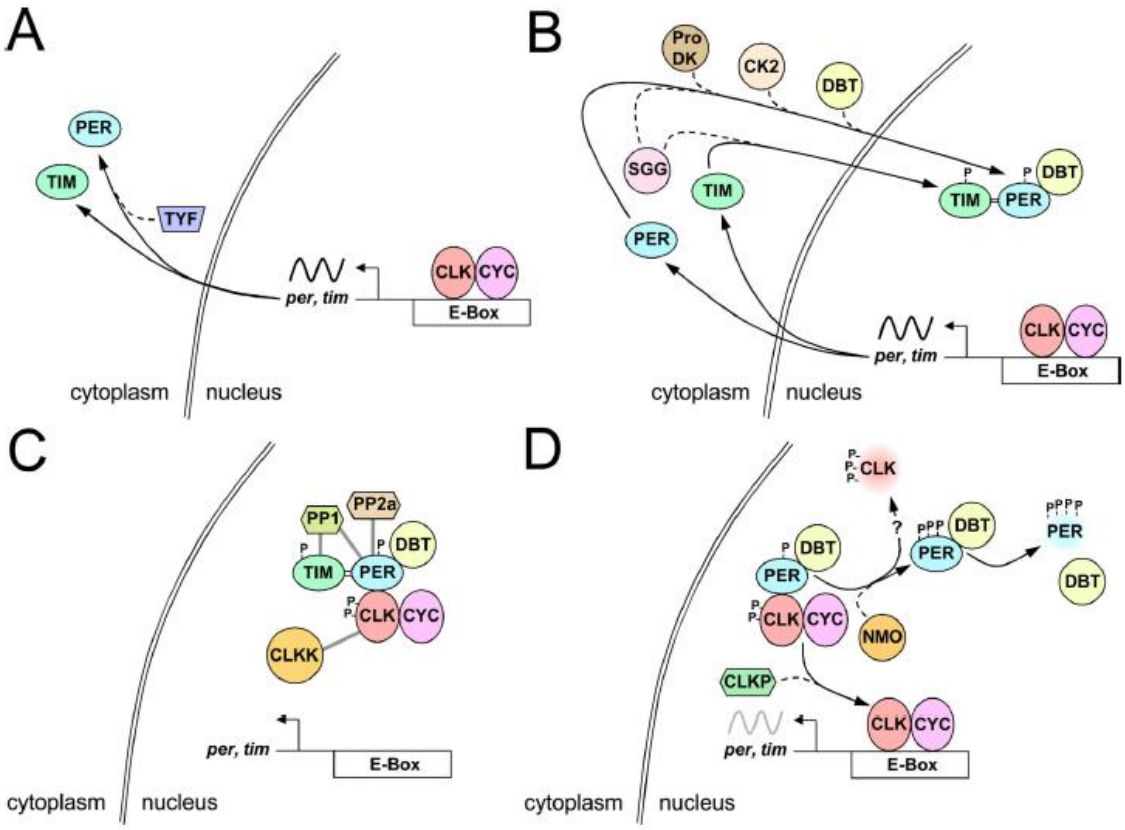

Figure 2: Post-transcriptional and -translational regulatory steps within the *Drosophila* core feedback loop. All gene, regulatory element, and protein names are as defined in the text. All symbols are as defined in Fig. 1. A. ~ZT6-ZT12: Delay in PER synthesis. B. ~ZT16-20: Movement of PER and TIM into the nucleus. C. ~ZT16-ZT0: Stabilization of nuclear PER. D. ~ZT3-ZT6: Release of PER repression and reactivation of CLK-CYC transcription. Double bar, stabilizing activity; TYF, twenty four; CLKK, CLK kinase; ProDK, proline-directed kinase; gray bars, kinase and phosphatase targets; faded protein symbols, protein degradation; ?, putative direct effect; gray sinusoidal line, initiation of transcription. (Hardin, 2011).

Based on the available evidence, the timing of CLK-CYC activation and PER-TIM repression is primarily regulated post-translationally, in part through rhythmic phosphorylation of CLK, PER and TIM to generate 24 h rhythms. The phosphorylation

state of a protein is controlled dynamically by both protein kinases and phosphatases. However, this important regulatory mechanism has been studied mainly at the level of the kinases involved in mediating circadian clock function. Many kinases such as DBT (ortholog of mammalian CASEIN KINASE I, CKI), CAESIN KINASE II (CK2), SHAGGY (SGG; ortholog of mammalian GLYCOGEN SYNTHASE KINASE 3B, GSK3), and NMO that control PER, TIM, and/or CLK levels, activity, and/or subcellular localization have already been identified (Fig. 2; Kloss et al., 1998 and 2001; Price et al., 1998; Martinek et al., 2001; Lin et al., 2002; Akten et al., 2003 and 2009; Chiu et al., 2008 and 2011; Yu et al., 2011; Szabo et al., 2013). In contrast, few phosphatases such as PROTEIN PHOSHATASE 2A (PP2A), PROTEIN PHOSHATASE 1 (PP1), and STRIPAK have been discovered that target PER, TIM, and/or CLK to regulate transcriptional rhythms in *Drosophila* (Fig. 2; Sathyanarayanan et al., 2004; Fang et al., 2007; Andreazza et al., 2015).

In vivo RNAi screen to identify candidate phosphatases

As previously described, in *Drosophila*, the PER-TIM-DBT complexes bind to and remove CLK-CYC from E-boxes, thereby promoting transcriptional repression (Fig. 1). However, PER-CLK binding in itself is not sufficient to remove CLK-CYC from E-boxes (Kim et al., 2007). DBT, a CKI homolog phosphorylates TIM-free PER protein and triggers its degradation (Kloss et al., and Price et al., 1998). As TIM accumulates, it binds to and stabilizes PER (Price et al., 1995). SGG (GSK3) phosphorylates TIM and CK2 phosphorylates PER to regulate nuclear entry of the PER/TIM/DBT complex,

thereby allowing repression of CLK/CYC function (Fig. 2; Martinek et al., 2001; Lin et al., 2002; Akten et al., 2003; Ko et al., 2010). In the absence of TIM, DBT promotes the phosphorylation and degradation of nuclear PER, thereby de-repressing CLK/CYC function and starting a new wave of transcription from E-boxes. Moreover, it is well established that NMO phosphorylates S596 on PER, which stimulates DBT-dependent phosphorylation of S589, S585 and likely T583. Phosphorylation in this *per*-short phospho-cluster somehow delays phosphorylation at other DBT-dependent sites on PER including S47, thus delaying the PER/SLIMB interaction and the daily degradation of PER (Edery et al., 1994; Ko et al., 2002 and 2010; Grima et al., 2002; Kim et al., 2007; Nawathean et al., 2007; Chiu et al., 2008 and 2011; Kivimae et al., 2008; Yu et al., 2011). PER-TIM-DBT dependent phosphorylation of CLK coincides with CLK-CYC release from E-boxes, suggesting that CLK phosphorylation represses transcription (Price et al., 1998; Nawathean and Rosbash, 2004; Yu et al., 2006). Upon release of PER-TIM-DBT, hyperphosphorylated CLK is replaced with transcriptionally competent hypophosphorylated CLK (Yu et al., 2006), likely via direct conversion of hyperphosphorylated CLK to hypophosphorylated CLK by phosphatases (Kim and Edery, 2006; Andreazza et al., 2015).

Due to the similarity among posttranslational regulatory events in different eukaryotic clock systems, it has been proposed that the molecules mediating the modifications and degradation of clock proteins may be the common foundation that allows the evolution of circadian clocks in eukaryotes (Dunlap et al., 1999). However, how these modifications regulate mechanisms of circadian processes in organisms is

only partially understood for a few clock components. Hence, my goal was to determine how phosphorylation regulates rhythmic transcription within the autoregulatory feedback loop that keeps circadian time in flies. Therefore, I carried out an RNAi screen (Fig. 3) to identify and characterize additional phosphatases that dephosphorylate clock proteins, thereby revealing novel features of the circadian timekeeping mechanism in *Drosophila* that are likely to be conserved in all animals including humans.

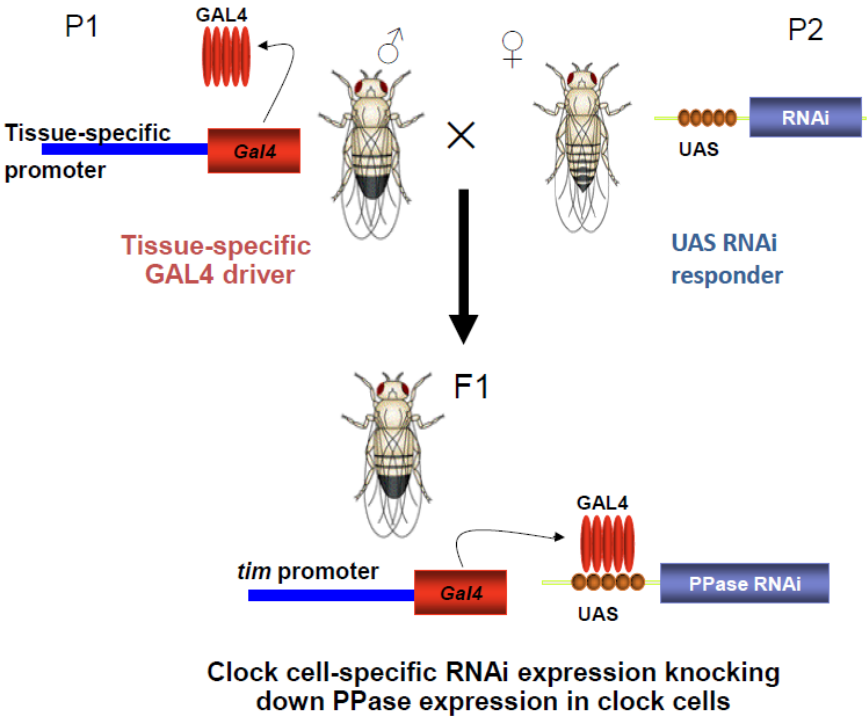

Figure 3: RNAi screen strategy to identify clock phosphatases in *Drosophila*. P1, P2, parent generations; F1, first filial generation; UAS, upstream activating sequence, an enhancer to which GAL4 specifically binds to activate gene transcription; PPase, phosphatase. Other details are as defined in the text.

We already know that PP1 functions within the *Drosophila* clock to dephosphorylate and stabilize TIM in cultured cells, thus stabilizing the PER-TIM-DBT complex, promoting transcriptional repression, and lengthening period (Fang et al., 2007). Overexpression of the endogenous Nuclear Inhibitor of PP1 (NIPP1) also leads to a lengthened circadian period and reduction in amplitude of behavioral rhythms (Fang et al., 2007). Reducing the expression or activity of PP2A, which dephosphorylates PER, has also been shown to lengthen circadian period presumably by decreasing PER stability (Sathyanarayanan et al., 2004). Moreover, reducing the activity or expression of kinases that promote PER degradation (e.g. DBT), or PER-TIM-DBT nuclear localization (e.g. CK2, SGG), also lengthen circadian period (Martinek et al., 2001; Lin et al., 2002; Akten et al., 2003, Muskus et al., 2007). These results suggest that the kinases/phosphatases that phosphorylate/dephosphorylate clock proteins can yield both fast and slow clocks depending on which phase of the cycle they act. Additional copies of *Clk* result in increased CLK-CYC transcriptional activity and shortening of the circadian period of otherwise wild-type flies (Kim and Edery, 2006). Hence, an RNAi knockdown of CLK phosphatases, which would increase CLK phosphorylation and decrease transcriptional activity, should also lengthen circadian period. My hypothesis therefore was that an increase in clock protein phosphorylation via the phosphatase/regulator RNAi knockdown should decrease CLK-CYC transcriptional activity and/or affect PER-TIM-DBT localization or degradation, and in turn lengthen/shorten the period of locomotor activity.

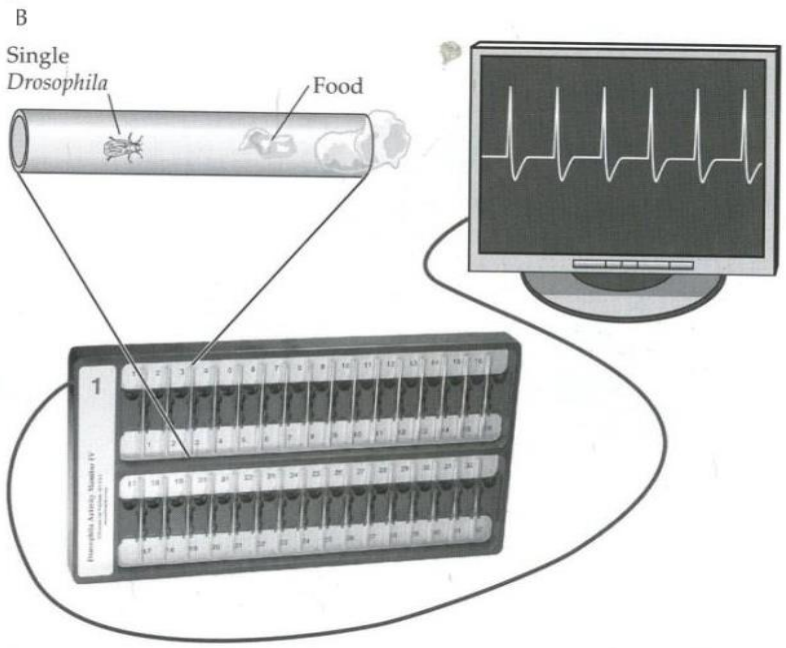

Figure 4: Schematic for monitoring *Drosophila* activity rhythms. Single fly from the F1 generation (Fig. 3) is introduced into the behavior tubes that are then fed into behavioral monitors equipped with infra-red beams. Activity is recorded whenever the beam breaks and is analyzed using Clocklab software as described in Methods. (Dunlap, 2004).

I propose that PER degradation permits CLK dephosphorylation by protein phosphatases. Such dephosphorylation would render CLK-CYC competent to bind E-boxes, thereby reactivating transcription. This hypothesis could be tested by identifying phosphatases that specifically dephosphorylate CLK and determining whether these phosphatases promote CLK-CYC binding to E-boxes and/or chromatin modifications that activate transcription. It is possible that new CLK synthesis could also account for the accumulation of hypophosphorylated CLK after transcriptional repression is released. However, if this were the case, hyperphosphorylated CLK would be degraded

and replaced by newly synthesized CLK. Since CLK does not drop to low levels before hypophosphorylated CLK accumulates, new CLK synthesis is a less likely explanation for the accumulation of hypophosphorylated CLK. Any reduction in the expression of CLK phosphatases/regulators is predicted to prolong repression, thereby lengthening the period of locomotor activity rhythms (Fig. 4).

Screening ~100 clock cell-specific RNAi knockdown lines targeting each annotated *Drosophila* phosphatase identified 22 genes as candidate clock phosphatases (Fig. 3 and the table on page 29). These include protein phosphatases that dephosphorylate target proteins at serine and threonine residues, tyrosine residues or both (dual-specificity phosphatases). Moreover, they function in multiple cellular processes regulating protein stability, localization and/or activity. I tested if these candidate phosphatases dephosphorylated core clock proteins, and/or had an impact on the output pathways. Dephosphorylation of clock proteins by direct action of phosphatases is a key event involved in releasing the repression of CLK-CYC transcription in fruit flies. The proposed study is fundamental to our understanding of the molecular mechanism of the circadian clocks. The findings will help us determine how clock protein dephosphorylation controls transcriptional rhythms, which are required for circadian timekeeping in flies. The clock phosphatases identified here represent potential genetic links to clock associated disorders in humans and novel targets for the development of drugs to treat such disorders.

Of the 22 phosphatases identified in the RNAi screen with aberrant rhythms, the receptor protein tyrosine phosphatase (RPTP) Leukocyte-Antigen Related (LAR; Streuli

et al., 1989) is required for rhythmic activity. Tyrosine phosphorylation of signal transduction proteins is regulated by protein-tyrosine kinases (PTKs) and protein-tyrosine phosphatases (PTPs). Both PTKs and PTPs have soluble, cytosolic members and receptor-like transmembrane members that contain a wide variety of structural and regulatory subunits in association with the catalytic domains (Walton and Dixon, 1993; Bixby, 2001). Phosphorylation of protein tyrosine residues plays a major role in the regulation of many biological processes, including cell growth, differentiation, and development (Zhang, 1998; Chagnon et al., 2004). Additionally, PTKs and PTPs are among the many signal-transducing molecules that have been implicated in axon outgrowth, extension, guidance, or steering (Goodman, 1996). In *Drosophila*, the RPTP family of Immuno-globulin (Ig) transmembrane receptors have also been shown to be crucial for proper axon guidance during embryogenesis (Seeger et al., 1993), and cell migration and positioning at later stages (Jhaveri et al., 2004). Despite their roles in development and a wealth of structural and enzymatic data, the function of RPTPs in circadian context is poorly understood.

There are six receptor PTPs identified in *Drosophila*, five of which are expressed predominantly on axons in the developing nervous system (Streuli et al., 1989; Yang et al., Tian et al., and Hariharan et al., 1991; Jeon et al., 2008). LAR is a member of this PTP subfamily that has ecto-domains consisting of N-terminal Ig-like domains and membrane-proximal fibronectin type III (FNIII) domains (Streuli et al., 1989); and a cytoplasmic domain consisting of two tandemly repeated PTPase domains, a membrane-proximal PTP-D1 and C-terminal PTP-D2. This ectodomain structure is also found in

adhesion molecules suggesting that LAR may play a role in cell-cell or cell-extracellular matrix interactions. Moreover, the PTPase domains of the LAR subfamily are extremely well conserved where the PTPase domains of *Drosophila* LAR and human LAR share 74% amino acid sequence identity suggesting a possible conservation in the function of *Lar*.

Based on the behavioral arrhythmicity displayed by *Lar* RNAi knockdowns, I set out to determine a role for *Lar* in *Drosophila* clocks. Genetic and molecular analysis revealed that it regulates the development of neuronal circuit underlying the communication between clock neurons in the fly brain (Agrawal and Hardin, 2016).

Organization of the circadian system in the *Drosophila* brain

The *Drosophila* circadian clock operates in many cells and tissues (Menet and Hardin, 2014). In the brain, this feedback loop operates in ~75 pacemaker neurons per hemisphere that function to drive activity rhythms (Fig. 5; Helfrich-Forster, 2003). These brain pacemaker neurons can be divided into multiple clusters based on their location, size and neuropeptide expression, including two anterior dorsal neuron 1s (DN_{1a}s), 15 posterior dorsal neuron 1s (DN_{1p}s), two dorsal neuron 2s (DN_2s), 38 dorsal neuron 3s (DN_3s), six dorsal lateral neurons (LN_ds), three lateral posterior neurons (LPNs), four pigment-dispersing factor (PDF) neuropeptide-expressing small ventral lateral neurons (sLN_vs), one PDF-negative 5^{th} sLN_v, and four large ventral lateral neurons (lLN_vs; Nitabach and Taghert, 2008; Shafer and Yao, 2014). These clusters of pacemaker neurons form a network that maintains synchrony and determines the pattern

of activity rhythms based on environmental inputs (Peschel and Helfrich-Forster, 2011; Yoshii et al., 2012). This network also exhibits circadian plasticity; the PDF-positive sLN_vs send axonal projections toward DN_1s and DN_2s that undergo daily changes in morphology (Fernandez et al., 2008; Depretis-Chauvin et al., 2014). However, a direct molecular link between the core clock and rhythmic remodeling of sLN_v axonal projections has not been identified.

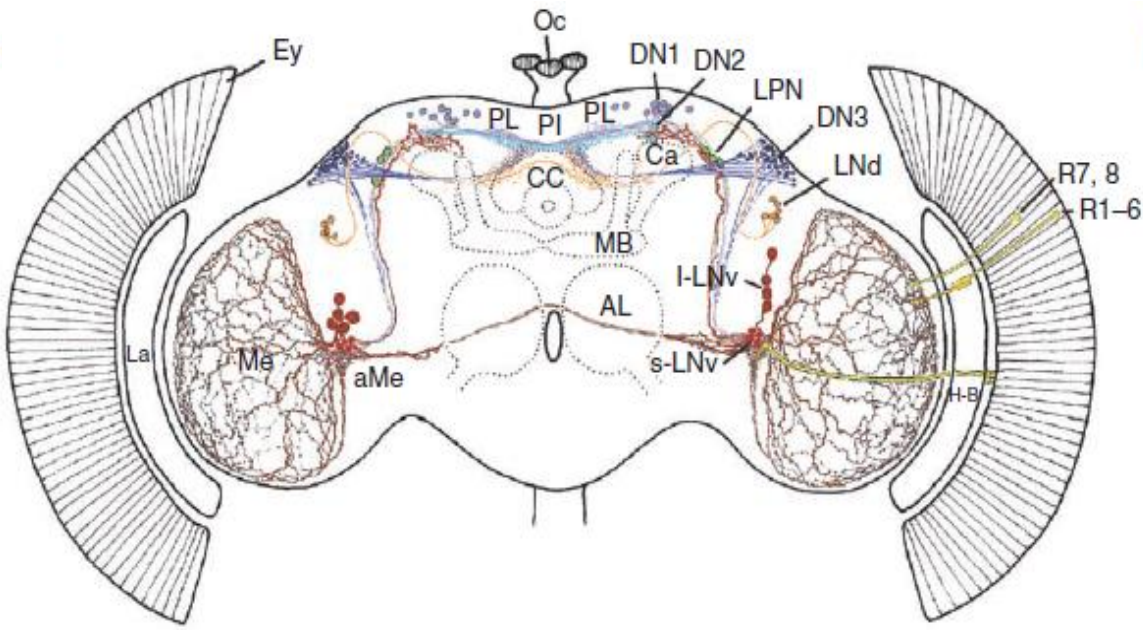

Figure 5: Circadian pacemaker neuron clusters and neural network in adult *Drosophila* brain. l-LN_v, large ventral lateral neuron; s-LN_v, small LN_v; LN_d, dorsal LN; DN, dorsal neuron; LPN, lateral posterior neuron; Ca, calyces of the mushroom bodies (MB); CC, central complex; PI/PL, pars intercerebralis/lateralis; Oc, ocelli; AL, antennal lobe; aMe, accessory medulla (Me); La, lamina; R1–8, photoreceptor cells of the compound eye (Ey). (Lim and Allada, 2013).

CRY function within and outside the *Drosophila* clock

Circadian clocks enable organisms to anticipate daily changes in the external environment. Although these ~24 h rhythms persist in constant conditions, daily environmental fluctuations entrain or reset rhythms to precisely 24 h periods and an appropriate rhythm-specific phase. In animals, environmental cycles of light, food, temperature and/or social cues set the phase of circadian oscillators so that overt rhythms in physiology, metabolism and behavior occur at the appropriate time of day. The most potent and reliable environmental cue is light, which mediates entrainment via different mechanisms depending on tissue type and species.

In *Drosophila*, neither genetic ablation of eyes nor mutations in the visual phototransduction pathway, block entrainment of circadian activity rhythms to light (Helfrich-Forster et al., 2001; Szular et al., 2012). For example, *Drosophila norpA* (a phospho-lipase C involved in the visual transduction pathway) and *ninaE* (Rh1 rhodopsin in R1-R6) mutants show robust and light-sensitive rhythms, suggesting the presence of an additional clock-relevant photoreceptor (Yang et al., and Suri et al., 1998). Action spectra for resetting adult locomotor activity rhythms and promoting TIM degradation in *Drosophila* are also significantly different from that for vision, suggesting a novel blue light circadian photoreceptor that entrains behavioral rhythms and peripheral clocks (Wheeler et al., 1993; Suri et al., and Yang et al., 1998).

Indeed, a screen for mutants that altered rhythmic *per*-driven luciferase reporter gene expression led to the discovery of CRYPTOCHROME (CRY), which functions as a blue light photoreceptor sufficient for clock resetting to light in flies (Stanewsky et al.,

1998; Helfrich-Forster et al., 2001). Under LD cycling conditions, PER-TIM mediated transcriptional repression is released when light in the morning promotes the rapid disappearance of TIM. *Drosophila* CRY resets the molecular feedback loop by directly interacting with core components of the circadian clock (Fig. 6; Ceriani et al., 1999). CRY binds to TIM in a light-dependent fashion, thereby promoting TIM phosphorylation on tyrosine residues by an unknown kinase(s), and the interaction of phosphorylated TIM with JETLAG, an F-box protein that degrades TIM through a ubiquitin-proteasome mechanism (Lin et al., 2001; Koh et al., 2006; Peschel et al., 2009). Moreover, flies overexpressing CRY are behaviorally hypersensitive to short light pulses, whereas cry^b mutant flies are unable to phase-shift their internal clock after such pulses (Emery et al., 1998 and 2000; Ishikawa et al., 1999). Furthermore, cry^b flies remain rhythmic under intense constant light, a condition that causes wild-type flies to immediately become arrhythmic. *Drosophila* uses CRY, the compound eyes, and the Hofbauer-Buchner (H-B) eyelet for entrainment to light:dark cycles (Helfrich-Forster et al., 2001; Ashmore and Sehgal, 2003). However, eyes and the H-B eyelet are unnecessary for circadian photoentrainment and photoresponses (Wheeler et al., 1993; Yang et al., 1998; Helfrich-Forster et al., 2001). Moreover, data showing that cry^b flies are rhythmic in intense constant light suggests that CRY is probably the only dedicated circadian photoreceptor. CRY is also involved in the light input into the larval clock; because only larvae lacking both CRY and the visual system are circadianly blind (Klarsfeld et al., 2004; Mazzoni et al., 2005).

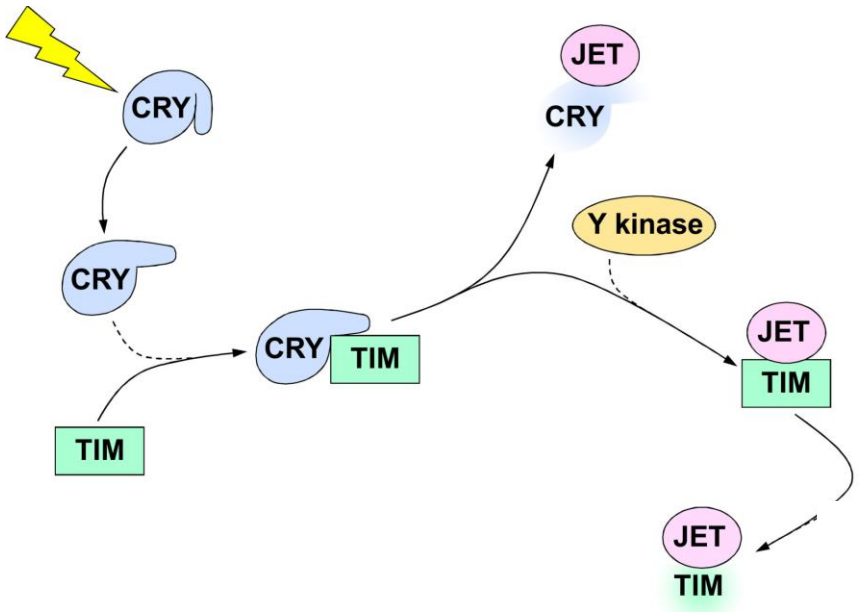

Figure 6: Light-induced phase resetting mechanism in *Drosophila*. All gene, regulatory element, and protein names are as defined in the text. All symbols are as defined in Figures 1 and 2. Y kinase, tyrosine kinase. Other details are as defined in the text. (Adapted from Hardin, 2011).

In mammals, the molecular clock mechanism is similar to that of *Drosophila*, but light-dependent resetting occurs through a different mechanism. Studies in mice show that specialized retinal ganglion cell photoreceptors are necessary to detect and transmit light information to the master clock in a brain region called the suprachiasmatic nucleus (SCN) (Buhr and Takahashi, 2013). The SCN then acts to entrain clocks in some peripheral organs, whereas clocks in other peripheral organs are reset directly by environmental cues such as food (Mohawk et al., 2012; Schibler et al., 2015). This contrasts with the situation in zebrafish and fruit flies, where cell autonomous photoreceptors entrain clocks in a wide variety of peripheral tissues, thereby

synchronizing molecular oscillations in isolated organs (Giebultowicz and Hege, and Plautz et al., 1997; Levine et al., 2002). Although CRY is involved in transducing photic information from the environment to the core oscillator in plants and flies (Cashmore, 2003), CRY plays a different role within the mouse clock. Mammalian CRY1 and CRY2 act as light-independent inhibitors of CLK-BMAL1 transcription, showing that mammalian CRYs play a central role in the circadian clock unrelated to that of *Drosophila* CRY. Mutations in mammalian CRYs lead to period alterations or arrhythmicity, with no evidence for photoreceptor function (Reppert and Weaver 2002; Ko and Takahashi, 2006).

In addition to the cell autonomous molecular clock mechanism, membrane excitability is a key component of normal maintenance of circadian molecular and behavioral rhythms in flies. Electrophysiological characterization of the small and large LN_vs (subsets of pacemaker neurons that control circadian activity and arousal) has shown that their membrane properties are clock regulated; spontaneous firing frequencies are higher during the early day, gradually dropping until dusk, and then rise again through the course of the night (Cao et al., 2008; Sheeba et al., 2010). Additionally, lLN_v spontaneous firing frequency elevates considerably in response to light in the absence of all opsin-based photoreceptors (Shang et al., 2008; Fogle et al., 2011). Light-evoked changes in membrane resting potential occur in about 100 milliseconds and these responses are selective for blue wavelengths corresponding to the spectral sensitivity of CRY. Consequently, *cry*-null lines are not light responsive, but restoring CRY expression in the lLN_v rescues light responsiveness. Surprisingly, CRY

expression in neurons that are normally unresponsive to light confers responsiveness. The CRY-mediated light response requires a flavin redox-based mechanism and depends on the voltage-gated potassium (K^+) channel ß-subunit (Kvß) Hyperkinetic (Hk) conductance, but is independent of the classical circadian CRY-TIM interaction (Fogle et al., 2015).

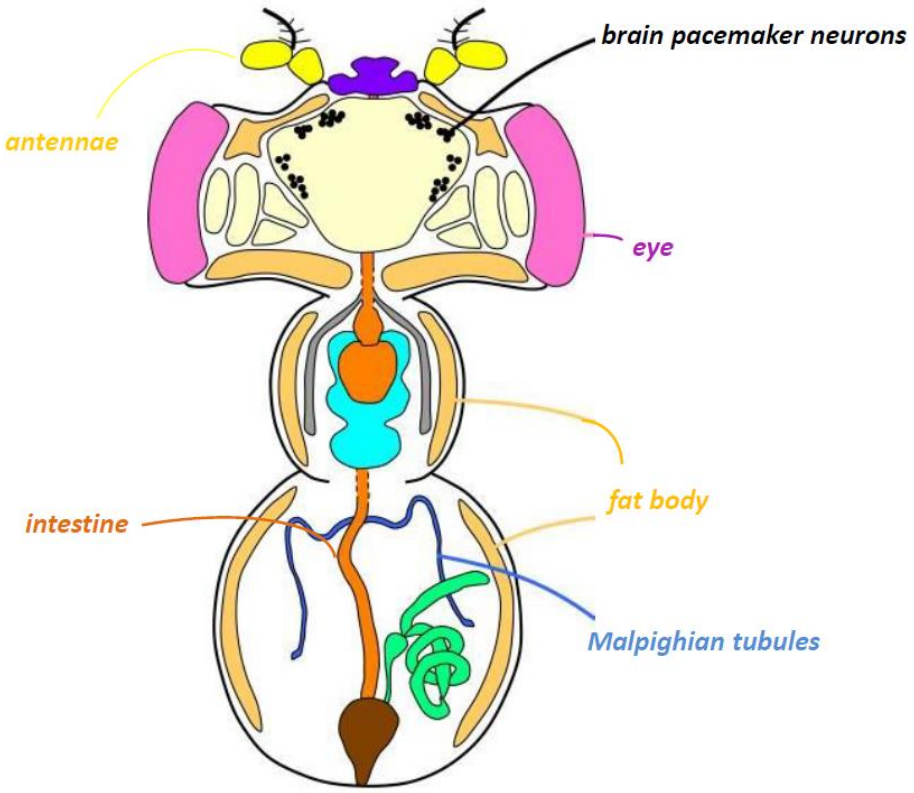

Figure 7: Clock distribution in different cells and tissues of *Drosophila melanogaster*. Yellow, antennae; cream, brain; tan, fat body; purple, proboscis; black, pacemaker neurons; pink, photoreceptors; orange, digestive tract; gray, salivary glands; aqua, ventral nerve chord; blue, Malpighian tubules; green, male reproductive tract; brown, rectum. (Adapted from Menet and Hardin, 2014).

In *Drosophila*, PDF expressing LN_v pacemaker neurons, that are also light-sensitive, are necessary and sufficient to drive circadian activity rhythms. However, pacemaker neurons are only a small fraction of the total number of clock-containing cells in a fly. Additional ‘‘peripheral’’ clocks exist in many tissues, including the eyes, antennae, and Malpighian tubules (MTs), where they likely control the local physiology of these organs (Menet and Hardin, 2014) (Fig. 7). The regulation of outputs in peripheral organs is mediated by clock driven molecular oscillations, which have been observed in many isolated peripheral organs (Emery et al., Giebultowicz and Hege, and Plautz et al., 1997). For instance, circadian oscillations in *per* expression occur in chemosensory cells of the antennae, even when the antennae are excised and maintained in isolated organ culture (Krishnan et al., 1999).

The *cry* gene is expressed in heads, including a subset of brain pacemaker neurons (Fig. 8) and in bodies, suggesting that CRY acts as a photoreceptor in both clock containing brain neurons and in peripheral tissues. Moreover, experiments showing that light can entrain the molecular clock in isolated peripheral tissues suggest that CRY is widely expressed (Emery et al., Giebultowicz and Hege, and Plautz et al., 1997), but this hasn’t been tested. Furthermore, numerous studies demonstrate a photoreceptor-independent role for CRY in peripheral tissues, implying that *Drosophila* CRY might be part of the pacemaker mechanism (Krishnan et al., 2001; Levine et al., 2002; Collins et al., 2006).

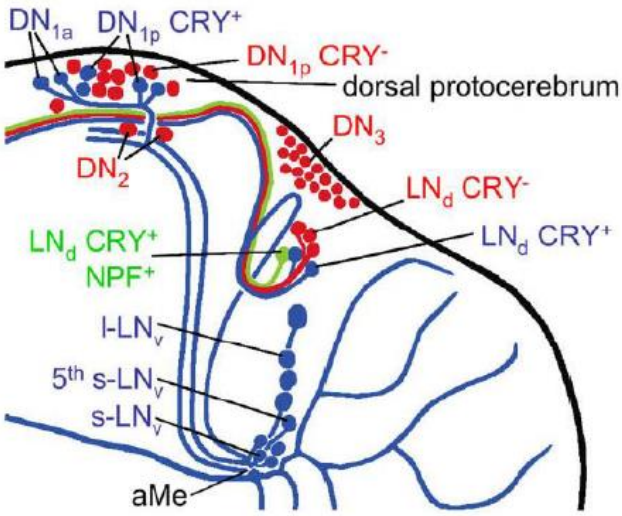

Figure 8: Schematic showing CRY distribution in different pacemaker neurons and processes. Blue, green, arborizations of the CRY positive cells; red, CRY negative cells; aMe, accessory medulla. (Yoshii et al., 2008).

Using a newly developed GFP-tagged-*cry* transgene and a mutant that lacks any detectable levels of CRY (*cry*^{03}; Dolezelova et al., 2007); I show for the first time that CRY is indeed expressed in fly peripheral tissues. I also demonstrate that CRY protein levels are dramatically reduced by light exposure in peripheral tissues and establish an essential role for CRY in light-induced degradation of TIM. Furthermore, my data suggest that CRY plays a dual role in MTs; apart from its photoreceptive function, CRY is indispensable for maintaining free-running PER and TIM oscillations in MTs, but not in LNs. I conclude that CRY is involved in TIM-mediated entrainment of both central LN and peripheral MT clocks, suggesting CRY is a major *Drosophila* photoreceptor

dedicated to the resetting of circadian rhythms in pacemaker neurons and in peripheral tissues.

Given that CRY mediates cell-autonomous membrane responses in lLN_vs, and multiple K^+ channel α-subunits that co-assemble with Hk mediate the CRY/Hk-coupled light response (Fogle et al., 2011), I wanted to investigate if CRY is coupled to membrane potential changes in fly peripheral tissues. In contrast to brain pacemaker neurons that are excitatory in nature, most peripheral tissues are not, thus I focused on assessing passive membrane properties. Using larval salivary glands which are amenable to electrophysiological recording and lack a circadian clock, I found a novel role for CRY in the regulation of passive properties of cell membrane physiology. *Drosophila* salivary glands consist of two major cell types: secretory cells and duct cells. Secretory cells synthesize and secrete high levels of protein whereas duct cells form simple tubes connecting the secretory cells to the larval mouth (Andrew et al., 2000). These are the largest secretory organs in the *Drosophila* embryo and larva. Numerous studies show that salivary glands are model tissues to study membrane properties of peripheral organs in animals including mammals (Dinudom et al., 2004; Romanenko et al., 2008). However, since these are non-excitable cells, I studied the impact of CRY on two key passive membrane properties, Resting Membrane Potential (RMP) and Input Resistance (R_i), in the fly larval gland cells.

My studies suggest that CRY is required to maintain low membrane conductance, or high input resistance, even in *Drosophila* peripheral tissues that lack a circadian clock. These findings for the first time define the expression profile of CRY in

the peripheral tissues, reveal that CRY protein is required for K^+ channel dependent changes in passive membrane properties that are light-independent, cell-autonomous and functions in peripheral tissues devoid of a canonical circadian clock.

CHAPTER II

AN RNAi SCREEN TO IDENTIFY PROTEIN PHOSPHATASES THAT FUNCTION WITHIN *Drosophila* CIRCADIAN CLOCK

Background

Circadian clocks in eukaryotes keep time via cell-autonomous transcriptional feedback loops. A well-characterized example of such a transcriptional feedback loop is in *Drosophila*, where CLOCK-CYCLE (CLK-CYC) complexes activate transcription of *period* (*per*) and *timeless* (*tim*) genes, rising levels of PER-TIM complexes feedback to repress CLK-CYC activity, and degradation of PER and TIM permits the next cycle of CLK-CYC transcription. The timing of CLK-CYC activation and PER-TIM repression is regulated post-translationally, in part through rhythmic phosphorylation of CLK, PER and TIM. Previous behavioral screens identified several kinases that control the levels, subcellular localization and/or activity of CLK, PER and TIM, but the two phosphatases that function within the clock were identified through the analysis of candidate genes from other pathways or model systems. To identify phosphatases that play a role in the *Drosophila* clock, I screened clock cell-specific RNA interference (RNAi) knockdowns of each annotated phosphatase in *Drosophila* for altered activity rhythms. This screen identified 22 such phosphatases that either lengthened or shortened circadian period by ≥ 1h (*p-value*: ≤ 0.05 compared to controls) or were arrhythmic.

The efficacy and specificity of RNAi mediated knockdown of candidate phosphatases was validated by testing additional RNAi line that targets other region of

the mRNA, transposon inserts and existing loss of function mutants for activity rhythm defects. In addition, CRISPR technology (Gratz et al., 2013) was used to generate mutants for one of these candidates that lacked loss of function mutants. Genetic validation and molecular analysis was carried out to define the role these genes play in regulating circadian oscillator function. The 15 candidates that remain after validation are expected to reveal novel features of the circadian timekeeping mechanism in *Drosophila* that are likely to be conserved in all animals including humans.

Results

To identify phosphatases that mediate circadian clock function, clock cell-specific RNAi knockdowns of all annotated *Drosophila* phosphatases were screened for altered locomotor activity rhythms. An RNAi screening strategy is advantageous because (1) lethality can be avoided by targeting RNAi to clock cells via the Gal4/UAS system, (2) RNAi is efficient method for knocking down target gene expression, and (3) transgenic UAS-RNAi lines are available for each phosphatase/regulator from either the Vienna *Drosophila* RNAi Center (VDRC), Transgenic RNAi Project at the Harvard Medical School plans (TRiP), or the National Institute of Genetics RNAi Stocks (NIG-Fly). A total of 144 annotated phosphatases and phosphatase regulatory subunits are present in the *Drosophila* genome (*Drosophila* RNAi Screening Center, DRSC). Of these phosphatases/regulators, ~100 are protein phosphatases.

Flies containing UAS-RNAi inserts that target a given phosphatase/regulator and a Gal4 driver expressed in all clock cells (e.g. *tim*-Gal4) were screened to identify

phosphatases that disrupt circadian activity rhythms. RNAi lines from VDRC were used because most are inserted at a single genomic site (e.g. KK lines) that affords efficient and comparable expression, whereas other lines are inserted at random genomic sites (e.g. GD lines), and all stocks are easily obtained. Flies bearing UAS-RNAi and the *tim*-Gal4 driver, or controls bearing UAS-RNAi alone and Gal4 driver alone, were placed into *Drosophila* Activity Monitors (Fig. 4), entrained for 3 days in LD cycles, and then released into DD (constant dark) for 7 days. Locomotor activity rhythms recorded during DD were analyzed for circadian rhythmicity and period via ClockLab software. This initial screen identified a total of 31 candidate phosphatases, all but one of which lengthened circadian period or abolished rhythmicity (Table 1). Since many RNAi lines with a lengthened period also reduced the proportion of rhythmic flies, I was concerned that widespread RNAi knockdown of these phosphatases or ectopic RNAi expression from this *tim*-Gal4 driver impaired fly health. Consequently, I used *pdf*-Gal4 to restrict RNAi expression to PDF neuropeptide expressing ventral lateral pacemaker neurons (LN_vs) and an independent *tim*-Gal4 insert to drive phosphatase RNAi expression. Out of the ~100 lines screened with all three Gal4 drivers, 22 RNAi lines with a ≥ 1 h period change (*p-value*: ≤ 0.05 compared to controls) or > 50% arrhythmicity were identified (Table 1).

Table 1: Activity rhythms for all of the annotated *Drosophila* phosphatases, using clock cell-specific RNAi knockdowns. The genotypes are listed using the GD or KK number for the UAS-RNAi responder flies; *tim*Gal4 (on 2nd or 3rd chromosome) and *pdf*Gal4 for the clock cell-specific Gal4 driver. Other details are as defined in the text and Methods.

Genotype	n	% Rhythmic	Period ± SEM
w^{1118};+/GD3018	13	100	23.57 ± 0.08
w^{1118};*tim*-Gal4/GD3018	16	100	24.4 ± 0.05
w^{1118};GD 3018/+;*tim*-Gal4/+	15	93	24.21 ± 0.16
w^{1118};GD3018/+;*pdf*-Gal4/+	15	100	24.13 ± 0.06
w^{1118};+/GD3116	13	92	23.92 ± 0.15
w^{1118};*tim*-Gal4/GD3116	16	94	24.5 ± 0.09
w^{1118};GD3116/+;*tim*-Gal4/+	9	78	24.36 ± 0.22
w^{1118};GD3116/+;*pdf*-Gal4/+	8	75	23.92 ± 0.18
w^{1118};+/GD7560	15	93	23.5 ± 0.0
w^{1118};*tim*-Gal4/GD7560	16	100	**24.66 ± 0.06**
w^{1118};GD7560/+;*tim*-Gal4/+	11	64	24.5 ± 0.27
w^{1118};GD7560/+;*pdf*-Gal4/+	10	100	24.35 ± 0.14
w^{1118};+/GD17123	16	94	23.5 ± 0
w^{1118};*tim*-Gal4/GD17123	16	81	24.08 ± 0.14
w^{1118};GD17123/+;*tim*-Gal4/+	15	100	24.0 ± 0.12
w^{1118};GD17123/+;*pdf*-Gal4/+	16	88	23.89 ± 0.13
w^{1118};+/GD17760	16	100	23.56 ± 0.04
w^{1118};*tim*-Gal4/GD17760	16	94	24.1 ± 0.11
w^{1118};GD17760/+;*tim*-Gal4/+	14	100	24.11 ± 0.14
w^{1118};GD17760/+;*pdf*-Gal4/+	13	85	23.86 ± 0.15
w^{1118};+/GD19078	16	100	23.5 ± 0.06
w^{1118};*tim*-Gal4/GD19078	16	100	23.81 ± 0.1
w^{1118};GD19078/+;*tim*-Gal4/+	16	88	24.36 ± 0.09
w^{1118};GD19078/+;*pdf*-Gal4/+	12	100	24.04 ± 0.11
w^{1118};+/GD21611	16	100	23.03 ± 0.03
w^{1118};*tim*-Gal4/GD21611	15	93	**24.64 ± 0.14**
w^{1118};GD21611/+;*tim*-Gal4/+	14	100	24.14 ± 0.16
w^{1118};GD21611/+;*pdf*-Gal4/+	16	100	23.66 ± 0.09
w^{1118};+/GD25317	14	100	23.71 ± 0.08
w^{1118};*tim*-Gal4/GD25317	14	100	**24.93 ± 0.09**
w^{1118};GD25317/+;*tim*-Gal4/+	15	93	24.39 ± 0.15
w^{1118};GD25317/+;*pdf*-Gal4/+	16	100	23.72 ± 0.09

Table 1 Continued

Genotype	n	% Rhythmic	Period ± SEM
w^{1118};+/GD26216	12	100	23.63 ± 0.13
w^{1118};*tim*-Gal4/GD26216	15	100	**24.9 ± 0.13**
w^{1118};GD26216/+;*tim*-Gal4/+	13	85	23.68 ± 0.12
w^{1118};GD26216/+;*pdf*-Gal4/+	15	100	24.3 ± 0.18
w^{1118};+/GD27232	16	100	23.5 ± 0.08
w^{1118};*tim*-Gal4/GD27232	16	100	24.41 ± 0.05
w^{1118};GD27232/+;*tim*-Gal4/+	8	75	24.5 ± 0.2
w^{1118};GD27232/+;*pdf*-Gal4/+	13	100	**24.54 ± 0.88**
w^{1118};+/GD32283	16	100	23.5 ± 0.04
w^{1118};*tim*-Gal4/GD32283	14	93	24.39 ± 0.23
w^{1118};GD32283/+;*tim*-Gal4/+	16	94	24.53 ± 0.1
w^{1118};GD32283/+;*pdf*-Gal4/+	14	93	24.0 ± 0.13
w^{1118};+/GD32956	16	94	23.9 ± 0.1
w^{1118};*tim*-Gal4/GD32956	15	93	24.54 ± 0.09
w^{1118};GD32956/+;*tim*-Gal4/+	14	**43**	24.58 ± 0.08
w^{1118};GD32956/+;*pdf*-Gal4/+	16	94	24.2 ± 0.08
w^{1118};+/GD35025	15	100	23.83 ± 0.1
w^{1118};*tim*-Gal4/GD35025	16	100	24.63 ± 0.08
w^{1118};GD35025/+;*tim*-Gal4/+	13	100	24.23 ± 0.12
w^{1118};GD35025/+;*pdf*-Gal4/+	16	100	24.34 ± 0.12
w^{1118};+/GD39175	16	100	23.88 ± 0.11
w^{1118};*tim*-Gal4/GD39175	15	93	23.71 ± 0.07
w^{1118};GD39175/+;*tim*-Gal4/+	15	80	24.25 ± 0.21
w^{1118};GD39175/+;*pdf*-Gal4/+	15	100	24.07 ± 0.13
w^{1118};+/GD40631	15	80	23.8 ± 0.09
w^{1118};*tim*-Gal4/GD40631	15	87	24.04 ± 0.17
w^{1118};GD40631/+;*tim*-Gal4/+	12	83	24.0 ± 0.14
w^{1118};GD40631/+;*pdf*-Gal4/+	15	100	23.97 ± 0.12
w^{1118};+/GD41912	16	100	23.69 ± 0.09
w^{1118};*tim*-Gal4/GD41912	15	100	24.57 ± 0.04
w^{1118};GD41912/+;*tim*-Gal4/+	15	80	24.04 ± 0.15
w^{1118};GD41912/+;*pdf*-Gal4/+	11	100	24.23 ± 0.16
w^{1118};+/GD41924	16	100	23.53 ± 0.03
w^{1118};*tim*-Gal4/GD41924	16	88	**25.14 ± 0.15**
w^{1118};GD41924/+;*tim*-Gal4/+	11	100	**24.73 ± 0.08**

Table 1 Continued

Genotype	n	% Rhythmic	Period ± SEM
w^{1118};GD41924/+;*pdf*-Gal4/+	14	93	**24.73 ± 0.08**
w^{1118};+/GD42051	14	86	23.71 ± 0.09
w^{1118};*tim*-Gal4/GD42051	16	100	**24.81 ± 0.06**
w^{1118};GD42051/+;*tim*-Gal4/+	16	94	**24.87 ± 0.11**
w^{1118};GD42051/+;*pdf*-Gal4/+	14	100	24.14 ± 0.12
w^{1118};+/GD42175	16	94	23.5 ± 0.0
w^{1118};*tim*-Gal4/GD42175	15	87	24.46 ± 0.21
w^{1118};GD42175/+;*tim*-Gal4/+	15	93	24.04 ± 0.11
w^{1118};GD42175/+;*pdf*-Gal4/+	16	100	24.06 ± 0.12
w^{1118};+/GD45415	15	93	23.78 ± 0.09
w^{1118};*tim*-Gal4/GD45415	15	100	24.67 ± 0.08
w^{1118};GD45415/+;*tim*-Gal4/+	15	80	24.33 ± 0.15
w^{1118};GD45415/+;*pdf*-Gal4/+	14	93	24.38 ± 0.10
w^{1118};+/GD46657	16	100	23.56 ± 0.06
w^{1118};*tim*-Gal4/GD46657	15	100	24.4 ± 0.1
w^{1118};GD46657/+;*tim*-Gal4/+	15	100	24.33 ± 0.12
w^{1118};GD46657/+;*pdf*-Gal4/+	15	100	24.1 ± 0.14
w^{1118};+/GD49671	15	100	23.7 ± 0.06
w^{1118};*tim*-Gal4/GD49671	30	-	-
w^{1118};GD49671/+;*tim*-Gal4/+	15	100	**26.13 ± 0.09**
w^{1118};GD49671/+;*pdf*-Gal4/+	16	94	**26.17 ± 0.20**
w^{1118};+/KK100076	16	100	23.5 ± 0.0
w^{1118};*tim*-Gal4/KK100076	14	**21**	**24.83 ± 0.14**
w^{1118};KK100076/+;*tim*-Gal4/+	13	69	**24.78 ± 0.29**
w^{1118};KK100076/+;*pdf*-Gal4/+	14	**14**	23.25 ± 0.18
w^{1118};+/KK100121	16	100	23.63 ± 0.07
w^{1118};*tim*-Gal4/KK100121	14	**29**	23.38 ± 0.13
w^{1118};KK100121/+;*tim*-Gal4/+	9	**0**	**AR**
w^{1118};KK100121/+;*pdf*-Gal4/+	15	**7**	23.5
w^{1118};+/KK100178	16	88	23.43 ± 0.05
w^{1118};*tim*-Gal4/KK100178	12	**0**	**AR**
w^{1118};KK100178/+;*tim*-Gal4/+	12	**33**	**25.88 ± 0.32**
w^{1118};KK100178/+;*pdf*-Gal4/+	12	**0**	**AR**
w^{1118};+/KK100216	16	94	23.5
w^{1118};*tim*-Gal4/KK100216	16	63	23.55 ± 0.05

Table 1 Continued

Genotype	n	% Rhythmic	Period ± SEM
w^{1118};KK100216/+;*tim*-Gal4/+	15	53	23.75 ± 0.15
w^{1118};KK100216/+;*pdf*-Gal4/+	14	100	23.61 ± 0.06
w^{1118};+/KK100283	15	100	23.07 ± 0.06
w^{1118};*tim*-Gal4/KK100283	16	81	23.89 ± 0.21
w^{1118};KK100283/+;*tim*-Gal4/+	14	93	24.04 ± 0.18
w^{1118};KK100283/+;*pdf*-Gal4/+	16	100	23.78 ± 0.11
w^{1118};+/KK100593	16	100	23.53 ± 0.03
w^{1118};*tim*-Gal4/KK100593	13	54	**25.21 ± 0.33**
w^{1118};KK100593/+;*tim*-Gal4/+	16	88	**25.46 ± 0.17**
w^{1118};KK100593/+;*pdf*-Gal4/+	13	**8**	23.5 ± 0.0
w^{1118};+/KK100914	16	100	23.53 ± 0.03
w^{1118};*tim*-Gal4/KK100914	16	100	23.78 ± 0.11
w^{1118};KK100914/+;*tim*-Gal4/+	15	80	23.5 ± 0.0
w^{1118};KK 100914/+;*pdf*-Gal4/+	16	100	23.53 ± 0.03
w^{1118};+/KK101257	28	89	23.5 ± 0.06
w^{1118};*tim*-Gal4/KK101257	15	**20**	**24.67 ± 0.44**
w^{1118};KK101257/+;*tim*-Gal4/+	13	**23**	**24.67 ± 0.17**
w^{1118};KK101257/+;*pdf*-Gal4/+	15	**40**	23.42 ± 0.08
w^{1118};+/KK101335	16	100	23.5 ± 0.0
w^{1118};*tim*-Gal4/KK101335	16	94	24.3 ± 0.12
w^{1118};KK101335/+;*tim*-Gal4/+	16	88	24.32 ± 0.53
w^{1118};KK101335/+;*pdf*-Gal4/+	16	88	23.75 ± 0.17
w^{1118};+/KK101406	15	87	23.42 ± 0.05
w^{1118};*tim*-Gal4/KK101406	16	88	24.2 ± 0.09
w^{1118};KK101406/+;*tim*-Gal4/+	15	53	**25.86 ± 0.23**
w^{1118};KK101406/+;*pdf*-Gal4/+	13	92	23.83 ± 0.09
w^{1118};+/KK101474	16	100	23.69 ± 0.09
w^{1118};*tim*-Gal4/KK101474	16	88	23.43 ± 0.16
w^{1118};KK101474/+;*tim*-Gal4/+	16	88	23.61 ± 0.14
w^{1118};KK101474/+;*pdf*-Gal4/+	14	100	23.57 ± 0.05
w^{1118};+/KK101547	16	94	23.47 ± 0.03
w^{1118};*tim*-Gal4/KK101547	14	**43**	**25.25 ± 0.35**
w^{1118};KK101547/+;*tim*-Gal4/+	16	**31**	**25.4 ± 0.17**
w^{1118};KK101547/+;*pdf*-Gal4/+	13	**23**	24.83 ± 0.59
w^{1118};+/KK101997	16	100	23.44 ± 0.04

Table 1 Continued

Genotype	n	% Rhythmic	Period ± SEM
w^{1118};*tim*-Gal4/KK101997	12	50	23.5 ± 0.2
w^{1118};KK101997/+;*tim*-Gal4/+	12	67	**24.81 ± 0.34**
w^{1118};KK101997/+;*pdf*-Gal4/+	10	**0**	**AR**
w^{1118};+/KK102021	16	100	23.47 ± 0.03
w^{1118};*tim*-Gal4/KK102021	15	93	24.21 ± 0.17
w^{1118};KK102021/+;*tim*-Gal4/+	14	64	23.78 ± 0.18
w^{1118};KK102021/+;*pdf*-Gal4/+	14	100	23.89 ± 0.18
w^{1118};+/KK102060	28	96	23.5 ± 0.03
w^{1118};*tim*-Gal4/KK102060	15	60	24.06 ± 0.18
w^{1118};KK102060/+;*tim*-Gal4/+	15	60	24.39 ± 0.14
w^{1118};KK102060/+;*pdf*-Gal4/+	13	92	23.92 ± 0.18
w^{1118};+/KK102071	25	100	23.53 ± 0.05
w^{1118};*tim*-Gal4/KK102071	15	67	23.55 ± 0.17
w^{1118};KK102071/+;*tim*-Gal4/+	16	75	24.00 ± 0.19
w^{1118};KK102071/+;*pdf*-Gal4/+	16	94	23.5 ± 0.05
w^{1118};+/KK102397	16	100	23.63 ± 0.07
w^{1118};*tim*-Gal4/KK102397	14	100	24.21 ± 0.11
w^{1118};KK102397/+;*tim*-Gal4/+	15	93	24.12 ± 0.14
w^{1118};KK102397/+;*pdf*-Gal4/+	15	80	23.54 ± 0.09
w^{1118};+/KK102474	15	100	23.73 ± 0.08
w^{1118};*tim*-Gal4/KK102474	16	100	24.59 ± 0.12
w^{1118};KK102474/+;*tim*-Gal4/+	14	93	23.73 ± 0.09
w^{1118};KK102474/+;*pdf*-Gal4/+	16	94	23.77 ± 0.08
w^{1118};+/KK102513	13	100	23.62 ± 0.1
w^{1118};*tim*-Gal4/KK102513	11	64	24.14 ± 0.17
w^{1118};KK102513/+;*tim*-Gal4/+	12	67	24.0 ± 0.18
w^{1118};KK102513/+;*pdf*-Gal4/+	12	100	23.58 ± 0.05
w^{1118};+/KK103044	16	81	23.38 ± 0.06
w^{1118};*tim*-Gal4/KK103044	16	75	23.71 ± 0.11
w^{1118};KK103044/+;*tim*-Gal4/+	15	67	**24.85 ± 0.1**
w^{1118};KK103044/+;*pdf*-Gal4/+	14	100	23.93 ± 0.07
w^{1118};+/KK103144	16	94	23.47 ± 0.06
w^{1118};*tim*-Gal4/KK103144	16	56	24.11 ± 0.27
w^{1118};KK103144/+;*tim*-Gal4/+	10	70	24.21 ± 0.32
w^{1118};KK103144/+;*pdf*-Gal4/+	13	92	23.88 ± 0.13

Table 1 Continued

Genotype	n	% Rhythmic	Period ± SEM
w^{1118};+/KK103317	16	100	23.53 ± 0.03
w^{1118};*tim*-Gal4/KK103317	16	94	23.83 ± 0.12
w^{1118};KK103317/+;*tim*-Gal4/+	12	100	23.96 ± 0.12
w^{1118};KK103317/+;*pdf*-Gal4/+	16	100	23.53 ± 0.05
w^{1118};+/KK103354	15	100	23.6 ± 0.05
w^{1118};*tim*-Gal4/KK103354	14	86	**24.88 ± 0.2**
w^{1118};KK103354/+;*tim*-Gal4/+	7	54	**25.0 ± 0.18**
w^{1118};KK103354/+;*pdf*-Gal4/+	12	**0**	**AR**
w^{1118};+/KK103357	15	100	23.57 ± 0.08
w^{1118};*tim*-Gal4/KK103357	12	**25**	23.83 ± 0.27
w^{1118};KK103357/+;*tim*-Gal4/+	13	**8**	**25.0 ± 0.0**
w^{1118};KK103357/+;*pdf*-Gal4/+	10	**0**	**AR**
w^{1118};+/KK103627	16	100	23.34 ± 0.06
w^{1118};*tim*-Gal4/KK103627	15	73	24.05 ± 0.22
w^{1118};KK103627/+;*tim*-Gal4/+	15	93	**25.32 ± 0.14**
w^{1118};KK103627/+;*pdf*-Gal4/+	13	**8**	**26.5**
w^{1118};+/KK103740	16	94	23.4 ± 0.05
w^{1118};*tim*-Gal4/KK103740	16	88	23.54 ± 0.03
w^{1118};KK103740/+;*tim*-Gal4/+	15	87	23.77 ± 0.14
w^{1118};KK103740/+;*pdf*-Gal4/+	16	100	23.5 ± 0.0
w^{1118};+/KK104081	11	100	23.5 ± 0.0
w^{1118};*tim*-Gal4/KK104081	16	100	23.63 ± 0.07
w^{1118};KK104081/+;*tim*-Gal4/+	16	88	23.61 ± 0.08
w^{1118};KK104081/+;*pdf*-Gal4/+	16	94	23.73 ± 0.09
w^{1118};+/KK104167	13	54	23.14 ± 0.09
w^{1118};*tim*-Gal4/KK104167	15	87	23.85 ± 0.14
w^{1118};KK104167/+;*tim*-Gal4/+	12	75	23.89 ± 0.2
w^{1118};KK104167/+;*pdf*-Gal4/+	16	94	23.8 ± 0.13
w^{1118};+/KK104211	15	93	23.42 ± 0.04
w^{1118};*tim*-Gal4/KK104211	14	**29**	**24.88 ± 0.52**
w^{1118};KK104211/+;*tim*-Gal4/+	12	58	**25.14 ± 0.37**
w^{1118};KK104211/+;*pdf*-Gal4/+	12	**8**	**25.5**
w^{1118};+/KK104374	14	86	23.5
w^{1118};*tim*-Gal4/KK104374	16	88	23.46 ± 0.04
w^{1118};KK104374/+;*tim*-Gal4/+	14	93	24.00 ± 0.17

Table 1 Continued

Genotype	n	% Rhythmic	Period ± SEM
w^{1118};KK104374/+;*pdf*-Gal4/+	15	100	24.03 ± 0.06
w^{1118};+/KK104427	16	94	23.57 ± 0.12
w^{1118};*tim*-Gal4/KK104427	13	**0**	**AR**
w^{1118};KK104427/+;*tim*-Gal4/+	13	54	**25 ± 0.68**
w^{1118};KK104427/+;*pdf*-Gal4/+	10	**10**	23.5
w^{1118};+/KK104452	16	100	23.5 ± 0.04
w^{1118};*tim*-Gal4/KK104452	16	**44**	**25.29 ± 0.33**
w^{1118};KK104452/+;*tim*-Gal4/+	15	67	24.35 ± 0.21
w^{1118};KK104452/+;*pdf*-Gal4/+	13	**15**	23.25 ± 0.18
w^{1118};+/KK104677	15	100	23.5 ± 0.0
w^{1118};*tim*-Gal4/KK104677	16	94	24.5 ± 0.0
w^{1118};KK104677/+;*tim*-Gal4/+	16	100	23.97 ± 0.13
w^{1118};KK104677/+;*pdf*-Gal4/+	16	100	24.31 ± 0.08
w^{1118};+/KK104729	16	88	23.29 ± 0.07
w^{1118};*tim*-Gal4/KK104729	13	69	23.61 ± 0.07
w^{1118};KK104729/+;*tim*-Gal4/+	11	91	23.7 ± 0.08
w^{1118};KK104729/+;*pdf*-Gal4/+	16	94	23.8 ± 0.12
w^{1118};+/KK104761	15	100	23.53 ± 0.03
w^{1118};*tim*-Gal4/KK104761	12	**17**	**24.75 ± 0.18**
w^{1118};KK104761/+;*tim*-Gal4/+	13	54	**25.43 ± 0.34**
w^{1118};KK104761/+;*pdf*-Gal4/+	8	**0**	**AR**
w^{1118};+/KK104774	15	100	23.47 ± 0.03
w^{1118};*tim*-Gal4/KK104774	15	93	24.18 ± 0.14
w^{1118};KK104774/+;*tim*-Gal4/+	14	86	**24.63 ± 0.24**
w^{1118};KK104774/+;*pdf*-Gal4/+	8	88	23.36 ± 0.09
w^{1118};+/KK104785	16	100	23.03 ± 0.03
w^{1118};*tim*-Gal4/KK104785	16	100	23.94 ± 0.13
w^{1118};KK104785/+;*tim*-Gal4/+	16	100	23.97 ± 0.11
w^{1118};KK104785/+;*pdf*-Gal4/+	16	94	23.7 ± 0.15
w^{1118};+/KK104860	16	100	23.5 ± 0.0
w^{1118};*tim*-Gal4/KK104860	13	92	24.25 ± 0.14
w^{1118};KK104860/+;*tim*-Gal4/+	15	80	**24.83 ± 0.31**
w^{1118};KK104860/+;*pdf*-Gal4/+	16	81	23.62 ± 0.11
w^{1118};+/KK104884	16	90	23.37 ± 0.04
w^{1118};*tim*-Gal4/KK104884	15	**33**	**24.4 ± 0.4**

Table 1 Continued

Genotype	n	% Rhythmic	Period ± SEM
w^{1118};KK104884/+;*tim*-Gal4/+	12	67	**25.44 ± 0.18**
w^{1118};KK104884/+;*pdf*-Gal4/+	11	**27**	24.00 ± 0.41
w^{1118};+/KK105122	16	88	23.46 ± 0.03
w^{1118};*tim*-Gal4/KK105122	16	94	23.83 ± 0.12
w^{1118};KK105122/+;*tim*-Gal4/+	16	100	23.69 ± 0.12
w^{1118};KK105122/+;*pdf*-Gal4/+	15	100	24.07 ± 0.16
w^{1118};+/KK105249	16	100	23.33 ± 0.04
w^{1118};*tim*-Gal4/KK105249	16	**31**	24.2 ± 0.3
w^{1118};KK105249/+;*tim*-Gal4/+	13	62	**25.56 ± 0.2**
w^{1118};KK105249/+;*pdf*-Gal4/+	16	100	23.78 ± 0.08
w^{1118};+/KK105399	13	100	23.65 ± 0.05
w^{1118};*tim*-Gal4/KK105399	12	**25**	23.17 ± 0.17
w^{1118};KK105399/+;*tim*-Gal4/+	7	**0**	**AR**
w^{1118};KK105399/+;*pdf*-Gal4/+	9	78	23.0 ± 0.25
w^{1118};+/KK105483	16	100	23.5 ± 0.0
w^{1118};*tim*-Gal4/KK105483	16	88	23.89 ± 0.10
w^{1118};KK105483/+;*tim*-Gal4/+	16	94	23.73 ± 0.13
w^{1118};KK105483/+;*pdf*-Gal4/+	13	100	24.5 ± 0.13
w^{1118};+/KK105484	13	77	23.25 ± 0.08
w^{1118};*tim*-Gal4/KK105484	16	50	23.69 ± 0.26
w^{1118};KK105484/+;*tim*-Gal4/+	14	**29**	23.63 ± 0.27
w^{1118};KK105484/+;*pdf*-Gal4/+	15	100	23.9 ± 0.05
w^{1118};+/KK105525	16	100	23.57 ± 0.05
w^{1118};*tim*-Gal4/KK105525	10	50	**25.2 ± 0.34**
w^{1118};KK105525/+;*tim*-Gal4/+	13	85	**25.5 ± 0.13**
w^{1118};KK105525/+;*pdf*-Gal4/+	16	94	**24.73 ± 0.12**
w^{1118};+/KK105565	14	100	23.5
w^{1118};*tim*-Gal4/KK105565	15	53	23.63 ± 0.08
w^{1118};KK105565/+;*tim*-Gal4/+	16	56	23.56 ± 0.05
w^{1118};KK105565/+;*pdf*-Gal4/+	11	55	23.47 ± 0.06
w^{1118};+/KK105568	16	100	23.5 ± 0
w^{1118};*tim*-Gal4/KK105568	16	56	24.28 ± 0.12
w^{1118};KK105568/+;*tim*-Gal4/+	14	71	23.9 ± 0.19
w^{1118};KK105568/+;*pdf*-Gal4/+	12	92	23.68 ± 0.1
w^{1118};+/KK105674	16	100	23.47 ± 0.03

Table 1 Continued

Genotype	n	% Rhythmic	Period ± SEM
w^{1118};*tim*-Gal4/KK105674	16	100	24.19 ± 0.12
w^{1118};KK105674/+;*tim*-Gal4/+	16	100	23.97 ± 0.13
w^{1118};KK105674/+;*pdf*-Gal4/+	16	100	23.5 ± 0.0
w^{1118};+/KK105752	13	92	23.38 ± 0.06
w^{1118};*tim*-Gal4/KK105752	16	**19**	**25.5 ± 0.62**
w^{1118};KK105752/+;*tim*-Gal4/+	15	**47**	**25.14 ± 0.13**
w^{1118};KK105752/+;*pdf*-Gal4/+	4	**0**	**AR**
w^{1118};+/KK106098	16	100	23.53 ± 0.03
w^{1118};*tim*-Gal4/KK106098	16	69	24.14 ± 0.27
w^{1118};KK106098/+;*tim*-Gal4/+	16	94	**25.07 ± 0.15**
w^{1118};KK106098/+;*pdf*-Gal4/+	13	54	24.0 ± 0.49
w^{1118};+/KK106180	16	94	23.5 ± 0.05
w^{1118};*tim*-Gal4/KK106180	14	**14**	**24.75 ± 0.18**
w^{1118};KK106180/+;*tim*-Gal4/+	15	73	**24.64 ± 0.27**
w^{1118};KK106180/+;*pdf*-Gal4/+	16	**13**	23.25 ± 0.18
w^{1118};+/KK106253	16	100	23.53 ± 0.03
w^{1118};*tim*-Gal4/KK106253	11	100	24.36 ± 0.15
w^{1118};KK106253/+;*tim*-Gal4/+	4	100	23.75 ± 0.22
w^{1118};KK106253/+;*pdf*-Gal4/+	16	100	23.47 ± 0.03
w^{1118};+/KK107057	31	87	23.48 ± 0.06
w^{1118};*tim*-Gal4/KK107057	16	50	**22.25 ± 0.34**
w^{1118};KK107057/+;*tim*-Gal4/+	12	**42**	**22.3 ± 0.34**
w^{1118};KK107057/+;*pdf*-Gal4/+	16	81	23.65 ± 0.14
w^{1118};+/KK107386	8	100	23.5 ± 0.0
w^{1118};*tim*-Gal4/KK107386	12	100	24.04 ± 0.12
w^{1118};KK107386/+;*tim*-Gal4/+	11	100	23.68 ± 0.16
w^{1118};KK107386/+;*pdf*-Gal4/+	15	100	23.57 ± 0.04
w^{1118};+/KK107621	16	100	23.56 ± 0.04
w^{1118};*tim*-Gal4/KK107621	16	81	23.65 ± 0.09
w^{1118};KK107621/+;*tim*-Gal4/+	16	100	23.66 ± 0.07
w^{1118};KK107621/+;*pdf*-Gal4/+	15	100	23.63 ± 0.1
w^{1118};+/KK107770	15	100	23.43 ± 0.04
w^{1118};*tim*-Gal4/KK107770	16	100	23.44 ± 0.08
w^{1118};KK107770/+;*tim*-Gal4/+	16	94	23.63 ± 0.07
w^{1118};KK107770/+;*pdf*-Gal4/+	15	93	23.43 ± 0.05

Table 1 Continued

Genotype	n	% Rhythmic	Period ± SEM
w^{1118};+/KK107996	16	100	23.53 ± 0.03
w^{1118};*tim*-Gal4/KK107996	12	**25**	24.17 ± 0.27
w^{1118};KK107996/+;*tim*-Gal4/+	16	**0**	**AR**
w^{1118};KK107996/+;*pdf*-Gal4/+	13	**0**	**AR**
w^{1118};+/KK107998	16	100	23.5 ± 0.0
w^{1118};*tim*-Gal4/KK107998	15	93	24.07 ± 0.1
w^{1118};KK107998/+;*tim*-Gal4/+	15	100	24.3 ± 0.15
w^{1118};KK107998/+;*pdf*-Gal4/+	16	100	23.44 ± 0.04
w^{1118};+/KK108071	16	100	23.5 ± 0.0
w^{1118};*tim*-Gal4/KK108071	16	88	24.11 ± 0.13
w^{1118};KK108071/+;*tim*-Gal4/+	16	100	23.66 ± 0.09
w^{1118};KK108071/+;*pdf*-Gal4/+	16	100	23.5 ± 0.0
w^{1118};+/KK108352	15	100	23.6 ± 0.05
w^{1118};*tim*-Gal4/KK108352	16	100	24.41 ± 0.08
w^{1118};KK108352/+;*tim*-Gal4/+	16	94	24.23 ± 0.09
w^{1118};KK108352/+;*pdf*-Gal4/+	15	87	23.62 ± 0.08
w^{1118};+/KK108505	16	100	23.5 ± 0.0
w^{1118};*tim*-Gal4/KK108505	13	92	23.71 ± 0.11
w^{1118};KK108505/+;*tim*-Gal4/+	16	100	23.56 ± 0.04
w^{1118};KK108505/+;*pdf*-Gal4/+	16	100	23.75 ± 0.09
w^{1118};+/KK108629	16	100	23.47 ± 0.03
w^{1118};*tim*-Gal4/KK108629	16	100	24.34 ± 0.13
w^{1118};KK108629/+;*tim*-Gal4/+	15	100	23.83 ± 0.15
w^{1118};KK108629/+;*pdf*-Gal4/+	16	88	23.68 ± 0.11
w^{1118};+/KK108744	15	87	23.38 ± 0.1
w^{1118};*tim*-Gal4/KK108744	14	86	24.00 ± 0.12
w^{1118};KK108744/+;*tim*-Gal4/+	15	**47**	24.29 ± 0.14
w^{1118};KK108744/+;*pdf*-Gal4/+	16	81	23.73 ± 0.14
w^{1118};+/KK108802	14	100	23.54 ± 0.03
w^{1118};*tim*-Gal4/KK108802	14	93	24.00 ± 0.09
w^{1118};KK108802/+;*tim*-Gal4/+	16	81	24.15 ± 0.14
w^{1118};KK108802/+;*pdf*-Gal4/+	15	93	23.79 ± 0.07
w^{1118};+/KK108859	15	80	23.46 ± 0.09
w^{1118};*tim*-Gal4/KK108859	16	75	23.86 ± 0.13
w^{1118};KK108859/+;*tim*-Gal4/+	12	83	**24.71 ± 0.23**

Table 1 Continued

Genotype	n	% Rhythmic	Period ± SEM
w^{1118};KK108859/+;*pdf*-Gal4/+	15	100	23.8 ± 0.09
w^{1118};+/KK108888	16	100	23.72 ± 0.08
w^{1118};*tim*-Gal4/KK108888	16	94	23.7 ± 0.14
w^{1118};KK108888/+;*tim*-Gal4/+	16	94	23.67 ± 0.09
w^{1118};KK108888/+;*pdf*-Gal4/+	16	94	23.7 ± 0.1
w^{1118};+/KK109147	16	100	23.75 ± 0.06
w^{1118};*tim*-Gal4/KK109147	14	**14**	23.5 ± 0.0
w^{1118};KK109147/+;*tim*-Gal4/+	11	**18**	**24.75 ± 0.18**
w^{1118};KK109147/+;*pdf*-Gal4/+	12	67	**25.06 ± 0.78**
w^{1118};+/KK109622	16	94	23.53 ± 0.03
w^{1118};*tim*-Gal4/KK109622	16	100	**24.5 ± 0.13**
w^{1118};KK109622/+;*tim*-Gal4/+	12	75	24.06 ± 0.17
w^{1118};KK109622/+;*pdf*-Gal4/+	16	94	23.6 ± 0.1
w^{1118};+/KK109858	16	100	23.5 ± 0
w^{1118};*tim*-Gal4/KK109858	11	**45**	24.08 ± 0.27
w^{1118};KK109858/+;*tim*-Gal4/+	10	**10**	23.5
w^{1118};KK109858/+;*pdf*-Gal4/+	11	**0**	**AR**
w^{1118};+/KK109898	16	100	23.44 ± 0.04
w^{1118};*tim*-Gal4/KK109898	15	**47**	23.64 ± 0.17
w^{1118};KK109898/+;*tim*-Gal4/+	13	62	**25.75 ± 0.27**
w^{1118};KK109898/+;*pdf*-Gal4/+	12	**42**	23.4 ± 0.09
w^{1118};+/KK110167	16	100	23.5 ± 0.0
w^{1118};*tim*-Gal4/KK110167	16	94	23.7 ± 0.1
w^{1118};KK110167/+;*tim*-Gal4/+	15	87	23.73 ± 0.21
w^{1118};KK110167/+;*pdf*-Gal4/+	13	85	23.45 ± 0.04
w^{1118};+/KK110360	16	88	23.4 ± 0.07
w^{1118};*tim*-Gal4/KK110360	14	93	24.00 ± 0.08
w^{1118};KK110360/+;*tim*-Gal4/+	16	100	23.75 ± 0.1
w^{1118};KK110360/+;*pdf*-Gal4/+	16	81	23.81 ± 0.27
w^{1118};+/KK110443	16	100	23.59 ± 0.05
w^{1118};*tim*-Gal4/KK110443	15	73	24.05 ± 0.25
w^{1118};KK110443/+;*tim*-Gal4/+	13	69	**25.28 ± 0.26**
w^{1118};KK110443/+;*pdf*-Gal4/+	14	71	23.55 ± 0.22
w^{1118};+/KK110595	16	100	23.72 ± 0.12
w^{1118};*tim*-Gal4/KK110595	12	67	24.42 ± 0.08

Table 1 Continued

Genotype	n	% Rhythmic	Period ± SEM
w^{1118};KK110595/+;*tim*-Gal4/+	16	63	24.7 ± 0.08
w^{1118};KK110595/+;*pdf*-Gal4/+	5	80	24.5 ± 0.31
w^{1118};+/KK110661	16	100	23.53 ± 0.03
w^{1118};*tim*-Gal4/KK110661	14	86	24.04 ± 0.18
w^{1118};KK110661/+;*tim*-Gal4/+	16	94	23.63 ± 0.09
w^{1118};KK110661/+;*pdf*-Gal4/+	16	100	24.44 ± 0.09
w^{1118};+/KK110786	16	100	23.5 ± 0.0
w^{1118};*tim*-Gal4/KK110786	16	88	**25.36 ± 0.08**
w^{1118};KK110786/+;*tim*-Gal4/+	16	94	**25.37 ± 0.11**
w^{1118};KK110786/+;*pdf*-Gal4/+	14	**7**	**27.0 ± 0.0**

Based on our criteria, candidate phosphatases that mediate *Drosophila* clock function include: *mts* (GD41924), *Pp2A-29B* (GD49671), CG3788 (KK100076), *IPP-2* (KK100121), CG17746 (KK100178), *Gbs-70E* (KK100593), *Ppm1* (KK101257), *I-2* (KK101547), CG7115 (KK103354), *Cep97* (KK103357), *PpD6* (KK104211), *Ptpmeg2* (KK104427), *Ptp69D* (KK104761), *MAPK PPase4* (KK104884), *PP1α-96A* (KK105525), CG14903 (KK105752), CG10417 (KK106180), *Lar* (KK107996), *Pp1-Y2* (KK109147), *Can A at 14F* (KK109858), *Laza* (KK109898) and CG3530 (KK110786). The efficacy and specificity of RNAi mediated knockdown of these candidate 'clock phosphatases' was then validated by testing RNAi lines that target another region of the mRNA and/or other genetic reagents (i.e. transposon inserts, overexpression strains and existing loss of function mutants) for activity rhythm defects. In addition, CRISPR technology was used to generate mutants for one candidate phosphatase that lacked loss of function mutants. For each candidate circadian protein phosphatase, I have provided a

description of the protein, its known function, and the results for the genetic reagents used to validate RNAi below.

Table 2: Activity rhythms of the independent genetic reagents tested for the different candidate clock phosphatases identified in the RNAi screen. Other details are as defined in Table 1 and Methods.

Genotype	n	% Rhythmic	Period ± SEM
w^{1118};+/GD35171	43	100	23.73 ± 0.04
w^{1118};*tim*-Gal4/GD35171	16	94	24.43 ± 0.08
w^{1118};GD35171/+;*tim*-Gal4/+	11	91	24.5 ± 0.19
w^{1118};GD35171/+;*pdf*-Gal4/+	15	93	23.82 ± 0.07
w^{1118};;UAS-*mts*/+	12	100	23.5 ± 0.0
w^{1118};*tim*-Gal4/+;UAS-*mts*/+	8	**0**	**AR**
w^{1118};;UAS-*mts*/*pdf*-Gal4	14	**43**	23.3 ± 0.18
w^{1118};P{EP}*Pp2A-29B*^{EP2332}/+	16	100	23.63 ± 0.05
w^{1118};P{EP}*Pp2A-29B*^{EP2332}/*tim*-Gal4	15	100	23.9 ± 0.13
w^{1118};P{RS3}*Pp2A-29B*$^{CB-5426-3}$	16	88	23.57 ± 0.05
w^{1118};PBac{WH}CG17746^{f05041}	11	91	23.3 ± 0.08
$y^{1}w^{*}$;P{EP}CG17746^{G4827}	16	94	23.53 ± 0.06
$y^{1}w^{1118}$;PBac{3HPy^{+}}*I-2*^{C362}	14	100	23.75 ± 0.13
w^{*};P{UAS-*I-2*.HA}G/+;P{UAS-*Pp1-87B*.HA}H-1/+	15	100	23.67 ± 0.11
w^{*};P{UAS-*I-2*.HA}G/*tim*-Gal4;P{UAS-*Pp1-87B*.HA}H-1/+	15	87	24.15 ± 0.15
w^{*};P{UAS-*I-2*.HA}G/+;P{UAS-*Pp1-87B*.HA}H-1/*pdf*-Gal4	9	100	24.22 ± 0.11
$y^{1}w^{67c23}$;P{SUPor-P}CG7115^{KG02655}	12	75	23.5 ± 0.14
w^{1118};UAS-*Cep97*/+	15	100	24.27 ± 0.14
w^{1118};UAS-*Cep97*/*tim*-Gal4	9	100	24.28 ± 0.08
w^{1118};UAS-*Cep97*/+;*pdf*-Gal4/+	13	100	24.67 ± 0.54
UAS-*Cep97*/Y	14	93	23.38 ± 0.06
UAS-*Cep97*/Y;*tim*-Gal4/+	15	60	23.83 ± 0.11
UAS-*Cep97*/Y;;*pdf*-Gal4/+	13	85	23.59 ± 0.06
w^{1118};;UAS-*Cep97*/+	15	100	23.5 ± 0.0
w^{1118};*tim*-Gal4/+;UAS-*Cep97*/+	16	100	23.97 ± 0.1
w^{1118};;UAS-*Cep97*/*pdf*-Gal4	16	100	24.31 ± 0.1

Table 2 Continued

Genotype	n	% Rhythmic	Period ± SEM
y^{1};P{SUPor-P}tocKG08989*PpD6*^{KG08989}	11	100	23.68 ± 0.12
$y^{1}w$*Mi{MIC}*Ptpmeg2*^{MI03011}/Y	15	100	23.73 ± 0.08
w^{67c23}P{lacW}*Ptpmeg2*^{G0232}/Y	16	63	24.65 ± 0.21
$y^{1}w^{67c23}$P{Mae-UAS.6.11}*Ptpmeg2*^{GG01129}/Y	16	94	23.57 ± 0.07
$y^{1}w^{67c23}$P{Mae-UAS.6.11}*Ptpmeg2*^{GG01129}/Y;*tim*-Gal4/+	10	90	24.22 ± 0.19
$y^{1}w^{67c23}$P{Mae-UAS.6.11}*Ptpmeg2*^{GG01129}/Y;;*pdf*-Gal4/+	15	100	23.8 ± 0.09
w^{1118}PBac{WH}*Ptpmeg2*^{f06600};l(2)*/+	13	100	23.62 ± 0.11
*w**;;*Ptp69D*^{1}	8	88	**26.57 ± 0.21**
*w**;;Df(3L)8ex25	10	60	**26.5 ± 00**
w^{1118};;*Ptp69D*^{10}	15	93	**26.96 ± 0.14**
w^{1118};;*Ptp69D*^{18}	16	50	**27.19 ± 0.15**
w^{1118};;*Ptp69D*^{20}	10	100	23.6 ± 0.06
w^{1118};;*Ptp69D*^{21}	16	100	23.53 ± 0.3
w^{1118};;UAS-*Ptp69D*/+	9	89	24.19 ± 0.22
w^{1118};;UAS-*Ptp69D*/*pdf*-Gal4	12	67	24.13 ± 0.19
w^{1118};;*tim*-Gal4/+;UAS-*Ptp69D*/+	12	92	**27.82 ± 0.28**
w^{1118};;UAS-DN*Ptp69D*/+	15	100	23.47 ± 0.09
w^{1118};;UAS-DN*Ptp69D*/*pdf*-Gal4	8	63	**27.2 ± 0.18**
w^{1118};;*tim*-Gal4/+;UAS-DN*Ptp69D*/+	15	100	23.5 ± 0.05
w^{1118};;*Ptp69D*$^{1}_{iso}$	8	100	23.44 ± 0.06
y^{1}P{SUPor-P}*MKP-4*^{KG03420}	13	100	24.23 ± 0.12
w^{1118};;P{GSV6}*Pp1α-96A*^{GS11179}/+	16	100	23.59 ± 0.08
w^{1118};*tim*-Gal4/+;P{GSV6}*Pp1α-96A*^{GS11179}/+	16	**25**	24.13 ± 0.21
w^{1118};;P{GSV6}*Pp1α-96A*^{GS11179}/*pdf*-Gal4	9	67	23.67 ± 0.15
w^{1118};;*PP1α-96A*^{2}/+	16	94	23.77 ± 0.12
w^{1118};;UAS-*PP1α-96A*.HA/+	16	100	23.38 ± 0.05
w^{1118};*tim*-Gal4/+;UAS-*PP1α-96A*.HA/+	16	94	23.87 ± 0.11
w^{1118};;UAS-*PP1α-96A*.HA/*pdf*-Gal4	16	94	23.33 ± 0.08
w^{1118};;*PP1α96A*-CRISPRmutant-1/+	17	82	23.52 ± 0.07
w^{1118};;*PP1α96A*-CRISPRmutant-2/+	13	92	23.58 ± 0.05
w^{1118};;*PP1α96A*-CRISPRmutant-3/+	9	100	23.44 ± 0.05
w^{1118};UAS-CG10417/+	16	100	23.44 ± 0.04
w^{1118};UAS-CG10417/*tim*-Gal4	14	100	**24.96 ± 0.09**
w^{1118};UAS-CG10417/+;*pdf*-Gal4/+	16	100	**24.97 ± 0.03**
*w**;*Lar*$^{13.2}$/+	14	93	23.54 ± 0.04

Table 2 Continued

Genotype	n	% Rhythmic	Period ± SEM
Df(2L)TW84,l(2)74i^{1},amos^{Tft}*Lar*^{TW84}/+	14	86	23.71 ± 0.11
Df(2L)E55,rdo^{1}hook^{1}*Lar*^{E55}pr^{1}/+	16	88	24.32 ± 0.08
w^{1118};;UAS-*Lar*/+	14	100	23.57 ± 0.04
w^{1118};*tim*-Gal4/+;UAS-*Lar*/+	15	93	24.06 ± 0.07
w^{1118};;UAS-*Lar*/*pdf*-Gal4	16	75	24.17 ± 0.07
w^{1118};*Lar*Df(2L)E55/*Lar*$^{13.2}$;+	14	0	**AR**
w^{1118};UAS-*CanA14F*myc/+	16	75	24.5 ± 0.2
w^{1118};UAS-*CanA14F*myc/*tim*-Gal4	16	63	23.6 ± 0.1
w^{1118};UAS-*CanA14F*myc/+;*pdf*-Gal4/+	15	100	24.03 ± 0.1
w^{1118};;UAS-*CanA14F*act-myc/+	9	100	23.94 ± 0.11
w^{1118};*tim*-Gal4/+;UAS-*CanA14F*act-myc/+	15	**0**	**AR**
w^{1118};;UAS-*CanA14F*act-myc/*pdf*-Gal4	16	94	**25.03 ± 0.15**
CanA14F-KO/Y	15	**13**	**25.0 ± 0.0**
CanA14F-KO$_{iso}$/Y	16	94	23.67 ± 0.08

Microtubule Star (MTS), GD41924: MTS is the catalytic subunit of protein phosphatase 2a (PP2A), which dephosphorylates proteins at serine and threonine residues. It functions in many cellular process including the mitotic cell cycle, cell surface receptor signaling and cell adhesion (Janssens and Goris, 2001; Chen et al., 2007). Importantly it is also known to play a role in regulating *Drosophila* circadian clocks (Fang et al., 2007; Andreazza et al., 2015). Behavioral analysis of an additional RNAi line that targeted another region of the mRNA did not validate the initial screen phenotype emphasizing the importance of validating RNAi phenotypes using independent genetic reagents. Indeed, overexpression of *mts* (UAS-*mts*) using clock cell-

specific Gal4 drivers disrupted activity rhythms, thus validating the RNAi screen results (Table 2).

Protein phosphatase 2A at 29B (PP2A-29B), GD49671: PP2A-29B is a protein phosphatase type 2A regulatory subunit. It functions in many cellular processes including chromosome segregation, centriole assembly, and phagocytosis (Stroschein-Stevenson et al., 2006; Dobbelaere et al., 2008). I tested additional P element transposon inserts to independently validate the RNAi phenotype, but activity rhythms were not altered (Table 2).

Protein phosphatase inhibitor 2 (IPP-2), KK100121: IPP-2 is a protein phosphatase inhibitor. It functions to regulate signal transduction and phosphoprotein phosphatase pathways. Although the phenotype of this RNAi knockdown was strongly arrhythmic, no other genetic reagents were available to confirm the RNAi phenotype.

CG17746, KK100178: CG17746 is a member of the protein phosphatase 2C family, which contains cation binding domains and dephosphorylate proteins at serine and threonine residues. I tested additional P element transposon inserts for activity rhythms, but these reagents did not validate the RNAi phenotype (Table 2).

Glycogen binding subunit 70E (Gbs-70E), KK100593: Gbs-70E is a protein phosphatase 1 regulatory subunit with a carbohydrate binding type-21 (CBM21) domain. It functions in regulation of glycogen metabolic process (Kerekes et al., 2014). However, there are no additional genetic reagents available for this gene to validate the arrhythmic RNAi phenotype.

Metal-dependent protein phosphatase 1 (PPM1), KK101257: PPM1 is a protein phosphatase, Mg^{+2}/Mn^{+2} dependent (PPM type), member of the protein phosphatase 2C family that dephosphorylates proteins at serine and threonine residues. There are no known cellular functions described for this phosphatase, and no additional genetic reagents were available to validate the RNAi phenotype.

Protein phosphatase inhibitor 2 (I-2), KK101547: I-2 is a protein phosphatase inhibitor that has protein phosphatase 1 binding activity (Sami et al., 2011). Behavioral analysis of P element transposon insert and overexpression (UAS-*I-2*) driven with clock cell-specific Gal4 drivers did not reproduce the defect in activity rhythms seen with RNAi knockdown (Table 2).

CG7115, KK103354: CG7115 is a PPM-type member of the protein phosphatase 2C family that dephosphorylates proteins at serine and threonine residues. It functions in many cellular processes including cell adhesion and regulation of cell shape (Sopko et al., 2014). I tested the only available P element insert to validate the long period/arrhythmicity associated with RNAi knockdown, but activity rhythms in this strain were not altered (Table 2).

Cep97, KK103357: Cep97 is a protein phosphatase type 1 regulator with characteristic leucine-rich repeat domain. It functions in centriole replication (Dobbelaere et al., 2008). Behavioral analysis of *Cep97* overexpression (UAS-*Cep97*) using clock cell-specific Gal4 drivers did not alter activity rhythms (Table 2).

Protein phosphatase D6 (PPD6), KK104211: PPD6 is a protein phosphatase that dephosphorylates proteins at serine and threonine residues. There are no known cellular

functions described for this phosphatase. I tested the only available P element transposon insert for this gene, but activity rhythms in this strain were not altered (Table 2).

Protein tyrosine phosphatase Meg2 (Ptpmeg2), KK104427: Ptpmeg2 also known as *lethal-1-G0232*, is a non-membrane spanning protein tyrosine phosphatase. It functions in many cellular processes including phagocytosis, neurogenesis and cell migration (Stroschein-Stevenson et al., 2006; Chen et al., 2012). I tested the available *Ptpmeg2* P element transposon insert lines and clock cell-specific *Ptpmeg2* overexpression strains, but none of these genetic reagents altered activity rhythms (Table 2).

Protein tyrosine phosphatase 69D (Ptp69D), KK104761: Ptp69D is a protein tyrosine phosphatase with characteristic Fibronectin type III, Immunoglobulin subtype, and tyrosine specific protein phosphatase domains. It is a transmembrane receptor protein tyrosine phosphatase that functions in many cellular processes including dendrite morphogenesis, axon guidance, and fasciculation-defasciculation of neuron axons (Desai et al., 1996; Desai and Purdy, 2003). When I tested additional reagents, including loss of function mutants and dominant negative for *Ptp69D*, many showed an even longer period phenotype compared to the RNAi, while others showing no phenotype (Table 2). When *Ptp69D* mutants that showed a long period were isogenized with wild-type (w^{1118}) or paired with a wild-type X chromosome, the long period phenotype was lost (Table 2). Upon further analysis, I confirmed that the long period (~26.5 h) phenotype was due to the per^{SLIH} allele (Hamblen et al., 1998), a naturally occurring *per* variant.

MAPK Phosphatase 4 (MAPK PPase4), KK104884: MAPK PPase4 is a dual specificity protein phosphatase that dephosphorylates proteins at tyrosine, serine and threonine residues. Its known cellular function is in negative regulation of JUN kinase activity (Sun et al., 2008). I tested additional P element transposon inserts to independently validate the RNAi phenotype, but activity rhythms were not altered (Table 2).

Protein phosphatase 1α at 96A (PP1α-96A), KK105525: PP1α-96A is a protein phosphatase, part of the PP-1 subfamily that dephosphorylates proteins at serine and threonine residues. It functions in many cellular processes including positive regulation of canonical Wnt signaling pathway and innate immune response (Schertel et al., 2013). Importantly PP-1 subfamily is known to play a role in regulating *Drosophila* circadian clocks (Sathyanarayanan et al., 2004). However, none of the available *PP1α-96A* P element inserts or clock cell-specific *PP1α-96A* overexpression strains altered activity rhythms (Table 2). Given the involvement of PP1 in *Drosophila* circadian clocks, I wanted to test loss of function mutants. Therefore, I used CRISPR/Cas9 system to generate three *PP1α-96A* deletion mutants (See Methods and figure on page 55). Unfortunately, none of these mutants were homozygous viable as adults, and, heterozygotes did not display altered activity rhythms (Table 2).

CG10417, KK106180: CG10417 is a PPM-type member of the protein phosphatase 2C family that dephosphorylates proteins at the serine and threonine residues (Sopko et al., 2014). No other genetic reagents were available for this gene. However, given its association with the PP2 family known to be involved in *Drosophila*

circadian clock function (Fang et al., 2007), I generated a UAS-CG10417 strain to over-express this phosphatase specifically in clock cells. Interestingly, CG10417 overexpression in clock cells resulted in a long period phenotype (Table 2). This phenotype is similar to that of the RNAi knockdown, demonstrating that increasing or decreasing the dephosphorylation of CG10417 targets, slows the pace of the clock. This is not unprecedented since RNAi knockdown and overexpression of PP2A subunit WDB also leads to long period rhythms (Sathyanarayanan et al., 2004; Andreazza et al., 2015).

Leukocyte-antigen-related-like (LAR), KK107996: LAR is a transmembrane receptor protein tyrosine phosphatase bearing Fibronectin type III, Immunoglobulin-like, and tyrosine specific protein phosphatase domains. It functions in many cellular processes including cell adhesion, axon guidance and regulation of nervous system development (Streuli et al., 1989; Yang et al., and Tian et al., 1991). Although multiple loss of function mutants were available for this phosphatase, none were homozygous viable. However, one heterozygous combination of *Lar* loss of function alleles survived and phenocopied the arrhythmicity seen in *Lar* RNAi knockdown flies (Table 2). Further analysis showed that *Lar* is required for the development of sLN_v projections into the dorsal brain that are essential for activity rhythms during constant darkness (Agrawal and Hardin, 2016).

Protein phosphatase 1, Y-linked 2 (PP1-Y2), KK109147: PP1-Y2 is a protein phosphatase that dephosphorylates proteins at the serine and threonine residues. The RNAi shows a strong arrhythmic and/or long period phenotype, but no additional genetic reagents were available to validate this RNAi phenotype.

Calcineurin A at 14F (CanA14F), KK109858: CanA14F is a protein phosphatase that dephosphorylates proteins at serine and threonine residues. It functions in many cellular processes such as promoting NFAT protein import into the nucleus and sleep (Nakai et al., 2011). Interestingly, a *CanA14F* knock out (KO), and expression of a constitutively active form of *CanA14F* (Nakai et al., 2011) showed strong arrhythmic and long period/arrhythmic phenotypes, respectively (Table 2). However, the arrhythmicity associated with the KO was lost upon isogenization of the mutant with wild-type (w^{1118}) flies (Table 2).

CG3530, KK110786: CG3530 is a protein phosphatase that dephosphorylates proteins at tyrosine residues. Its known cellular function is in the mitotic cell cycle (Chen et al., 2007). There are no independent genetic reagents available to validate the RNAi phenotype.

Conclusions

An *in vivo* screen of ~100 RNAi lines, representing all annotated *Drosophila* phosphatases for altered activity rhythms, was carried out. The screen identified a total of 22 candidate genes (Table 1), of which 19 were protein phosphatases and 3 were protein phosphatase regulators/ inhibitors or nucleotide/carbohydrate phosphatases that altered clock function upon RNAi knockdown in *Drosophila* clock cells. The efficacy and specificity of RNAi mediated knockdown of these candidate phosphatases was validated by testing RNAi lines that targeted another region of the mRNA, transposon inserts in or near the gene, overexpression and/or loss of function mutants for activity

rhythm defects (Table 2). Further genetic validation showed that the RPTP *Lar* is required for the development of the sLN_v dorsal projections that are required for rhythmic activity in constant darkness but not during LD cycles (Agrawal and Hardin, 2016). During the course of my screen and validation of candidates, the STRIPAK/PP2a phosphatase was independently identified (Andreazza et al., 2015). This phosphatase is proposed to dephosphorylate CLK and enable transcriptional activation, which was an important target of my screen. Nevertheless, 15 viable candidate clock phosphatases remain, and *Lar* has already provided novel insight into the function of PDF signaling among pacemaker neurons to control locomotor activity rhythms.

Methods

Fly strains

The w^{1118} and w^{1118};Cyo/Sco;TM2/TM6B strains were used as wild-type controls for activity rhythms and as balancers to generate lines used for screening and analysis, respectively. The following Gal4 strains were used to drive RNAi expression in clock cells: w^{1118};*tim*Gal4^{62}, w^{1118};;*pdf*Gal4, and w^{1118};;*tim*Gal4^{16}. The following RNAi strains from the Vienna *Drosophila* RNAi Center (VDRC) were used to knock down phosphatase expression in clock cells, listed as the gene name or CG number followed by the VDRC line number in parenthesis: *puckered* (GD3018), *Protein tyrosine phosphatase 52F* (GD3116), *IA-2 protein tyrosine phosphatase* (GD7560), *TbCMF46* (GD17123), *string* (GD17760), CG17124 (GD19078), *Calcineurin B* (GD21611), *Protein phosphatase 19C* (GD25317), CG3530 (GD26216), *Protein tyrosine*

phosphatase 4E (GD27232), *Calcineurin A1* (GD32283), CG17598 (GD32956), *Protein phosphatase 1 at 87B* (GD35025), *Protein tyrosine phosphatase 52F* (GD39175), *Protein tyrosine phosphatase 69D* (GD40631), *Phosphotyrosyl phosphatase activator* (GD41912), *microtubule star* (GD41924), *sds22* (GD42051), *Nuclear inhibitor of Protein phosphatase 1* (GD42175), *Mitogen-activated protein kinase phosphatase 3* (GD45415), CG32588 (GD46657), *Protein phosphatase 2A at 29B* (GD49671), CG3788 (KK100076), CG6380 (KK100121), CG17746 (KK100178), CG2104 (KK100216), *Mapmodulin* (KK100283), *Glycogen binding subunit 70E* (KK100593), CG42327 (KK100914), *Ppm1* (KK101257), CG10376 (KK101335), *widerborst* (KK101406), *CIB2 ortholog* (KK101474), *Inhibitor-2* (KK101547), *Protein phosphatase V* (KK101997), *Protein phosphatase Y at 55A* (KK102021), *Protein phosphatase N at 58A* (KK102060), CG14297 (KK102071), *Protein tyrosine phosphatase 36E* (KK102397), CG31469 (KK102474), *viriato* (KK102513), *Glycogen binding subunit 76A* (KK103044), *Protein phosphatase 2B at 14D* (KK103144), CG32568 (KK103317), CG7115 (KK103354), *Cep97* (KK103357), *cell division cycle 14* (KK103627), *Protein tyrosine phosphatase Meg* (KK103740), CG32812 (KK104081), *twins* (KK104167), *Protein phosphatase D6* (KK104211), *MAP kinase-specific phosphatase* (KK104374), *Protein tyrosine phosphatase Meg2* (KK104427), *Protein phosphatase D5* (KK104452), *flapwing* (KK104677), CG11597 (KK104729), *Protein tyrosine phosphatase 69D* (KK104761), *PTEN-like phosphatase* (KK104774), *Dullard* (KK104785), *myopic* (KK104860), *MAPK Phosphatase 4* (KK104884), CG13197 (KK105122), *Protein phosphatase 2C* (KK105249), *Protein phosphatase 4 regulatory subunit 2-related*

protein (KK105399), *alphabet* (KK105483), CG15528 (KK105484), *Protein phosphatase 1α at 96A* (KK105525), *inhibitor-t* (KK105565), CG6036 (KK105568), CG5026 (KK105674), CG14903 (KK105752), CG7378 (KK106098), CG10417 (KK106180), *TFIIF-interacting CTD phosphatase* (KK106253), *PP2A-B'* (KK107057), *Protein phosphatase D3* (KK107386), CG4733 (KK107621), *Protein phosphatase 1 at 13C* (KK107770), *Leukocyte-antigen-related-like* (KK107996), *slingshot* (KK107998), *eyes absent* (KK108071), *corkscrew* (KK108352), *Protein tyrosine phosphatase 99A* (KK108505), CG8909 (KK108629), CG10089 (KK108744), CG8509 (KK108802), *Nuclear inhibitor of Protein phosphatase 1* (KK108859), *Protein tyrosine phosphatase 61F* (KK108888), *Protein phosphatase 1, Y-linked 2* (KK109147), CG14411 (KK109622), *Calcineurin A at 14F* (KK109858), *lazaro* (KK109898), CG3632 (KK110167), *PH domain leucine-rich repeat protein phosphatase* (KK110360), *Protein tyrosine phosphatase 10D* (KK110443), *IA-2 protein tyrosine phosphatase* (KK110595), *astray* (KK110661), and CG3530 (KK110786). The following strains were used to characterize candidate clock protein phosphatases: UAS-*mts*RNAi (GD35171), w^{1118};;UAS-*mts*, w^{1118};P{EP}*Pp2A-29B*^{EP2332}, w^{1118};P{RS3}*Pp2A-29B*$^{CB-5426-3}$, w^{1118};PBac{WH}CG17746^{f05041}, $y^{1}w$*;P{EP}CG17746^{G4827}, $y^{1}w^{1118}$;PBac{3HPy^{+}}*I-2*^{C362}, *w**;P{UAS-*I-2*.HA}G/+;P{UAS-*Pp1-87B*.HA}H-1, $y^{1}w^{67c23}$;P{SUPor-P}CG7115^{KG02655}, w^{1118};UAS-*Cep97*, UAS-*Cep97*/Y, w^{1118};;UAS-*Cep97*, y^{1};P{SUPor-P}tocKG08989*PpD6*^{KG08989}, $y^{1}w$*Mi{MIC}*Ptpmeg2*^{MI03011}/Y, w^{67c23}P{lacW}*Ptpmeg2*^{G0232}/Y, $y^{1}w^{67c23}$P{Mae-UAS.6.11}*Ptpmeg2*^{GG01129}/Y, w^{1118}PBac{WH}*Ptpmeg2*^{f06600};l(2)*, *w**;;*Ptp69D*^{1}, *w**;;Df(3L)8ex25, w^{1118};;*Ptp69D*^{10},

w^{1118};;*Ptp69D*^{18}, w^{1118};;*Ptp69D*^{20}, w^{1118};;*Ptp69D*^{21}, w^{1118};;UAS-*Ptp69D*, w^{1118};;UAS-DN*Ptp69D*, y^{1}P{SUPor-P}*MKP-4*^{KG03420}, w^{1118};;P{GSV6}*Pp1α-96A*^{GS11179}, w^{1118};;*PP1α-96A*^{2}, w^{1118};;UAS-P*P1α-96A*.HA, w^{1118};;*PP1α96A*-CRISPRmutant-1/+, w^{1118};;*PP1α96A*-CRISPRmutant-2/+, w^{1118};;*PP1α96A*-CRISPRmutant-3/+, w^{1118};UAS-*PP2C-like*, *w**;*Lar*$^{13.2}$/+, Df(2L)TW84,l(2)74i^{1},*amos*^{Tft}*Lar*^{TW84}/+, Df(2L)E55,rdo^{1}hook^{1}*Lar*^{E55}pr^{1}/+, w^{1118};;UAS-*Lar*, w^{1118};UAS-*CanA14F*myc, w^{1118};;UAS-*CanA14F*act-myc and *CanA14F*-KO/Y.

Drosophila activity monitoring and behavior analysis

One to three day old male flies were entrained for three days in 12:12 light-dark (LD) and transferred to constant darkness (DD) for seven days at 25°C. The screen employed testing of each UAS-RNAi alone (as a control), driver alone (as a control) and a combination of UAS-RNAi line with *tim*-Gal4 or *pdf*-Gal4 (the test). Locomotor activity was monitored using the *Drosophila* Activity Monitor (DAM) system (Trikinetics). Analyses of period, power and rhythm strength during DD was carried out using ClockLab (Actimetrics) software as previously described (Pfeiffenberger et al., 2010). UAS-RNAi lines that produce consistent period lengthening or shortening of ≥ 1 h with *p*-value ≤ 0.05 compared to UAS-RNAi and Gal4 driver controls and/or > 50% arrhythmicity were analyzed further for defects in behavioral rhythms. Different genetic backgrounds could contribute to a ≤ 1 h period change and therefore were not considered significant.

Generation of PP1-96α CRISPR mutants

Two gRNAs were designed using the CRISPR database (Fig. 9; http://www.flyrnai.org/crispr/). With two gRNAs, each recruiting Cas9 nuclease, a deletion of nucleotides within the target gene is possible. The sequences of the two gRNAs ordered were: 5'ATGATATCCGACATCTTTGT3' and its complement; and 5'TGCAGTGCGCGGTGCACGAC3' and its complement. The two oligonucleotides were then annealed together for insertion into the U6-BK-gRNA vector (Ren et al., 2013). The DH5-α strain of *E.coli* was used for the transformation of the plasmid. Using Qiagen plasmid midiprep, the plasmid was extracted from bacteria and presence of a correct insertion was confirmed using sequencing analysis at the Gene Technologies Laboratory at Texas A&M University. The isolated plasmid was then sent to BestGene Inc. (Chino Hills, CA) for injection and upon receiving the injected larvae, PCR analysis was carried out to screen for any deletion mutants.

A

CAGGAAGCTGAGCAAGCGGGCCCACAAAGATGTCGGATATCATGAACATCGACAGTATCATCT
CGCGCCTGCTGGAGGgtaggtgttagggctccaacttttgattaccttgcccccacccatcatcacccattccccaca
tgccttgccacccaaccaccgcccactctcatcaccttaacgtaaattttccctgcttggttttccattgcagTGCGCGGT
GCACGACCGGGAAAGAATGTTCAGCTATCAGAGAGCGAGATCCGCAGCCTGTGCCTCAAGTC
CCGCGAGATATTCCTG

B

Sequence	No. of nucleotides deleted
5'- GGGCCCACAAAGATGTCGGATATCATGAAC-3'	wild-type
5'- GGGCCCACA----TGTCGGATATCATGAAC-3'	-4
5'- GGGCCCACAA-GATGTCGGATA-CATGAAC-3'	-2
5'- GGGCCCACA----TGTCGGATATCATGAAC-3'	-4

Figure 9: CRISPR/Cas9 technology to generate mutants for *PPI-96α* phosphatase. A. Part of coding sequence with gRNA gene targets shown in red; yellow box, start codon and green underline indicate the sequence shown in (B). B. Deletion mutations caused by the gRNA sequence. Other details are as defined in the text and Methods.

CHAPTER III

LAR IS REQUIRED FOR DEVELOPMENT OF CIRCADIAN PACEMAKER NEURON PROCESSES*

Background

In *Drosophila* brain, feedback loop operates in ~75 pacemaker neurons per hemisphere that function to drive activity rhythms (Helfrich-Forster, 2003). These brain pacemaker neurons can be divided into multiple clusters based on their location, size and neuropeptide expression, including pigment-dispersing factor (PDF) neuropeptide-expressing four small ventral lateral neurons (sLN_vs), and four large ventral lateral neurons (lLN_vs) (Nitabach and Taghert, 2008; Shafer and Yao, 2014). These clusters of pacemaker neurons form a network that maintains synchrony and determines the pattern of activity rhythms based on environmental inputs (Peschel and Helfrich-Forster, 2011; Yoshii et al., 2012), and also exhibits circadian plasticity where the PDF-positive sLN_vs send axonal projections toward DN_1s and DN_2s that undergo daily changes in morphology (Fernandez et al., 2008).

Of the 22 phosphatases identified in RNAi screen with aberrant rhythms, the receptor protein tyrosine phosphatase (RPTP) leukocyte-antigen related (LAR; Streuli et al., 1989), is required for rhythmic activity. Despite this behavioral arrhythmicity, clock

*This chapter is reprinted with permission from Agrawal P, Hardin PE (2016). The *Drosophila* receptor protein tyrosine phosphatase LAR is required for development of circadian pacemaker neuron processes that support rhythmic activity in constant darkness but not during Light/Dark cycles. J Neurosci 36:3860-3870.

protein rhythms persist in brain pacemaker neurons from *Lar* mutants and RNAi knockdown flies, which suggests that *Lar* mediates clock output. Indeed, PDF accumulation in sLN_v dorsal projections is eliminated in *Lar* mutant and RNAi knockdown flies, but PDF expression persists in sLN_v cell bodies. During fly development, LAR is previously shown to regulate neuronal morphology, axon guidance and growth in embryos via multiple signaling pathways (e.g., BMP, WNT) (Krueger et al., 1996; Desai et al., 1997; Wills et al., 1999; Kaufmann et al., 2002; Berke et al., 2013). I have now shown that the lack of PDF accumulation in sLN_v dorsal projections in *Lar* mutant and RNAi knockdown flies is in fact due to defects in the arborization of these projections during development.

Strikingly, unlike flies deficient in PDF expression or PDF neurons, which lack lights-on anticipation and show premature lights-off anticipation (Renn et al., 1999), *Lar* RNAi knockdown flies show normal lights-on and lights-off anticipation during LD cycles. Because PDF expression in sLN_v and lLN_v cell bodies and their surviving projections distinguish *Lar* mutants and RNAi knockdown flies from flies lacking PDF entirely, my results suggest that the remaining PDF expression in sLN_v and lLN_vs mediate lights-on and lights-off anticipation during light/dark cycles.

Results

Reducing LAR expression in clock cells abolishes activity rhythms

In *Drosophila*, release of transcriptional repression by the degradation of PER and TIM proteins occurs simultaneously with the replacement of hyperphosphorylated CLK by

transcriptionally competent hypophosphorylated CLK (Yu et al., 2006). Likewise, multiple kinases and phosphatases control the phosphorylation state of PER and TIM, which determines the timing of transcriptional repression by regulating their nuclear localization and stability (Hardin, 2011). I therefore sought to identify phosphatases that promote CLK-CYC transcriptional activation upon dephosphorylation of core clock components. The loss of such phosphatases is predicted to delay CLK-CYC transcriptional activity, slow PER-TIM degradation, and/or their nuclear localization; all of which act to lengthen circadian period (Sathyanarayanan et al., 2004; Fang et al., 2007; Andreazza et al., 2015).

To identify phosphatases that dephosphorylate clock proteins, I used clock cell-specific RNAi knockdown to screen a total of ~100 phosphatases for altered locomotor activity rhythms. The *tim*Gal4 and *pdf*Gal4 drivers were used to express UAS-phosphatase RNAi in either all clock cells or in PDF-positive LN_vs alone. The screen identified 22 genes that either lengthened or shortened circadian period by ≥ 1 h (*p-value* ≤ 0.05 compared with controls) or were significantly arrhythmic. An RNAi line targeting the RPTP *Lar* (UAS-*Lar*RNAi) was largely arrhythmic when driven by either *tim*Gal4 or *pdf*Gal4 during DD, whereas *tim*Gal4, *pdf*Gal4 and UAS-*Lar*RNAi controls showed high levels of rhythmicity (Table 3; Fig. 10). When UAS-*Dicer2* was used to enhance the RNAi potency (Dietzl et al., 2007), flies expressing *Lar* RNAi in all clock cells or PDF-positive LN_vs were almost entirely arrhythmic (Table 3). Whether or not *Dicer2* was used to enhance *Lar* RNAi potency, knocking down *Lar* expression in clock cells caused a significant (*p-value* < 0.01) increase in arrhythmicity.

Table 3: Activity rhythms are disrupted in clock cell-specific *Lar* RNAi knockdown and *Lar* mutant flies. *Rhythm strength is significantly different ($p<0.01$) than w^{1118} and controls containing either the Gal4 driver or UAS responder alone with or without *Dicer2*. #Rhythm strength is significantly different ($p<0.001$) than w^{1118}, w^{1118};*Lar* Df/+;+, and w^{1118};$Lar^{13.2}$/+;+ flies.

Genotype	Total	% Rhythmic	Period ± SEM	Strength (P-S) ± SEM
w^{1118};+;+	16	100	23.50 ± 0.00	160.34 ± 21.62
w^{1118};*tim*Gal4/+;+	16	88	23.54 ± 0.04	129.26 ± 11.33
w^{1118};+;*pdf*Gal4/+	16	100	23.66 ± 0.06	118.24 ± 14.20
w^{1118};UAS-*Lar*RNAi/+;+	16	100	23.53 ± 0.03	26.44 ± 9.06
w^{1118};UAS-*Lar*RNAi/*tim*Gal4;+	12	25	24.17 ± 0.27	8.68 ± 1.25*
w^{1118};UAS-*Lar*RNAi/+;*pdf*Gal4/+	16	0	n.a.	2.20 ± 1.03*
UAS-*Dicer2*;*tim*G4/+;+	16	100	24.81 ± 0.12	80.85 ± 12.26
UAS-*Dicer2*;UAS-*Lar*RNAi/*tim*Gal4;+	11	0	n.a.	5.00 ± 1.43*
w^{1118};UAS-*Dicer2*/+;*pdf*Gal4/+	15	80	24.17 ± 0.09	62.66 ± 11.51
w^{1118};UAS-*Dicer2*/UAS-*Lar*RNAi;*pdf*Gal4/+	10	10	23.50	5.78 ± 1.22*
w^{1118};$Lar^{13.2}$/+;+	14	93	23.54 ± 0.04	59.37 ± 3.23
w^{1118};*Lar* Df/+;+	14	100	23.71 ± 0.11	113.54 ± 29.01
w^{1118};*Lar* Df/$Lar^{13.2}$;+	14	0	n.a.	1.83 ± 0.17#

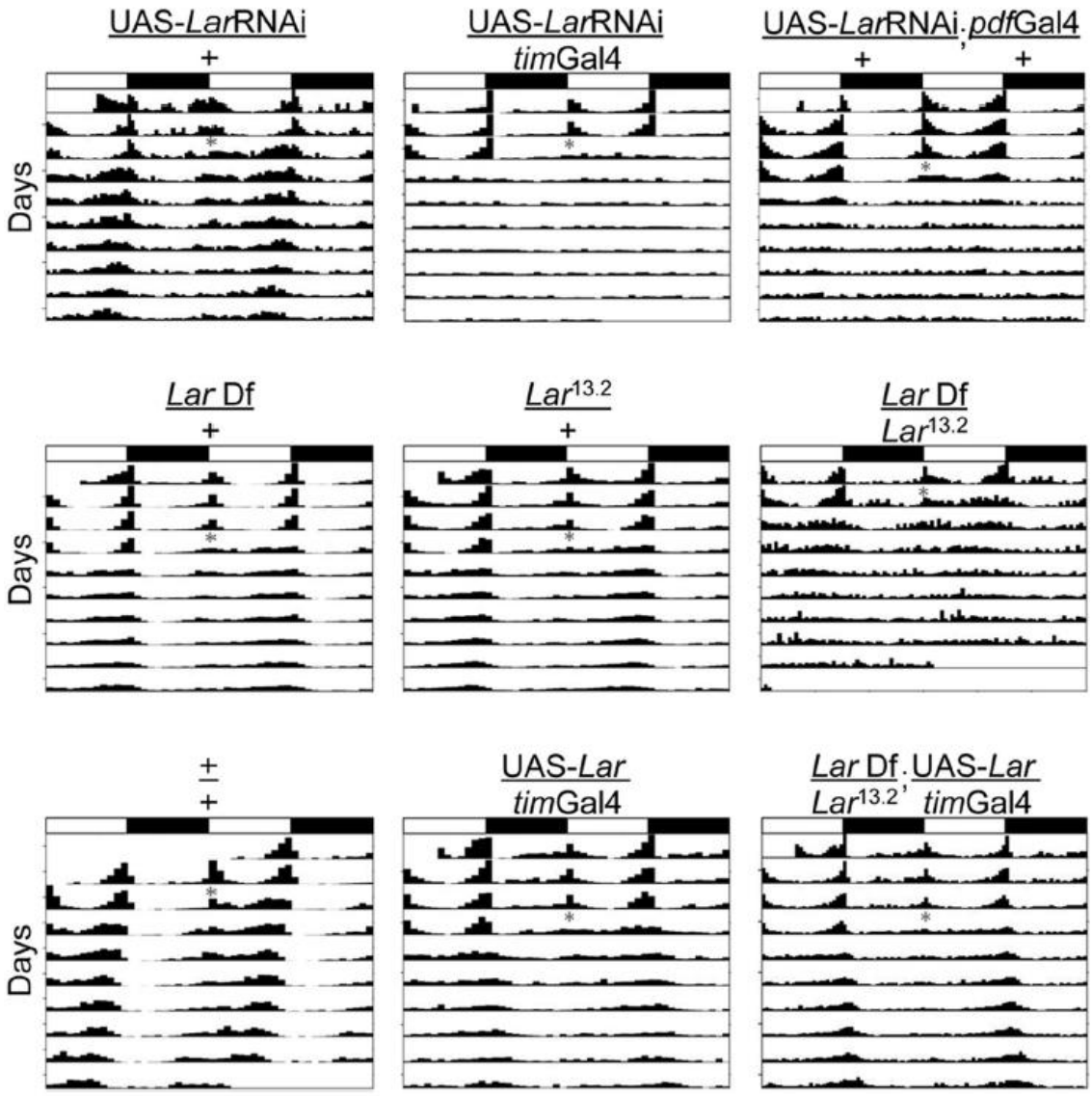

Figure 10: Locomotor activity analysis of clock cell-specific *Lar* RNAi knockdown and *Lar* mutant flies. Analysis of activity in DD and fly genotypes are as described in Materials and Methods. Representative double-plotted actograms for single flies of each genotype are shown. White boxes, lights-on period; black boxes, lights-off period; vertical bars, fly activity. The height of vertical bars indicates relative level of activity.

To independently confirm that decreased *Lar* expression abolishes activity rhythms, I tested loss of function *Lar* mutants for behavioral defects. *Lar*-null mutants, although capable of completing embryogenesis and early larval development, die as late third instar larvae or pupae (Krueger et al., 1996). Because homozygous *Lar*-null mutants do not survive to adulthood, I tested transheterozygous combinations of isogenized *Lar* loss-of-function alleles for locomotor activity rhythms. One allelic combination, *Lar* deficiency Df(2L)E55 over point mutant $Lar^{13.2}$ (*Lar* Df/$Lar^{13.2}$), was viable, even though both alleles are predicted to be null for LAR function (Krueger et al., 1996). Activity rhythms in *Lar* Df/$Lar^{13.2}$ flies were abolished, as reflected by a significant (*p-value* < 0.001) decrease in rhythm strength compared with *Lar* Df/+ and $Lar^{13.2}$/+ flies (Table 3; Fig. 10), thus confirming the behavioral phenotype and the specificity of *Lar* RNAi.

Because reduced levels of *Lar* in clock cell-specific *Lar* RNAi knockdown and *Lar* Df/$Lar^{13.2}$ flies caused high levels of arrhythmicity, I reasoned that expressing *Lar* specifically in clock cells would rescue the arrhythmic phenotype associated with these genotypes. To express *Lar* in clock cells, *tim*Gal4 was used to drive UAS-*Lar*. When *tim*Gal4 was used to express UAS-*Lar* in clock cell-specific *Lar* RNAi knockdown or *Lar* Df/$Lar^{13.2}$ mutant flies, rhythmic activity was restored (Table 4; Fig. 10), consistent with the significant increase in rhythm strength compared with control *tim*Gal4 driven *Lar* RNAi (*p-value* = 0.0032) and *Lar* Df/$Lar^{13.2}$ (*p-value* = 0.02) flies (Table 3). Rescue of clock cell-specific *Lar* RNAi knockdown and *Lar* Df/$Lar^{13.2}$ arrhythmicity by clock

cell-specific *Lar* expression further demonstrates that LAR levels and/or activity are required for rhythmic activity.

Table 4: *Lar* expression in clock cells rescues activity rhythms in *Lar* mutant and RNAi knockdown flies. *Rhythm strength is significantly different ($p < 0.004$) than w^{1118};*Lar* $^{13.2}$/+;+ and w^{1118};*Lar* Df/+;+ flies (Table 1). #Rhythm strength is significantly different ($p = 0.02$) than UAS-*Dicer2*;UAS-*Lar*RNAi/*tim*Gal4;+ flies (Table 1). +Rhythm strength is significantly different ($p = 0.011$) than w^{1118};+;UAS-*Lar*/+, but not significantly different ($p = 0.39$) than w^{1118};+;*tim*Gal4/+.

Genotype	**Total**	**% Rhythmic**	**Period ± SEM**	**Strength (P-S) ± SEM**
w^{1118};+;UAS-*Lar*/+	14	100	23.57 ± 0.04	92.86 ± 9.91
w^{1118};+;*tim*-Gal4/+	15	93	23.58 ± 0.06	58.54 ± 4.63
w^{1118};+;UAS-*Lar*/*tim*-Gal4	16	88	24.20 ± 0.32	65.16 ± 5.98+
w^{1118};*Lar* Df/*Lar*$^{13.2}$;UAS-*Lar*/*tim*-Gal4	14	86	24.67 ± 0.10	26.7 ± 7.05*
w^{1118};UAS-*Dicer2*/+;UAS-*Lar*/*tim*-Gal4	15	80	24.21 ± 0.22	29.95 ± 8.61
w^{1118};UAS-*Dicer2*/UAS-*Lar*RNAi;UAS-*Lar*/*tim*-Gal4	16	88	24.54 ± 0.24	14.61 ± 1.14#

Molecular clock gene oscillations are preserved in Lar knockdown flies

Because *Lar* is an RPTP, I expected that reducing LAR levels would result in increased clock protein phosphorylation, thus disrupting feedback loop progression and/or function. To determine whether reducing *Lar* expression alters PER, TIM and/or CLK phosphorylation or abundance, antibodies against these proteins were used to probe Western blots containing head extracts from *tim*Gal4 driven UAS-*Lar*RNAi and UAS-*Lar*RNAi flies without a Gal4 driver collected at different Zeitgeber times (ZTs; where

ZT0 is lights-on and ZT12 is lights-off) during LD cycles or different CTs (where CT0 is subjective lights-on and CT12 is subjective lights-off) during DD. CT2, CT10, and CT22 time points were selected to detect differences in abundance and/or phosphorylation because higher levels and/or hyperphosphorylated forms of clock proteins are present at CT22 and CT2 and lower levels and/or hypophosphorylated forms of clock proteins are present at CT10. Neither CLK, PER, and TIM phosphorylation, as measured by the lower mobility forms, nor abundance were noticeably different in head extracts from *tim*Gal4 driven UAS-*Lar*RNAi and control UAS-*Lar*-RNAi/+ flies during LD (data not shown) or DD conditions (Fig. 11*A*). This result demonstrates that the molecular oscillator in clock cell-specific *Lar* RNAi knockdown flies is functioning similar to that in controls having normal *Lar* levels, at least in fly heads, where >90% clock protein signal comes from photoreceptor expression (Glossop and Hardin, 2002).

To directly assess clock protein localization and cycling in pacemaker neurons in clock cell-specific *Lar* RNAi knockdown and *Lar* Df/*Lar*$^{13.2}$ flies, PER distribution was monitored in dissected brains during LD (data not shown) and DD. Newly eclosed UAS-*Lar*RNAi/+, *tim*Gal4 driven UAS-*Lar*RNAi and *Lar* Df/*Lar*$^{13.2}$ adults were synchronized in LD and collected for dissection at the predicted PER peak (CT22) and trough (CT10) time points on the third day after transfer to DD. Remarkably, PER expression in *tim*Gal4 driven UAS-*Lar*RNAi and *Lar D*f/*Lar*$^{13.2}$ brains was indistinguishable from UAS-*Lar*RNAi/+ controls at both peak and trough time points during LD (data not shown) and DD (Fig. 11*B–G*). In each of these genotypes, PER was readily detected in all pacemaker neuron groups at CT22 (Fig. 11*B–D*), but was undetectable at CT10 (Fig.

11*E–G*). Cycling of PER protein in whole heads from *tim*Gal4 driven UAS-*Lar*RNAi flies and pacemaker neurons from *tim*Gal4 driven UAS-*Lar*RNAi and *Lar* Df/*Lar*$^{13.2}$ flies demonstrates that *Lar* does not disrupt molecular oscillator function. These results suggest that *Lar* functions downstream of the molecular oscillator to disrupt activity rhythms.

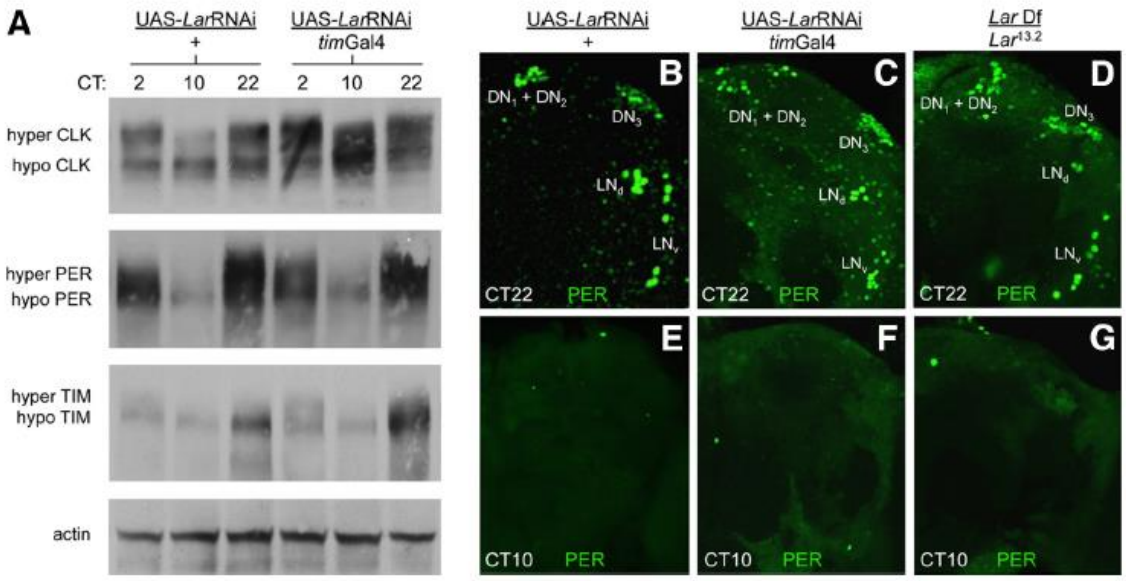

Figure 11: Rhythms in clock gene expression are intact in *Lar* knockdown flies. *A*, Western blots of head extracts from w^{1118};UAS-*Lar*RNAi/+ and UAS-*Dicer2*/+;UAS-*Lar*RNAi/*tim*Gal4 (UAS-*Lar*RNAi/*tim*Gal4) flies were probed with CLK, PER, and TIM antisera. *B–G*, Brains dissected from adult flies collected at CT22 or CT10 were immunostained with PER antisera and imaged by confocal microscopy.

PDF accumulation is impaired in Lar knockdown flies

A key regulator of locomotor activity rhythms is the neuropeptide PDF (Renn et al., 1999), which rhythmically accumulates in the sLN_v projections into the dorsal brain

(hereafter sLN_v dorsal projections) with a peak early in the day (Park et al., 2000). To determine whether defects in PDF expression give rise to the arrhythmic activity seen in clock cell-specific *Lar* RNAi knockdown and *Lar* Df/*Lar*$^{13.2}$ mutant flies, PDF was monitored in brains from PDF neuron-specific *Lar* RNAi knockdown, *Lar* Df/*Lar*$^{13.2}$ mutant and control flies at ZT2. In *pdf*Gal4 driven UAS*Lar*RNAi flies, PDF immunostaining is markedly reduced or absent (18 of 18 brain hemispheres) in sLN_v dorsal projections compared with the normal PDF immunostaining (18 of 18 brain hemispheres) seen in sLN_v dorsal projections from control UAS-*Lar*RNAi flies (Fig. 12*A*–*F*). In contrast, PDF immunostaining in lLN_v projections to the medulla and accessory medulla (aMe) showed no alterations in *pdf*Gal4 driven UAS-*Lar*RNAi or control UAS-*Lar*RNAi flies (18 of 18 brain hemispheres for each genotype; Fig. 12*A*–*F*), whereas PDF immunstaining in lLN_v projections to the posterior optic tract (POT) were absent or disrupted in most *pdf*Gal4 driven UAS*Lar*RNAi flies (10 of 18 brain hemispheres) but normal in UAS-*Lar*RNAi controls (18 of 18 brain hemispheres) (Fig. 12*A*–*F*). Likewise, wild-type PDF immunostaining was detected in sLN_v dorsal projections from *Lar* Df/+ and *Lar*$^{13.2}$/+ control flies (16 of 16 brain hemispheres for each genotype), but PDF immunostaining was absent in sLN_v dorsal projections in *Lar* Df/*Lar*$^{13.2}$ mutants (16 of 16 brain hemispheres; Fig. 12*G*–*O*). PDF expression in lLN_v projections to the medulla and aMe were present but appeared less intense in *Lar* Df/*Lar*$^{13.2}$ mutants than in control *Lar* Df/+ and *Lar*$^{13.2}$/+ flies (16 of 16 brain hemispheres), and PDF levels in the POT projection were drastically reduced or absent

in *Lar* Df/*Lar*$^{13.2}$ mutant flies (8 of 16 brain hemispheres) compared with *Lar* Df/+ and *Lar*$^{13.2}$/+ controls (Fig. 12*G–O*).

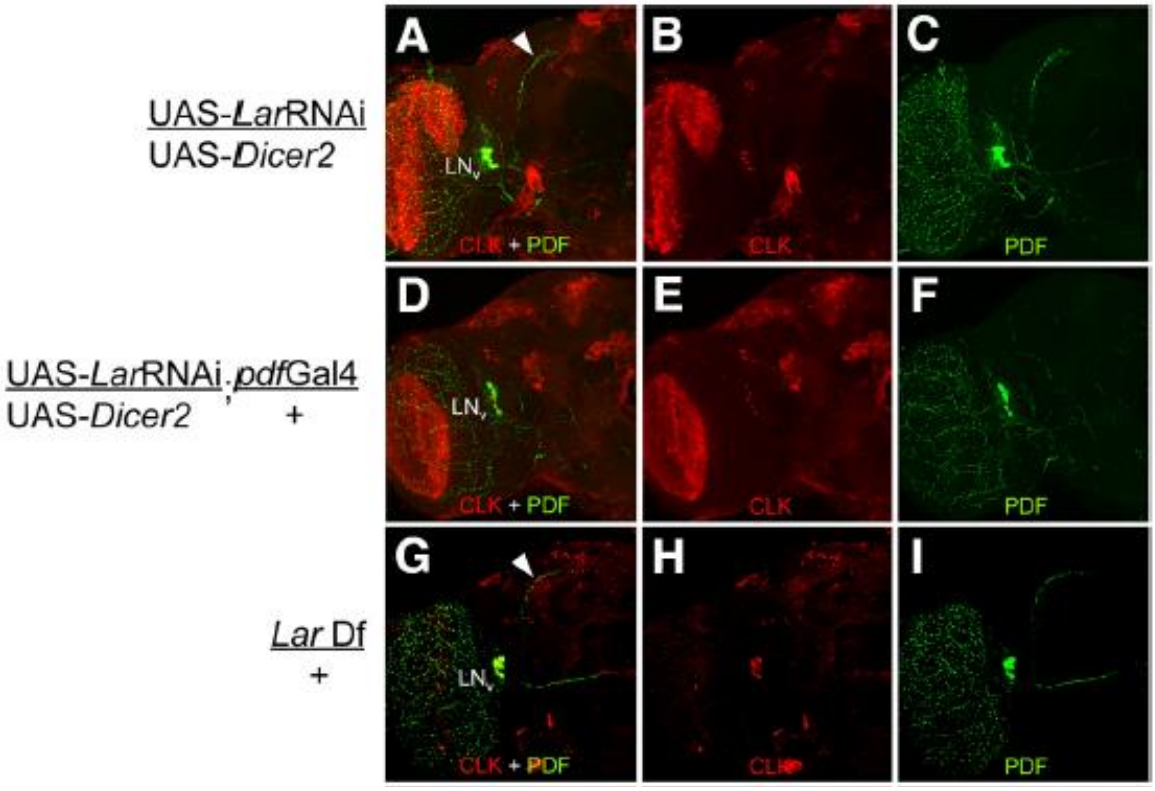

Figure 12: PDF expression is absent in sLN$_v$ dorsal projections of PDF neuron-specific *Lar* RNAi knockdown flies. *A–C,* Projected *Z*-series image (76 μm) of a UAS-*Lar*RNAi/UAS-*Dicer2* brain. *D–F,* Projected *Z*-series image (90 μm) of a UAS-*Lar*RNAi/UAS-*Dicer2*;*pdf*-Gal4/+ brain. *G–I,* Projected *Z*-series image (76 μm) of a *Lar* Df/+ brain. *J–L,* Projected *Z*-series image (78 μm) of a *Lar*$^{13.2}$/+ brain. *M–O,* Projected *Z*-series image (88 μm) of a *Lar* Df/*Lar*$^{13.2}$ brain. *P–R,* Projected *Z*-series image (82 μm) of a *Lar* Df/*Lar*$^{13.2}$;*tim*Gal4/UAS-*Lar* brain.

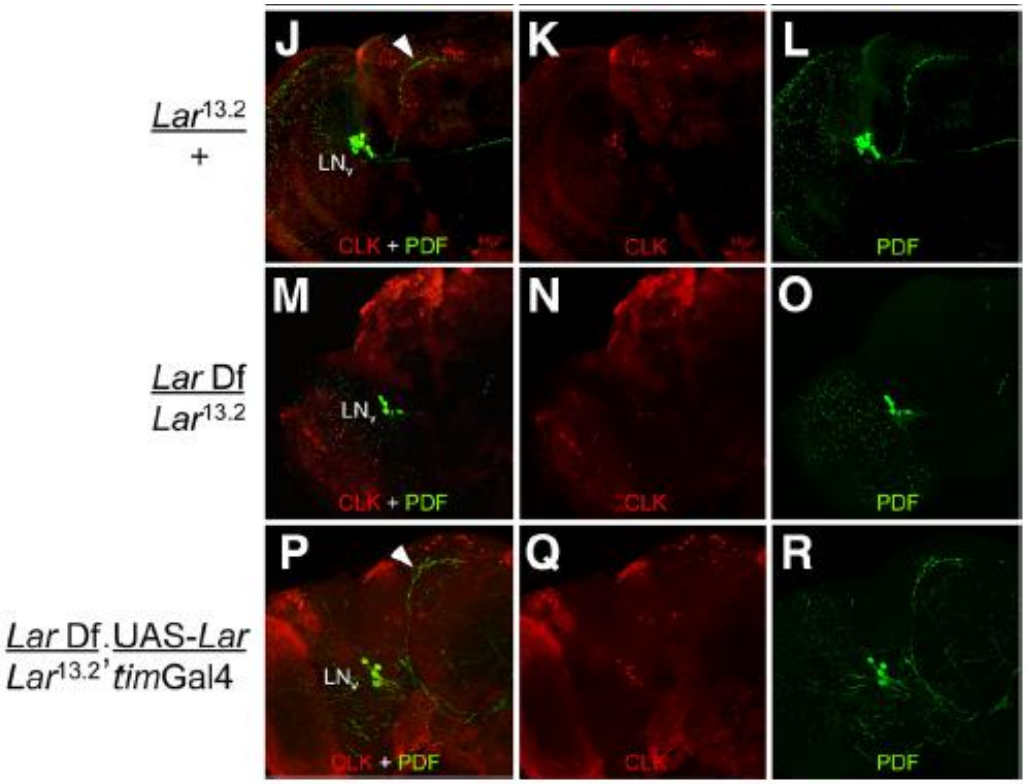

Figure 12 Continued

If the lack of PDF accumulation in sLN_v dorsal projections is due to decreased *Lar* levels, then expressing *Lar* in clock cells should restore PDF expression in these projections. Indeed, when *tim*Gal4 was used to drive UAS-*Lar* in *Lar* Df/*Lar*$^{13.2}$ flies, wild-type PDF immunostaining was detected in sLN_v dorsal projections and lLN_v medulla projections (16 of 16 brain hemispheres; Fig. 12*P–R*). However, PDF expression in lLN_v POT projections was not completely restored by expressing *Lar* in all clock neurons (8 of 16 brain hemispheres were disrupted or absent; Fig. 12*P–R*). The lack of PDF accumulation in sLN_v dorsal projections is not due to the loss of sLN_vs in flies with impaired *Lar* expression; CLK is expressed in sLN_v nuclei of *pdf*Gal4 driven

UAS-*Lar*RNAi flies, *Lar* Df/*Lar*$^{13.2}$ mutants and control flies with varying levels of PDF (Fig. 13). CLK levels in *pdf*Gal4 driven UAS-*Lar*RNAi and *Lar* Df/*Lar*$^{13.2}$ mutant flies were not significantly different (*p-value* > 0.05) than the UAS-*Lar*RNAi and *Lar* Df/+ or *Lar*$^{13.2}$/+ controls, respectively. These data demonstrate that LAR expression in PDF neurons is required for PDF accumulation in sLN_v dorsal projections.

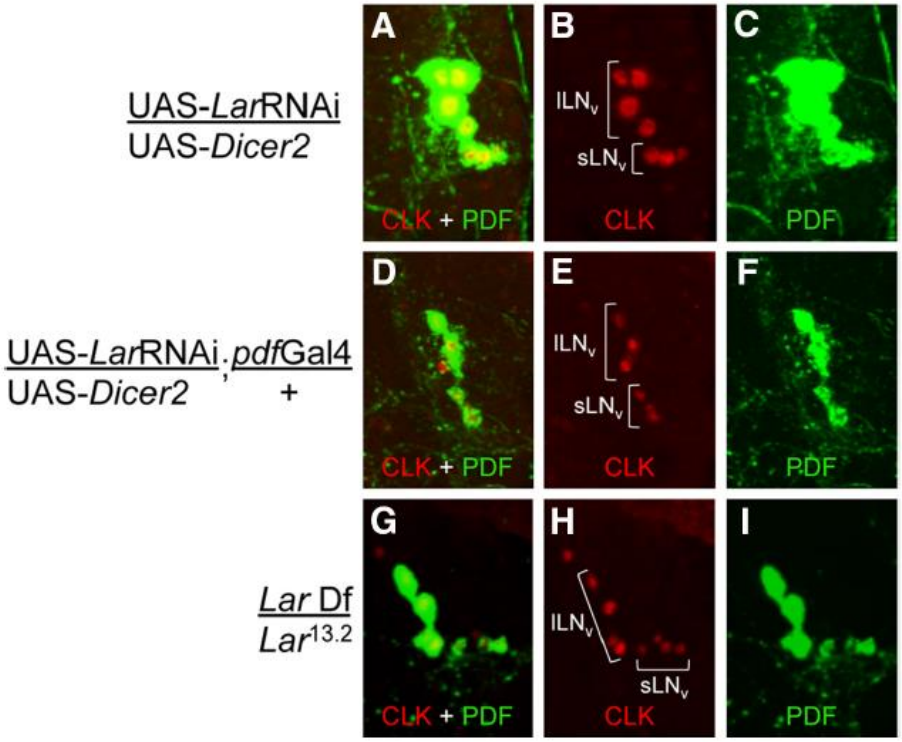

Figure 13: Both lLN_vs and sLN_vs are present in PDF neuron-specific *Lar* RNAi knockdown and *Lar* Df/*Lar* $^{13.2}$ mutant flies. *A–C,* Projected *Z*-series (18 μm) from a UAS-*Lar*RNAi/UAS-*Dicer2* brain. *D–F,* Twelve micrometer projected *Z*-series image from a UAS-*Lar*RNAi/UAS-*Dicer2*;*pdf*Gal4/+ brain. *G–I,* Fourteen micrometer projected *Z*-series image from a *Lar* Df/*Lar*$^{13.2}$ brain.

Lar is required during development for PDF accumulation in sLN_v dorsal projections and activity rhythms

Loss of *Lar* expression in pacemaker neurons could abolish activity rhythms and PDF accumulation in sLN_v dorsal projections by blocking clock output pathway development, maintenance, or both. To determine whether LAR is required in adults for locomotor activity rhythms, *Lar* RNAi was expressed in PDF expressing neurons post-eclosion using the $Gal80^{ts}$ TARGET system (McGuire et al., 2003). In flies raised and tested at the permissive temperature (18°C), $Gal80^{ts}$ inhibits *pdf*Gal4 driven UAS-*Lar*RNAi, resulting in rhythms with a period of 23.54 h (Table 5, row 12), and strengths that were either not different (*p-value* > 0.28) or stronger (*p-value* < 0.02) than controls unable to express *Lar* RNAi (Table 5, rows 9-11). When *pdf*-Gal4 driven UAS-*Lar*RNAi flies were raised at 18°C and transferred to restrictive temperature (30°C) after eclosion, *Lar* RNAi is only expressed in PDF neurons of adults. However, these flies were just as rhythmic (*p-value* > 0.29) as control flies that are unable to express *Lar* RNAi after eclosion and had comparable periods (Table 5, compare row 4 to rows 1-3). These results suggest that LAR expression in PDF neurons after adults emerge is not required for activity rhythms. This implies that *Lar* function is required in sLN_vs during development since knocking down *Lar* in PDF neurons during development and in adults essentially eliminates activity rhythms (Table 3, rows 6 and 10).

Table 5: PDF neuron-specific *Lar* RNAi knockdown during development, but not in adults, abolishes activity rhythms. *Significantly different ($p<0.05$) rhythm strength compared to controls exposed to the same temperature regime.

Genotype (temperature raised » temperature tested)	Total	% Rhythmic	Period ± SEM	Strength (P-S) ± SEM
w^{1118};+;+ (18°C»30°C)	16	94	23.50 ± 0.12	29.35 ± 12.45
w^{1118};*tub*-Gal80^{ts}/+;*pdf*Gal4/+ (18°C»30°C)	18	89	23.94 ± 0.13	14.05 ± 2.55
w^{1118};UAS-*Lar*RNAi/+;+ (18°C»30°C)	15	100	23.59 ± 0.08	21.41 ± 4.46
w^{1118};UAS-*Lar*RNAi/*tub*-Gal80^{ts};*pdf*Gal4/+ (18°C»30°C)	18	94	23.46 ± 0.21	17.62 ± 3.05
w^{1118}; +;+ (30°C»30°C)	12	92	24.41 ± 0.11	17.48 ± 2.01
w^{1118};*tub*-Gal80^{ts}/+;*pdf*Gal4/+ (30°C»30°C)	15	87	24.04 ± 0.13	31.75 ± 10.01
w^{1118};UAS-*Lar*RNAi/+;+ (30°C»30°C)	14	93	23.61 ± 0.14	16.21 ± 1.8
w^{1118};UAS-*Lar*RNAi/*tub*-Gal80^{ts};*pdf*Gal4/+ (30°C»30°C)	18	6	24.50	3.44 ± 1.17*
w^{1118};+;+ (18°C»18°C)	12	83	23.45 ± 0.05	35.13 ± 9.46
w^{1118};*tub*-Gal80^{ts}/+;*pdf*Gal4/+ (18°C»18°C)	12	83	23.30 ± 0.08	43.76 ± 7.94
w^{1118};UAS-*Lar*RNAi/+;+ (18°C»18°C)	16	88	23.50 ± 0.10	15.01 ± 1.34
w^{1118};UAS-*Lar*RNAi/*tub*-Gal80^{ts};*pdf*Gal4/+ (18°C»18°C)	17	88	23.61 ± 0.09	47.37 ± 6.31
w^{1118};+;+ (30°C»18°C)	12	92	23.43 ± 0.03	27.79 ± 6.23
w^{1118};*tub*-Gal80^{ts}/+;*pdf*Gal4/+ (30°C»18°C)	15	80	23.71 ± 0.16	30.67 ± 18.72
w^{1118};UAS-*Lar*RNAi/+;+ (30°C»18°C)	12	83	23.56 ± 0.07	13.48 ± 2.06
w^{1118};UAS-*Lar*RNAi/*tub*-Gal80^{ts};*pdf*Gal4/+ (30°C»18°C)	15	13	24.75 ± 0.11	6.85 ± 1.47*

To confirm a role for LAR during development, I tested *pdf*Gal4 driven UAS-*Lar*RNAi flies for defects in activity rhythms when raised and tested at 30°C at the adult stage (continuous *Lar* knockdown) or raised at 30°C and transferred to 18°C at the adult stage (development-only *Lar* knockdown). Both continuous and development-only *Lar* knockdown flies displayed significantly higher arrhythmicity (*p-value* < 0.05) compared with control strains that showed rhythms with 23.5-24.5 h circadian periods (Table 5, compare row 8 to rows 5-7 and row 16 to rows 13-15). These results confirm that *Lar* is required during early stages of fly development for rhythms in locomotor activity.

Given that the expression of *Lar* RNAi in PDF neurons after eclosion does not alter rhythmic activity, I expected PDF to accumulate in sLN_v dorsal projections. Indeed, I observed PDF staining in sLN_v cell bodies and dorsal projections from flies expressing *Lar* RNAi in PDF neurons after eclosion that was comparable to controls (Fig. 14*A–F*). In contrast, flies that express *Lar* RNAi in PDF neurons during development lacked PDF staining when tested at 18°C as adults (Fig. 14*G–L*). Together, these results demonstrate that *Lar* functions during development to permit PDF accumulation in sLN_v dorsal projections and drive activity rhythms.

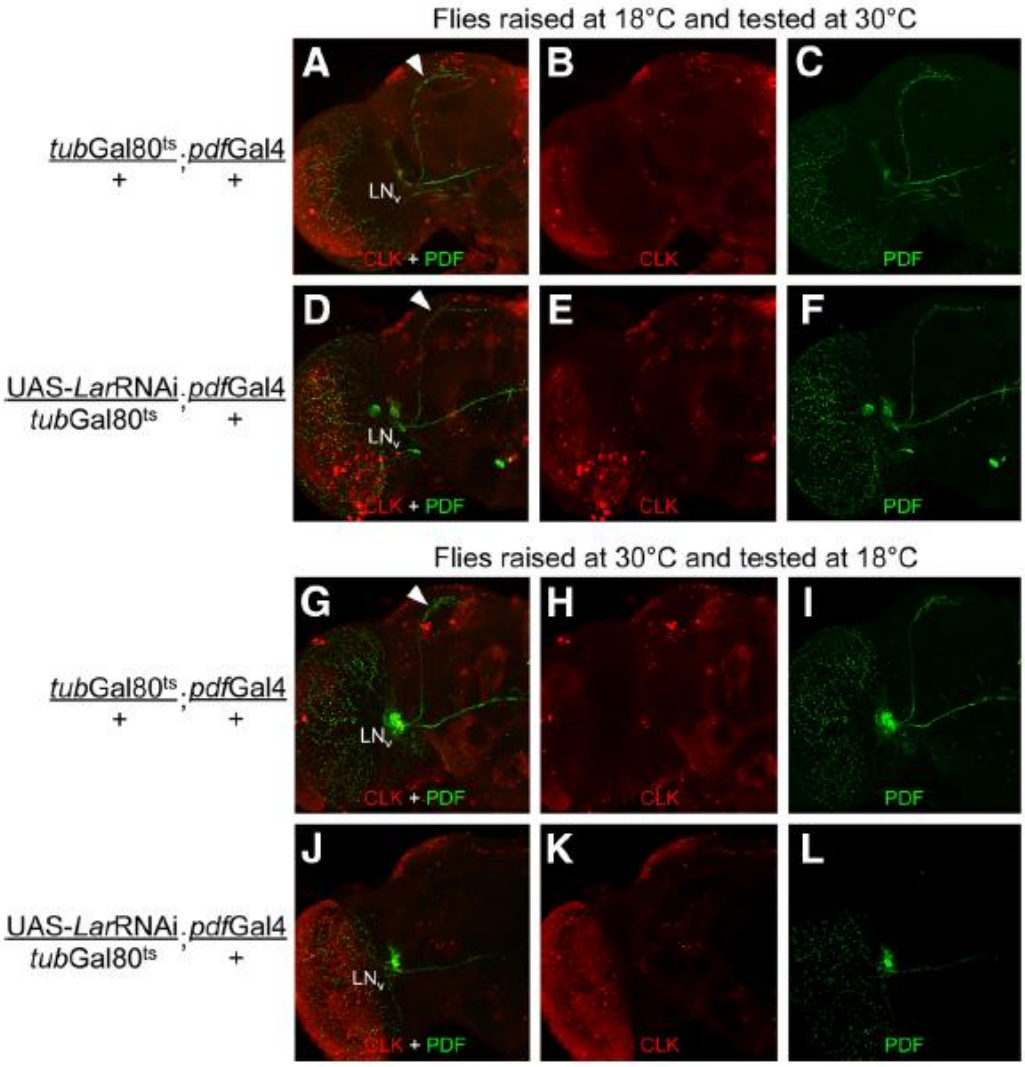

Figure 14: *Lar* is required during development, but not in adults, for PDF accumulation in sLN_v dorsal projections. *A–F*, Flies were raised at 18°C to block Gal4 activation, shifted to 30°C after eclosion to permit Gal4 activation, and collected at ZT2. *A–C*, Seventy four micrometer projected *Z*-series image of a *tub*Gal80^{ts}/+;*pdf*Gal4/+brain. *D–F*, Eighty-two micrometer projected *Z*-series image of a UAS-*Lar*RNAi/*tub*Gal80 ^{ts};*pdf*Gal4/+ brain. *G–L*, Flies were raised at 30°C to permit Gal4 activation, shifted to 18°C after eclosion to block Gal4 activation, and collected at ZT2. *G–I*, Eighty-six projected *Z*-series image of a *tub*Gal80^{ts}/+;*pdf*Gal4/+ brain. *J–L*, Eighty-two micrometer projected *Z*-series image of a UAS-*Lar*RNAi/*tub*Gal80 ^{ts};*pdf*Gal4/+ brain.

Lar disrupts the development of sLN$_v$ dorsal projections

During fly development, LAR was previously shown to regulate neuronal morphology, axon guidance and growth in embryos via multiple signaling pathways (eg, BMP, WNT) (Krueger et al., 1996; Desai et al., 1997; Wills et al., 1999; Kaufmann et al., 2002; Berke et al., 2013). Given that *Lar* plays a role in axonal development, I tested whether sLN$_v$ dorsal projections were disrupted in PDF neuron-specific *Lar* RNAi knockdown flies. sLN$_v$ axonal morphology was visualized with a membrane-tethered version of GFP (mCD8-GFP) expressed in PDF-positive neurons. GFP was detected in sLN$_v$ dorsal projections from control brains at ZT2 (Fig. 15*A*), when the axonal arbor is at its maximum (Fernandez et al., 2008). Strikingly, sLN$_v$ dorsal projections were either completely absent (17 of 18 brain hemispheres) or weakly detected (1 of 18 brain hemispheres) in UAS-*Lar*RNAi/UAS-mCD8GFP;*pdf*-Gal4/+ adults beyond the dorsomedial defasciculation point (Fig. 15*B*). Likewise, lLN$_v$ projections to the medulla and the POT were aberrant (8 of 18 brain hemispheres with absent or altered projections) and GFP staining was weak in UAS-*Lar*RNAi/UASmCD8GFP;*pdf*Gal4/+ flies (Fig. 15*B*). These results show that *Lar* plays a critical role in the development of sLN$_v$ dorsal projections (and to a lesser extent in lLN$_v$ projections), consistent with the loss of PDF accumulation in these processes and loss of behavioral rhythms.

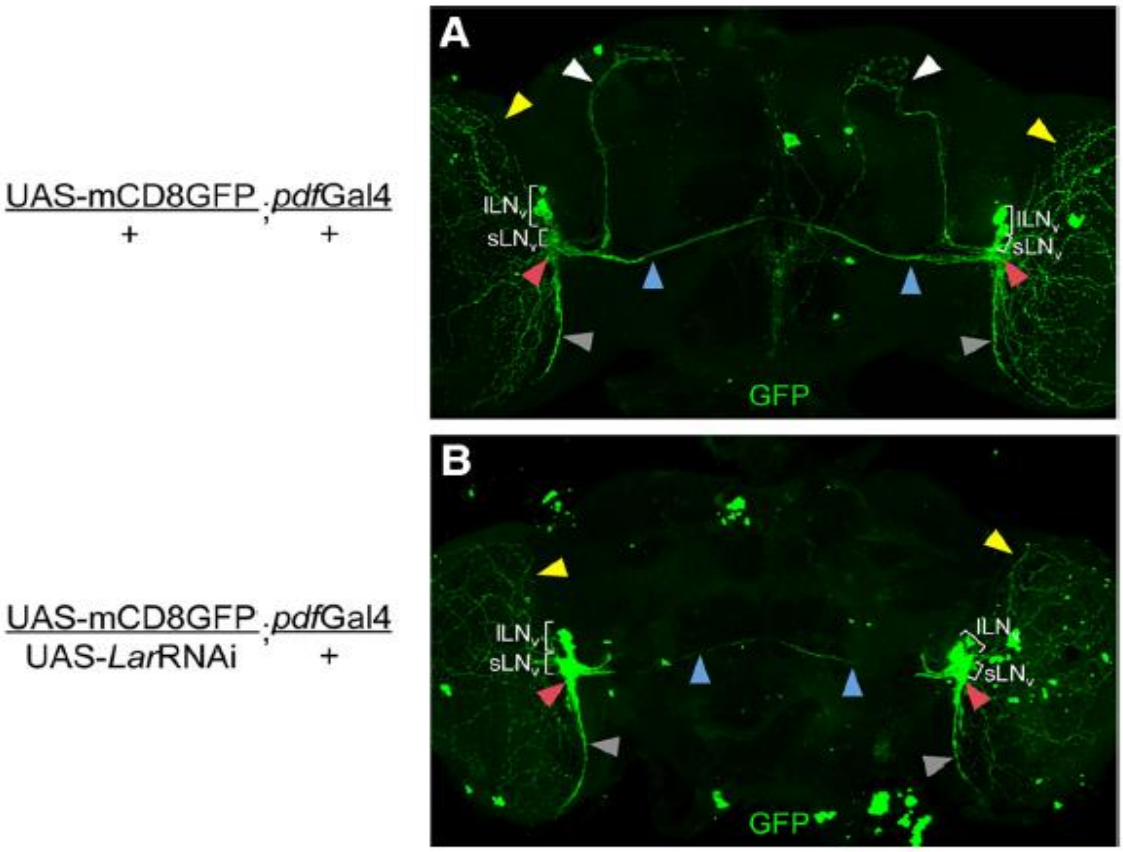

Figure 15: PDF neuron-specific *Lar* RNAi knockdown eliminates the sLN_v dorsal projection. *A*, Seventy-six micrometer projected *Z*-series image from a control UAS-mCD8GFP/+;*pdf*Gal4/+ fly brain. *B*, Seventy-eight micrometer projected *Z*-series image from a UAS-mCD8GFP/UAS-*Lar*-RNAi;*pdf*Gal4/+ fly brain. White arrowhead, sLN_v dorsal projection; blue arrowhead, lLN_v POT projection; yellow arrowhead, lLN_v medulla projection; red arrowhead, sLN_v and lLN_v aMe projections; gray arrowhead, lLN_v aMe ventral elongation projection.

Although *Lar* mutants and RNAi knockdowns eliminate PDF expression in sLN_v dorsal projections (Fig. 12), PDF continues to accumulate in sLN_v and lLN_v cell bodies and their projections into the medulla, the aMe, and (to a lesser extent) the POT (Figs. 12, 14, 15). The presence of PDF in sLN_v and lLN_v cell bodies and their remaining

projections distinguishes *Lar* mutant and RNAi knockdown flies from the pdf^{01} mutant, which eliminates PDF without altering sLN_v structure, or PDF neuron ablation flies, which eliminate both PDF and LN_vs (Renn et al., 1999). Despite their differences in PDF expression and sLN_v structure, *Lar* mutant and RNAi knockdown, pdf^{01} mutant and LN_v ablation flies all abolish activity rhythms in DD. However, activity rhythms of pdf^{01} mutant and LN_v ablated flies are also disrupted in diurnal (LD) cycles; the evening activity peak is advanced by 0.5-1 h and anticipation of lights-on is abolished (Renn et al., 1999). *Lar* RNAi knockdown flies were therefore tested to determine whether their diurnal activity reflected that of pdf^{01} mutant flies, but surprisingly the phase of their evening activity peak was similar to wild-type controls (*p-value* ≥ 0.07) and significantly later (*p-value* < 0.001) than the pdf^{01} mutant, and they could anticipate lights-on significantly better (*p-value* < 0.05) than the pdf^{01} mutant (Fig. 16; Table 6). Because PDF expression in LN_v cell bodies and their projections into the medulla, aMe and POT persist in *Lar* RNAi knockdown flies, PDF secretion from LN_vs could account for the difference in light driven activity.

Table 6: LD activity in clock cell-specific *Lar* RNAi knockdown flies does not display defects seen in *pdf*^{01} mutants. *Significantly different ($p<0.001$) compared to clock cell-specific *Lar* RNAi knockdown and control strains. #Significantly different ($p<0.05$) compared to clock cell-specific *Lar* RNAi knockdown and control strains. ^Significantly better anticipation ($p = 0.02$) than w^{1118};UAS-*Lar*RNAi/+;+ control.

Genotype	Total	Evening peak ± SEM	Morning peak ± SEM	Anticipation index ± SEM
w^{1118};UAS-*Lar*RNAi/+;+	16	12.0 ± 0.08	0.6 ± 0.08	0.79 ± 0.04
w^{1118};UAS-*Lar*RNAi/*tim*-Gal4;+	16	12.1 ± 0.06	0.5 ± 0.00	0.95 ± 0.03^
w^{1118};+;UAS-*Lar*RNAi/+;*pdf*-Gal4/+	14	12.3 ± 0.07	0.5 ± 0.04	0.82 ± 0.06
yw;+;*pdf*^{01}/ *pdf*^{01}	14	9.8 ± 0.03*	0.6 ± 0.08	0.6 ± 0.06#

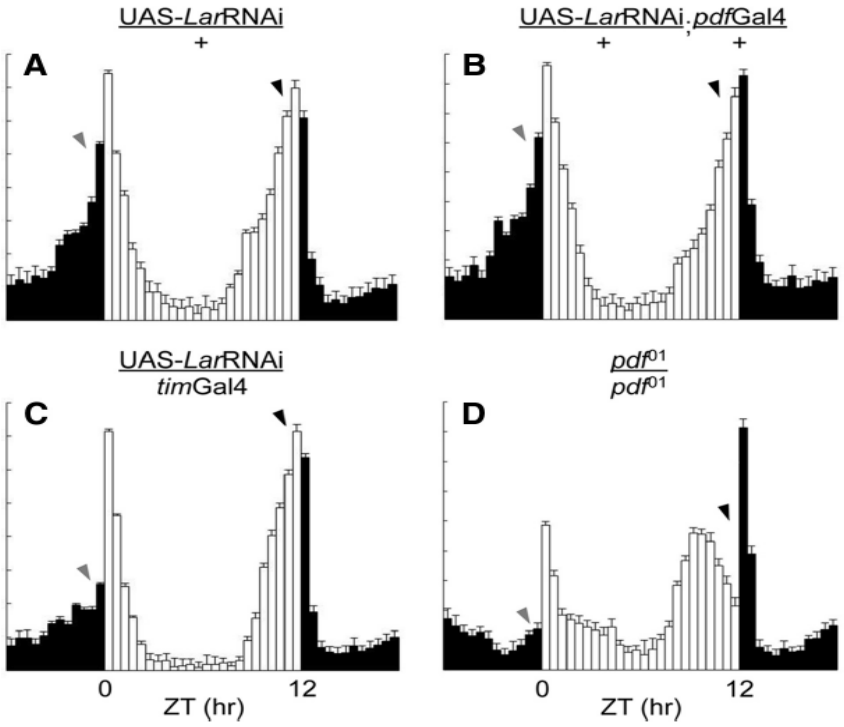

Figure 16: Activity profiles of clock cell-specific *Lar* RNAi knockdown, *pdf*^{01} and control flies during LD cycles. *A*, UAS-*Lar*RNAi/+ flies (n=16). *B*, UAS-*Lar*RNAi/+;*pdf*Gal4/+ flies (n=14). *C*, UAS-*Lar*RNAi/+;*tim*Gal4/+flies (n=16). *D*, *pdf*^{01} mutant flies (n=14).

Conclusions

In a screen to identify clock protein phosphatases, I found that RNAi knockdown of the RPTP LAR (*Leukocyte-antigen-related-like*) abolishes locomotor activity rhythms (Table 3; Fig. 10). A transheterozygous combination of *Lar* Df and $Lar^{13.2}$ mutant alleles also displayed arrhythmic activity, thus confirming the RNAi knockdown phenotype. The loss of rhythmicity in clock cell-specific *Lar* RNAi knockdown flies and *Lar* Df/$Lar^{13.2}$ mutants is not due to a defect in core oscillator function; CLK, PER and TIM phosphorylation and abundance were similar in *tim*Gal4 driven UAS-*Lar*RNAi and control UAS-*Lar*RNAi fly head extracts (Fig. 11*A*). Likewise, PER oscillations in pacemaker neurons from *Lar* RNAi knockdown flies were indistinguishable from controls lacking *Lar* RNAi expression (Fig. 11*B*). The presence of an intact molecular clock in *Lar* Df/$Lar^{13.2}$ mutant and clock cell-specific RNAi knockdown flies suggests that *Lar* disrupts output from the circadian oscillator.

The loss of activity rhythms in *Lar* mutant and RNAi knockdown flies is reminiscent of the arrhythmicity seen in pdf^{01} flies during constant darkness (Renn et al., 1999). Mutations that eliminate PDF (or the PDF receptor) are thought to disrupt output signaling from the sLN_vs to other tissues and synchronizing cues to different groups of pacemaker neurons, thereby causing arrhythmicity in constant darkness (Renn et al., 1999; Peng et al., 2003; Lin et al., 2004; Hyun et al., 2005; Lear et al., and Mertens et al., 2005). Given these roles for PDF, I hypothesized that loss of *Lar* disrupts PDF expression or release. Indeed, PDF neuron specific *Lar* RNAi knockdown and *Lar* Df/$Lar^{13.2}$ mutants displayed defective PDF staining in sLN_v dorsal projections, but PDF

staining persisted in LN_v cell bodies and their remaining projections (Figs. 12 and 13). These results suggest that the arrhythmic activity seen in PDF neuron specific *Lar* RNAi knockdown flies was due to the absence of PDF expression in sLN_v dorsal projections. Expressing *Lar* in clock neurons from *Lar* Df/$Lar^{13.2}$ mutants rescued PDF expression in sLN_v dorsal projections and behavioral rhythms (Table 4; Fig. 12*P–R*), demonstrating that *Lar* acts in clock cells to mediate PDF release and/or accumulation in sLN_v dorsal projections and drive rhythmic activity.

PDF expression in sLN_v dorsal projections is first detected in L1 larval brains (Helfrich-Forster, 1997). Since *Lar* participates in axon guidance through the midline during development of the embryonic CNS (Seeger et al., 1993), positioning sensory terminals in the olfactory lobe (Jhaveri et al., 2004), and proper compartmentalization of the visual system (Tayler et al., 2004), *Lar* could function during development, in adults, or both, to promote PDF accumulation in sLN_v dorsal projections. Using the $Gal80^{ts}$ TARGET system to express PDF neuron-specific *Lar* RNAi during development, in adults, or both, I found that *Lar* acts during development to enable PDF accumulation in sLN_v dorsal projections (Table 5; Fig. 14). Because PDF functions to synchronize pacemaker neurons and drive behavioral outputs (Park et al., 2000; Peng et al., 2003; Lin et al., 2004; Collins et al., 2012; Cavanaugh et al., 2014), loss of PDF in sLN_v dorsal projections likely accounts for the lack of activity rhythms.

Given that *Lar* is involved in axonal development, *Lar* could also be required for sLN_v dorsal projection development rather than PDF accumulation *per se*. Indeed, sLN_v dorsal processes marked by mCD8-GFP were severely disrupted or absent in PDF

neuron specific *Lar* RNAi knockdown flies (Fig. 15*B*). The lack of sLN_v dorsal projections in PDF neuron-specific *Lar* RNAi knockdown flies implies that *Lar* functions when sLN_v dorsal projections are forming during or before the L1 larval stage (Helfrich-Forster, 1997). My results suggest that loss of *Lar* alters sLN_v axonal targeting in the dorsal protocerebrum during embryonic or early larval development, thereby impairing PDF signaling, synchronization of the circadian network, and rhythmic activity.

By eliminating sLN_v dorsal projections, *Lar* mutants and RNAi knockdowns disrupt PDF signaling in a novel fashion; pdf^{01} flies have intact sLN_vs but lack PDF expression and PDF neuron ablated flies eliminate sLN_vs entirely and lack PDF expression (Renn et al., 1999). In addition to their arrhythmic activity in DD, pdf^{01} mutants and PDF neuron ablated flies lack morning activity in anticipation of lights-on and display an evening peak in activity ~0.5-1 h earlier than wild-type flies in LD, suggesting that the loss of PDF accounts for both of these diurnal phenotypes (Renn et al., 1999). Unexpectedly, *Lar* RNAi knockdown flies were active in anticipation of lights-on and showed an evening activity peak having a wild-type phase in LD cycles (Fig. 16; Table 6). Although PDF signaling to the dorsal brain is disrupted in *Lar* mutants and RNAi knockdowns, PDF continues to be expressed in sLN_v and lLN_v cell bodies and projections that target the medulla, POT and aMe (Figs. 12, 14, and 15). These results imply that PDF signaling from the remaining sLN_v and lLN_v projections mediates normal diurnal activity with a morning (M) peak at dawn and an evening (E) peak at dusk.

Methods

Fly strains

The following *Drosophila* strains were used in this study: w^{1118}, w^{1118};Cyo/Sco;TM2/TM6B, w^{1118};*tim*Gal4, w^{1118};;*pdf*Gal4, *w;;tim*Gal4, UAS-*Lar*RNAi (P{KK100581}, VDRC), UAS-*Lar* (*w*;P{UAS*Lar*.K}P4B, BDSC), UAS-*Dicer2*;*tim*Gal4, and *w*;UAS-*Dicer2*;*pdf*Gal4 (gifts from Jeffery Price, University of Missouri, Kansas City MO), UAS-mCD8::GFP (*w*;P{UAS-mCD8::GFP.L}LL6, BDSC), *tub*Gal80^{ts} (P{tubP-Gal80^{ts}}20, BDSC), $Lar^{13.2}$ (*w*;$Lar^{13.2}$/CyO, BDSC), *Lar* Df (Df(2L)E55, rdo^{1} $hook^{1}$ *Lar* E55 pr^{1}/CyO, BDSC), and *yw*;;pdf^{01} (a gift from Paul Taghert Washington University, St. Louis, MO). Flies were reared on standard cornmeal/agar medium supplemented with yeast and kept in 12h light/12h dark (LD) cycles at 25°C. The *Lar* mutant strains, $Lar^{13.2}$ and *Lar* Df were backcrossed seven times to y^{1};P{SUPor-P}*Lar* KG04810/CyO;ry^{506} flies (BDSC) to minimize effects due to differences in genetic background.

Drosophila activity monitoring and behavior analysis

One- to 3-d-old male flies were entrained for 3 d in LD cycles and transferred to constant darkness (DD) for 7 d at 25°C. To knockdown *Lar* only in adults using the TARGET system (McGuire et al., 2003), w^{1118};UAS-*Lar*RNAi/*tub*Gal80^{ts};*pdf*Gal4/+ males were raised at the permissive temperature (18°C) for *tub*Gal80^{ts} to block Gal4-dependent expression of *Lar* RNAi. After eclosion, flies were entrained for 3 d in LD and monitored for 7 d in DD at the restrictive temperature (30°C), which allows Gal4-

dependent expression of *Lar* RNAi. Controls lacking *Lar* expression in adults and during development were raised and tested at 18°C. To express *Lar* RNAi only during development, w^{1118};UAS-*Lar*RNAi/*tub*Gal80^{ts};*pdf*Gal4/+ males were raised at 30°C to allow Gal4-dependent *Lar* RNAi expression. After eclosion, flies were entrained for 3 d in LD and monitored for 7 d in DD at the permissive temperature (18°C). Controls that express *Lar* during development and in adults were raised and tested at 30°C. Locomotor activity was monitored using the *Drosophila* Activity Monitor system (Trikinetics). To determine period and rhythm strength during DD, X^2 periodogram analysis was performed using ClockLab (Actimetrics) software as previously described (Pfeiffenberger et al., 2010). Flies were considered rhythmic if their X^2 power value was ≥ 10 above the significance line (i.e., strength ≥ 10) and they were clearly rhythmic by visual inspection of the actogram. For analysis of activity during LD conditions, flies were monitored for 7 d. The number of activity events were recorded in 30 min bins, and average numbers of activity events per 30 min bin per fly were calculated to generate histograms. The times of morning and evening activity peaks (phase values) were computed using ClockLab. Morning Anticipation Index values were calculated as the ratio of activity counts occurring 3 h before lights-on over activity counts occurring 6 h before lights-on as described previously (Harrisingh et al., 2007; De et al., 2013). All *p* values were calculated using a Student's two-tailed *t* test with unequal variance.

Immunohistochemistry

Antibody staining of larval CNSs and adult fly brains was performed as previously described (Houl et al., 2008). Briefly, larval CNSs and adult brains were dissected in 1X PBS and fixed with 3.7% formaldehyde in 1X PBS at room temperature (RT) for 15 mins. Samples were then washed and incubated with blocking solution containing 1X PBS, 5% BSA, 5% goat serum (5% donkey serum for primary antibodies raised in goat), 0.03% sodium deoxycholate, and 0.03% TritonX100 at RT for 1 h followed by incubation with primary antibodies overnight (ON) at 4°C in blocking solution. Primary antibodies and their dilutions used were as follows: guinea pig anti-CLK GP50 1:3000 (Houl et al., 2008), goat anti-CLK dC-17 (Santa Cruz Biotechnology) 1:100, rabbit anti-GFP ab6556 (Abcam) 1:500, pre-absorbed rabbit anti-PER (a gift from Michael Rosbash, Brandeis University, Waltham, MA) 1:15,000, and mouse anti-PDF (Developmental Studies Hybridoma Bank) 1:500. For detection of primary antisera, the following secondary antibodies were used at a dilution of 1:200 (incubated ON at 4°C) in blocking solution: goat anti-rabbit AlexaFluor 488 (Invitrogen), donkey anti-rabbit AlexaFluor 647 (Invitrogen), goat anti-guinea pig Cy-3 (Jackson ImmunoResearch Laboratories), donkey anti-guinea pig AlexaFluor 488 (Invitrogen), goat anti-mouse AlexaFluor 488 and AlexaFluor 647 (Invitrogen), and donkey anti-goat AlexaFluor 488 (Invitrogen). Brains were then mounted in Vectashield mounting medium (Vector Labora-tories) for imaging. Entrained L3 larvae or 1- to 5-d-old adults were used for dissection.

Imaging

Larval CNSs and adult fly brains were imaged using an Olympus FV1000 confocal microscope (Olympus America) as described previously (Liu et al., 2015). Briefly, serial optical scans were obtained at 2 µm intervals without using Kalman-averaging. For coimmunostaining experiments, sequential scans of the Argon 488 nm and HeNe (543 nm for Cy3, 633 nm for AlexaFluor 647 and Cy5) lasers were used to avoid bleed-through between channels. For imaging AlexaFluor 488 and Cy3; Argon 488 nm and HeNe 543 nm lasers were used, with the 405/488/543 nm dichronic mirror for excitation whereas for imaging AlexaFluor 488 and either AlexaFluor 647 or Cy5; Argon 488 nm and HeNe 633 nm lasers were used, with the 488/543/633 nm dichronic mirror for excitation. Fluorescence signals were separated by a beam splitter (560 nm long pass) and recorded on spectral detectors set to 500-530 nm for AlexaFluor 488, 555-655 nm for Cy3, and a detector with 650 nm long pass filter for AlexaFluor 647 or Cy5. The Fluoview "Hi-Lo" lookup table was used to set the maximal signal below saturation and set the background to near zero using the high voltage and offset controls. Original Olympus images were saved as 12 bit oib format and processed using FV1000 confocal software to generate Z-stack series. Images were adjusted for brightness and contrast using FV1000 confocal software when needed. For each genotype and developmental stage, brain images were acquired using the same settings (power, gain, offset) at the same time.

Western blot analysis

For preparing protein extract from adult fly heads, flies were entrained in LD cycles for at least 3 d and collected at circadian time (CT)2, CT10, and CT22 on day 1 of constant darkness. Lysis was performed in radioimmunoprecipitation assay buffer (20 mM Tris, pH 7.5, 150 mM NaCl, 1 mM EDTA, 0.05 mM EGTA, 10% glycerol, 1% Triton X-100, 0.4% sodium deoxycholate, 0.1% SDS) containing protease inhibitor mixture (0.5 mM phenylmethylsulfonyl fluoride, 10 µg/ml aprotinin, 10 µg/ml leupeptin, 2 µg/ml pepstatin A, 1 mM Na_3VO_4, and 1 mM NaF). This homogenate was sonicated five to eight times for 10 s each, using a Microson ultrasonic cell disruptor at a setting of 4-5, and then centrifuged at 20,000 X *g* for 10 mins. The supernatant was collected and protein concentration was determined by the Coomassie-based Bradford Assay. Three hundred nanograms of total protein for each genotype were loaded in each lane. Soluble protein extracts were separated on 5% polyacrylamide electrophoresis gels, transferred to supported nitrocellulose membranes (MSI) and incubated with GP50 anti-CLK (1:4000), pre-absorbed rabbit anti-PER (1:65,000, a gift from Michael Rosbash), rat anti-TIM (1:1000, a gift from Amita Sehgal, University of Pennsylvania, Philadelphia, PA), or anti-β-ACTIN (1:5000; Sigma-Aldrich) antibodies. Goat anti-rabbit, anti-guinea-pig, anti-rat, and anti-mouse conjugated to horseradish peroxidase were used at a 1:2000 dilution (Jackson Immunoresearch) as secondary antibodies. Chemiluminescent detection was used to develop the reaction using ECL plus (GE Healthcare) reagent.

CHAPTER IV

CHARACTERIZING CRYPTOCHROME EXPRESSION AND FUNCTION IN PERIPHERAL TISSUES OF *Drosophila melanogaster*

Background

Circadian (~24 h) clocks regulate daily cycles in gene expression to control overt rhythms in physiology, metabolism and behavior. In *Drosophila*, rhythmic gene expression is activated by CLOCK-CYCLE (CLK-CYC) complexes, repressed by PERIOD-TIMELESS (PER-TIM) complexes, and synchronized to light:dark (LD) cycles primarily by the blue light photoreceptor CRYPTOCHROME (CRY). Upon detection of light, CRY binds TIM and promotes its light-dependent degradation, thus entraining the molecular clockwork to LD cycles. Furthermore, CRY alters K^+ channel conductance in a subset of *Drosophila* pacemaker neurons, the lLN_vs, in response to light, thereby affecting neuronal and behavioral excitability.

CRY proteins also have light-independent transcriptional functions in many animals and, like other canonical clock proteins, CRY may play non-circadian roles. Although CRY expression has been characterized in brain neurons of *Drosophila*, it remains unclear which CRY functions extend to peripheral clock and non-clock tissues. To address these questions, I first showed that an N-terminally GFP-tagged-*cry* transgene rescues light-induced phase resetting in the cry^{03} null mutant flies, demonstrating that GFP-CRY protein functions similar to wild-type CRY with respect to behavioral rhythms. Immunostaining with anti-GFP reveals the expected GFP-CRY

expression pattern in the brain, and GFP-CRY promotes light-dependent TIM degradation in a model peripheral tissue containing clocks, the Malpighian tubules (MTs). Using larval salivary glands, which lack a functional circadian clock and are amenable to electrophysiological recording, I found that CRY regulates cell membrane physiology; membrane input resistance (R_i) in *cry*^{03} null mutant glands decreased significantly compared to the wild-type, and was rescued by the GFP-*cry* transgene. The impact of CRY on the membrane properties of these non-excitable cells is light-independent and is likely mediated by K^+ channels. In support of a role for these ion channels in CRY function, salivary gland cells of transheterozygous *cry* and K^+ channel subunit mutants show decreased R_i similar to that of homozygous *cry* or K^+ channel subunit mutants. These findings for the first time define the expression profile of CRY in the peripheral tissues and reveal that CRY protein is required for light-independent, cell-autonomous and K^+ channel-dependent changes in membrane function in peripheral tissues devoid of a canonical circadian clock.

Results

Since CRY is proposed to act as a circadian photoreceptor and is required for oscillator function in many peripheral tissues, I anticipated that CRY protein should be expressed in all peripheral clock tissues. Several methods have been used previously to analyze *cry* spatial expression primarily in the brains of adult flies. However, these results vary depending on the genetic and immunological reagents used (Egan et al., 1999; Emery et al., 2000; Zhao et al., 2003; Klarsfeld et al., 2004; Yoshii et al., and Benito et al., 2008).

Nonetheless, a common theme emerges from these results; CRY is only expressed in a subset of brain pacemaker neurons, which suggests that pacemaker neurons lacking CRY are indirectly entrained to light. The loss of circadian oscillator function and/or synchrony in peripheral tissues of cry^{b} flies implies that CRY is expressed in these tissues, yet CRY expression has not been directly assessed in *Drosophila* peripheral tissues. Furthermore, since CRY may function to control oscillator function in some of these tissues by rhythmically repressing CLK-CYC activity in the nucleus (Collins et al., 2006), it is possible that rhythms in CRY nuclear translocation could also occur in the peripheral clocks. Therefore, I sought to characterize the spatial and subcellular localization of CRY protein in *Drosophila* peripheral tissues during the circadian cycle.

To detect CRY expression with high sensitivity, a BAC transgene was generated that expresses an N-terminal GFP-tagged *cry* (see Methods). As expected, the GFP-*cry* transgene in cry^{03} null mutant background had a wild-type period of ~24 h in constant darkness (DD) (Table 7 and Fig. 17), demonstrating that the GFP-CRY fusion protein has no impact on oscillator function in pacemaker neurons. CRY plays a prominent role in behavioral photoresponses and photosensitivity; in response to brief light pulses, wild-type flies manifest phase delays during the early night (ZT15) and phase advances late at night (ZT21), but light-dependent phase shifts are not seen in *cry* mutants (Stanewsky et al., 1998; Emery et al., 1998 and 2000; Dolezelova et al., 2007). Flies containing the GFP-*cry* transgene in cry^{03} mutant background showed phase shifts with bright light pulse both in the delay zone, at ZT15, and the advance zone, at ZT21, consistent with the wild-type CRY function in clock-resetting (Table 7 and Fig. 17). Furthermore, constant

light (LL) results in intensity dependent arrhythmia in wild-type *Drosophila*, whereas cry^{03} flies remain robustly rhythmic (Table 7; Emery et al., 2000). As in wild-type flies, activity rhythms in GFP-*cry*;cry^{03} transgenic flies were abolished in LL, demonstrating that GFP-CRY functions similarly to CRY in wild-type flies.

Table 7: GFP-*cry* transgenic flies rescue behavioral arrhythmicity of cry^{03} null mutants in LL. Analysis of activity rhythms in DD, LL and fly genotypes are as described in Methods.

Genotype	**Total**	**% Rhythmic**	**Period ± SEM**
w^{1118};+;+	9	78	23.64 ± 0.13
w^{1118};+;cry^{03}	11	82	24.41 ± 0.13
w^{1118};GFP-*cry*;cry^{03}	15	93	23.32 ± 0.06
w^{1118};+;+ (LL)	13	0	n.a.
w^{1118};+;cry^{03} (LL)	13	92	24.88 ± 0.24
w^{1118};GFP-*cry*;cry^{03} (LL)	12	0	n.a.

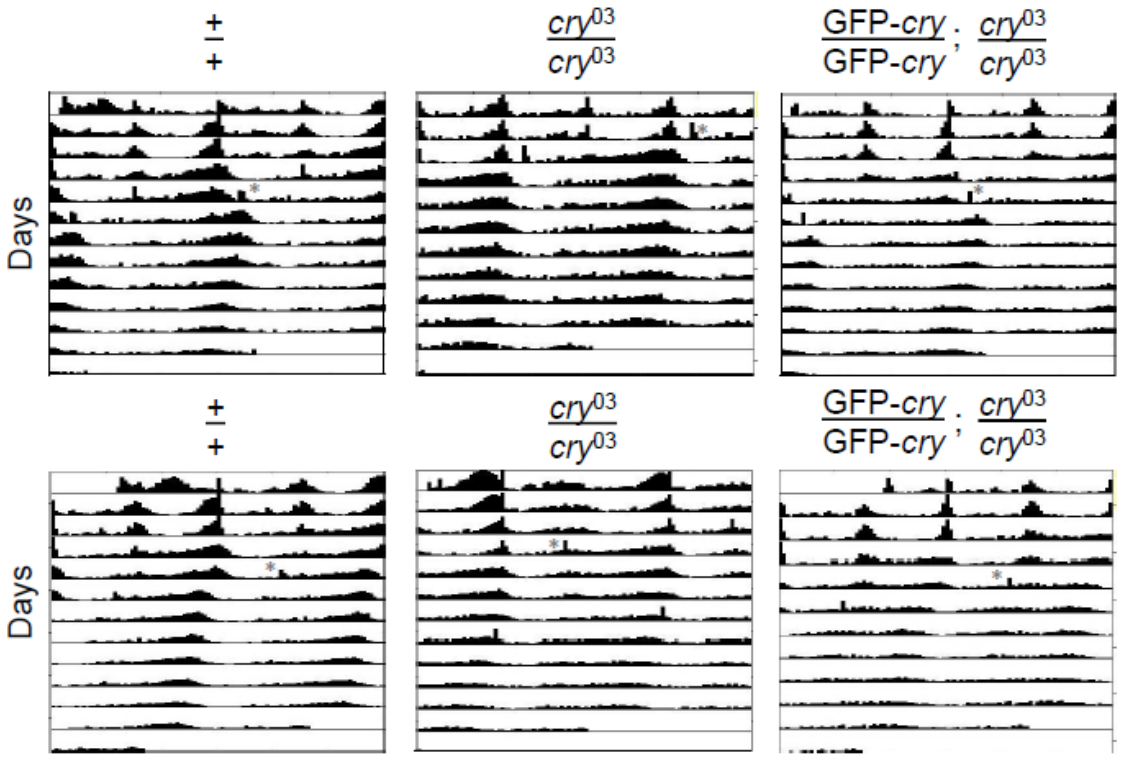

Figure 17: GFP-*cry* transgenic flies rescue light induced phase shifts of *cry*^{03} null mutants. Representative double-plotted actograms for average of total number of flies of each genotype are shown. White boxes, lights-on period; black boxes, lights-off period; vertical bars, fly activity. The height of vertical bars indicates relative level of activity.

Localization of GFP-CRY in the brain and peripheral tissues

To determine the subcellular localization of GFP-CRY, brains from GFP-*cry*;*cry*^{03} flies were visualized by confocal microscopy. GFP-CRY was detected in all clock brain neurons previously identified via CRY antibody staining including the small LN_vs (sLN_vs), large LN_vs (lLN_vs), and a subset of LN_ds and DN_1s. No staining was detected in DN_2s, DN_3s and the LPNs, as previously reported (Fig. 18A; Yoshii et al., and Benito et

al., 2008). In a majority of the CRY positive cells, some immunofluorescent signal was distributed throughout the cytoplasm, but most of the signal was detected in the nucleus and perinuclear region starting ZT16 (Fig. 18A). Previous studies show that CRY is degraded in response to light and accumulates to high levels in the dark (Emery et al., 1998; Yoshii et al., 2008). Consistent with this observation, Western blot analysis of GFP-CRY protein showed rhythmicity in response to LD cycles in GFP-*cry*;*cry*^{03} transgenic fly brains, and accumulation to constant high levels under constant dark conditions (Fig. 18B). Similarly, when flies were reared in DD, CRY immunoreactivity was constantly high in all the expected cells; and was also detected in some projections and additional non-clock cells (ellipsoid body neurons) along with faint expression in some DN_3s (Fig. 18A). No labeling was observed in the clock neurons, in the ellipsoid body neurons, or in the projections of *cry*^{03} mutant brains reared in LD or DD (data not shown), demonstrating the specificity of GFP immunostaining.

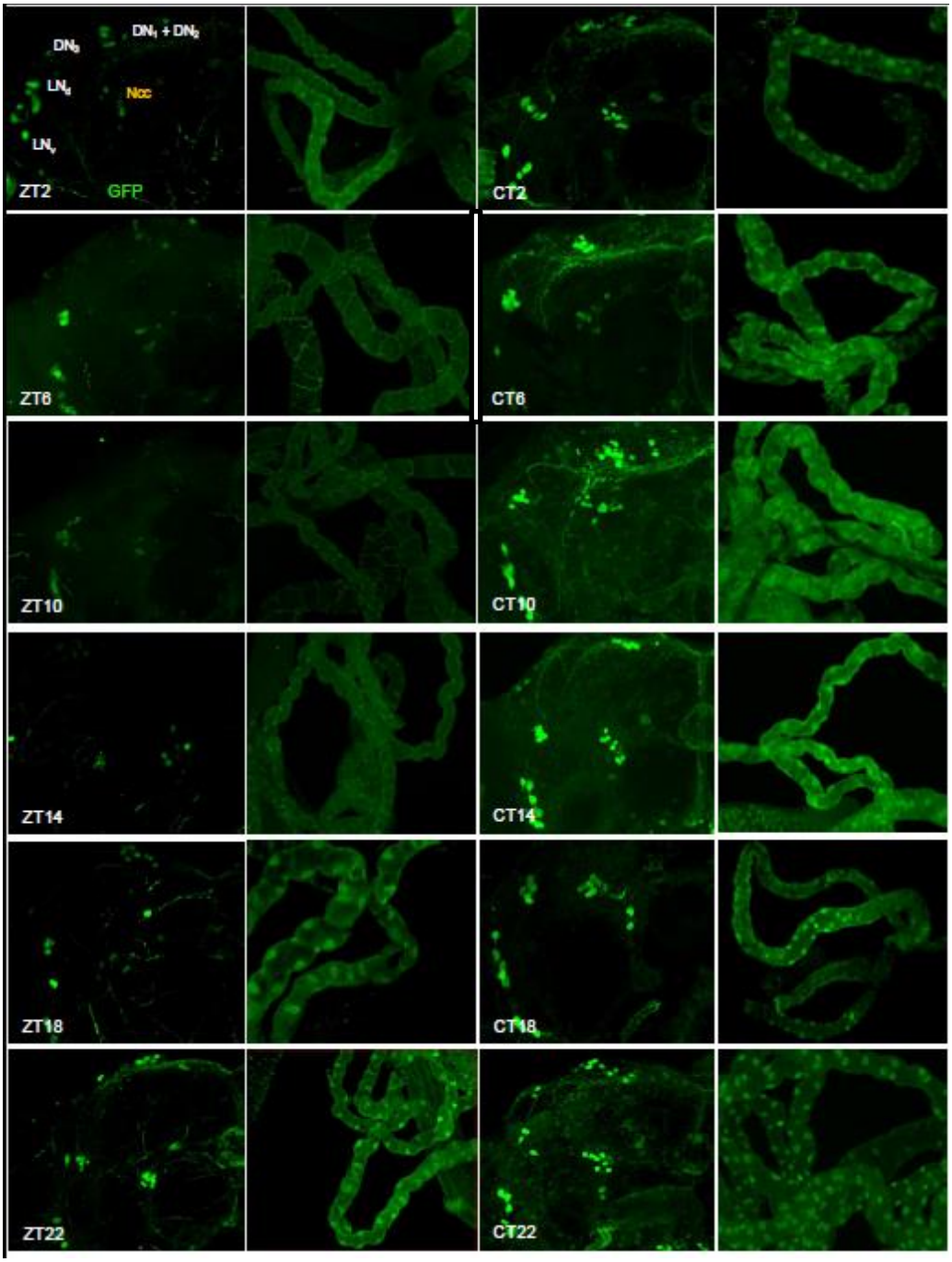

Figure 18: GFP-CRY is rhythmically expressed in the adult fly brains, Malpighian tubules and head extracts in an LD cycle but accumulates in DD. A. Brains and MTs dissected from adult flies collected during a circadian cycle were immunostained with GFP antisera and imaged by confocal microscopy. B. Western blots of head extracts from w^{1118};GFP-*cry*;*cry*^{03} flies, probed with GFP and actin antisera.

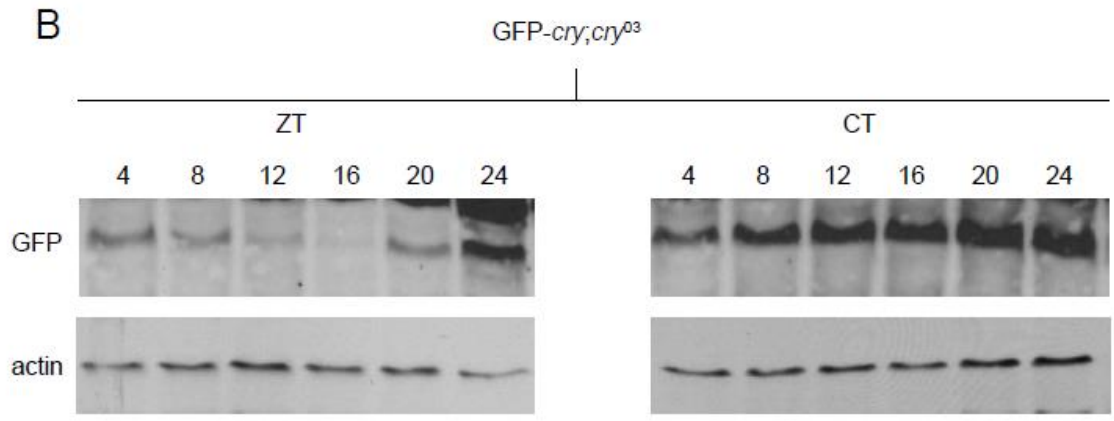

Figure 18 Continued

A previous study shows that CRY is expressed in the compound eyes (Yoshii et al., 2008), but CRY expression has not been characterized in other fly peripheral tissues. I used the GFP-*cry* transgene to assess CRY expression in the peripheral tissues, with a focus on MTs as a representative peripheral tissue. As seen in brain pacemaker neurons, GFP-CRY staining was observed in both the nucleus and cytoplasm, but staining in the nucleus appeared to be stronger than in the cytoplasm at peak time points in the adult MTs (Fig. 18A). The expression profile of GFP-CRY in the LD cycle in the MTs indicates CRY is low during the day and high during the night (Fig. 18A), implying a light-dependent degradation of CRY even in the peripheral tissues. Moreover, GFP-CRY immunoreactivity in MTs during DD showed no obvious cycling of CRY protein (Fig. 18A). Hence, the GFP-*cry* transgene is expressed in all the expected brain pacemaker neurons, in the MTs, and in other clock-containing peripheral tissues (e.g. the fat body, antennae, and intestine; data not shown).

Loss of TIM responsiveness to light in Malpighian tubules of cry^{03} mutants

To investigate whether CRY mediates TIM degradation in response to light in peripheral tissues, I monitored levels of TIM and PER in whole-mount preparations of MTs from *cry*^{03} and GFP-*cry*;*cry*^{03} flies collected during the night (ZT14 for PER and ZT22 for TIM) and during the day (ZT2 for PER and ZT10 for TIM). In GFP-*cry*;*cry*^{03} rescue controls, high PER (ZT2) and TIM (ZT22) staining could be detected during the peak times (Fig. 19) compared to the trough, reflecting rhythmic PER and TIM expression in this peripheral tissue. However, the *cry*^{03} mutation abolished fluctuations of PER and TIM immunoreactivity in MTs (Fig. 19), similar to what has been observed in *cry*^{b} mutant flies (Ivachenko et al., and Krishnan et al., 2001).

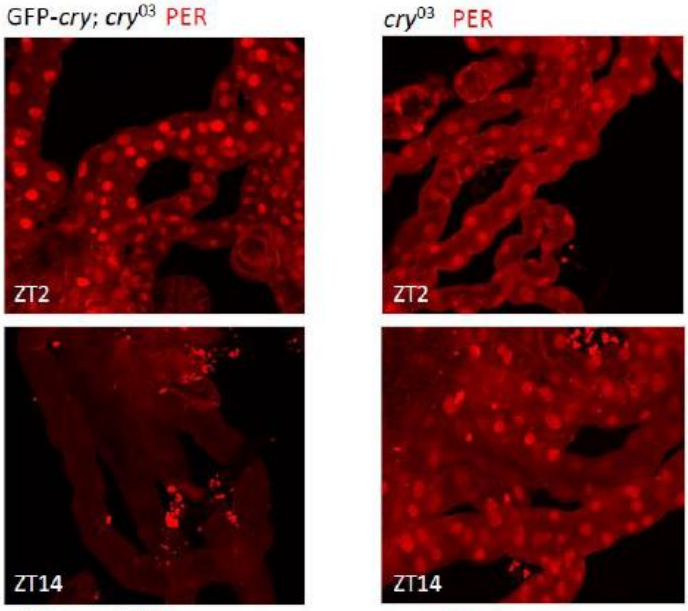

Figure 19: CRY is required for oscillator function in adult fly Malpighian tubules. MTs dissected from adult *w*^{1118};GFP-*cry*;*cry*^{03} and *w*^{1118};+;*cry*^{03} flies collected at the indicated time points during a circadian cycle were immunostained with PER or TIM antisera and imaged by confocal microscopy.

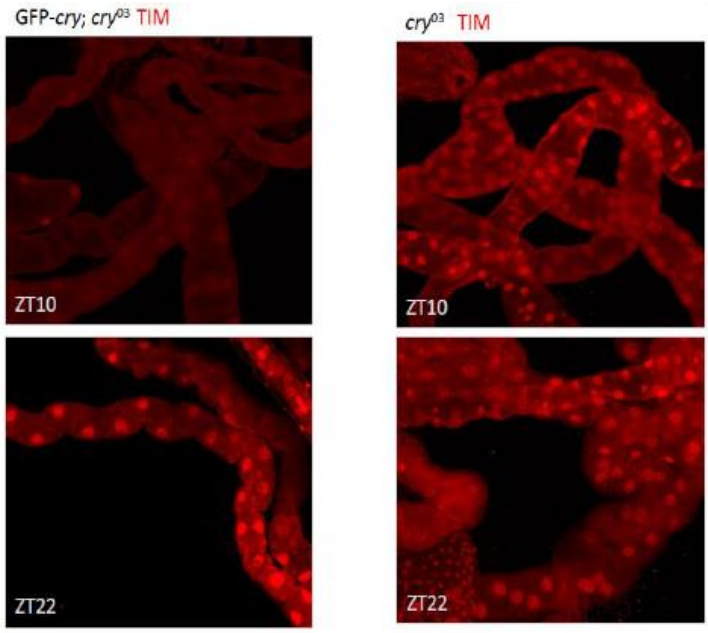

Figure 19 Continued

I further investigated whether GFP-CRY mediated light-dependent TIM degradation in MTs. I exposed GFP-*cry*;*cry*^{03} transgenic flies and *cry*^{03} mutant flies to 60 min in light pulses and assessed GFP and TIM levels by co-immunostaining at the end of the light exposure, which corresponded to ZT16 and ZT22 respectively. Like brain pacemaker neurons in wild-type flies, GFP-CRY and TIM are degraded in MTs from light-treated GFP-*cry*;*cry*^{03} at both times of day (Fig. 20*A*-*R*). In contrast, control (non-light-treated) GFP-*cry*;*cry*^{03} flies and *cry*^{03} flies showed TIM staining in the nuclei of LN_v (data not shown) and MT cells at ZT16 (Fig. 20*A*-*I*) and ZT22 (Fig. 20*J*-*R*). These observations demonstrate that GFP-*cry*;*cry*^{03} transgenic flies rescue light-dependent CRY mediated TIM degradation in peripheral tissues. The absence of TIM degradation

in *cry*^{03} flies is consistent with previous work showing that light doesn't cause TIM degradation in the *cry*^{b} mutant (Ivachenko et al., 2001).

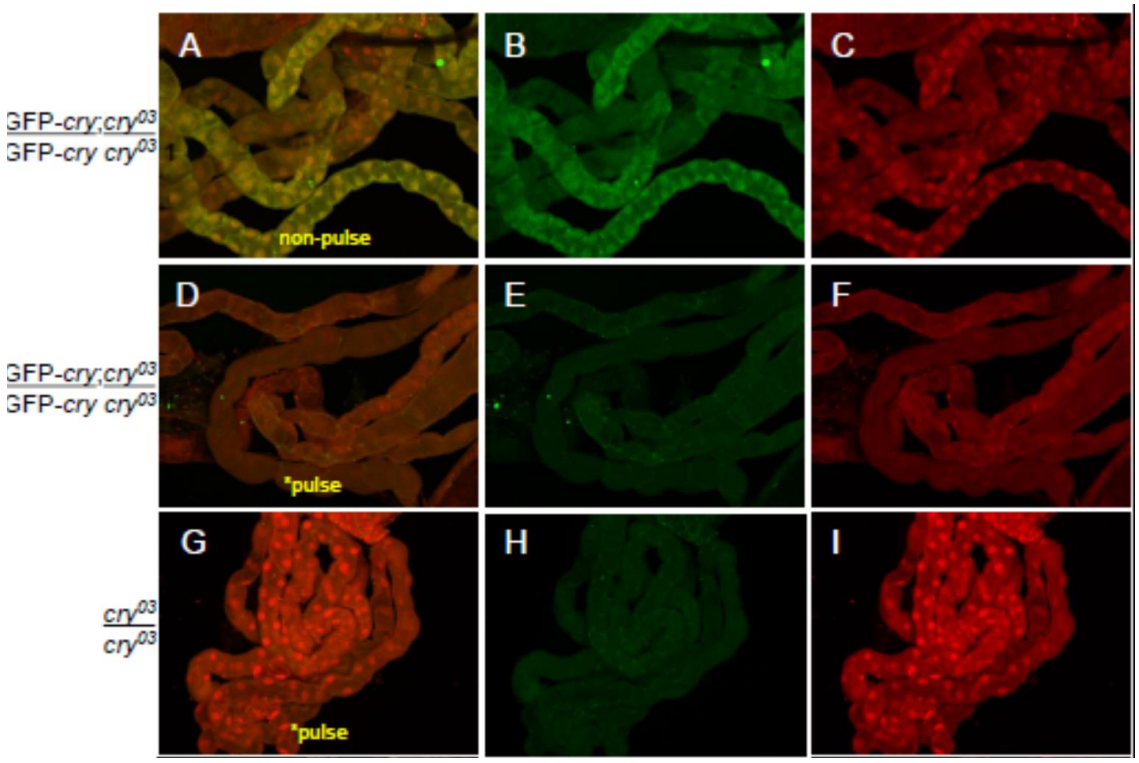

Figure 20: CRY in MTs is photo-responsive and triggers light-dependent TIM degradation. A. MTs dissected from adult flies collected after the indicated light exposure regime, were immunostained with GFP and TIM antisera and imaged by confocal microscopy. Other details are as described in the text. B. Light dependent interaction between GFP-CRY and TIM in fly bodies. CRY complexes pulled down using GFP-nanobodies from *w*^{1118};GFP-*cry*;*cry*^{03} fly bodies and then probed with GFP and TIM antisera for Western blot analysis. Other details are as described in the text and Methods.

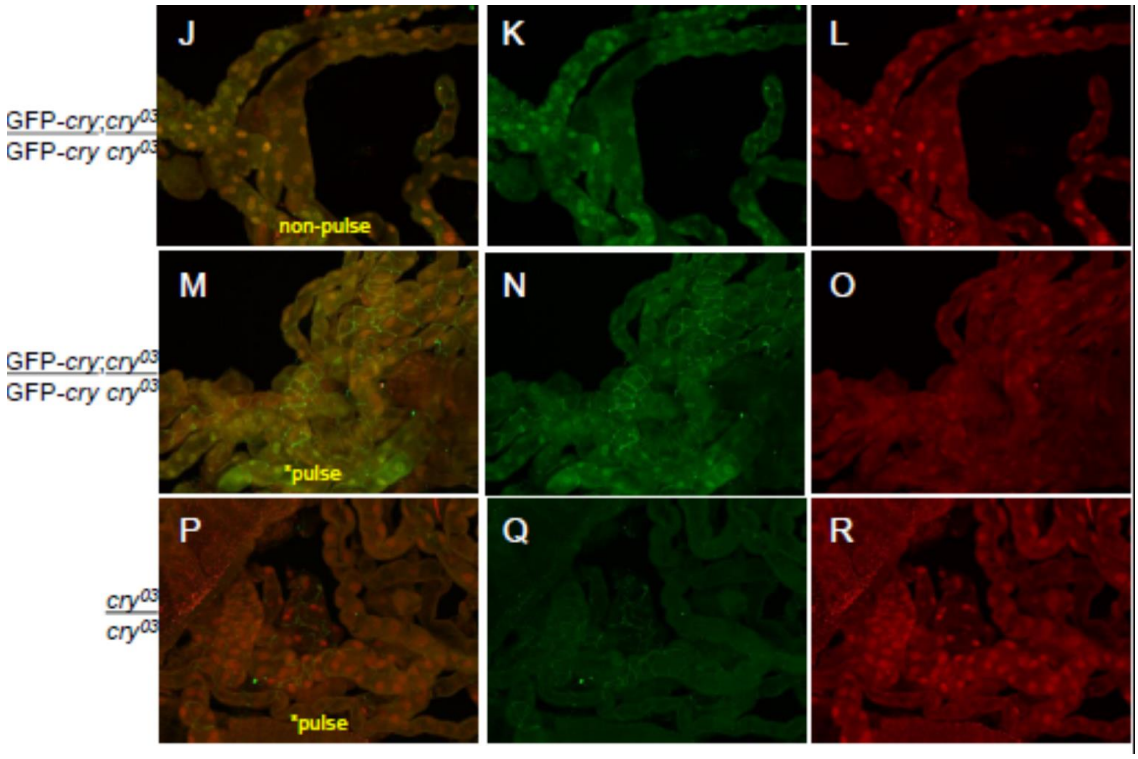

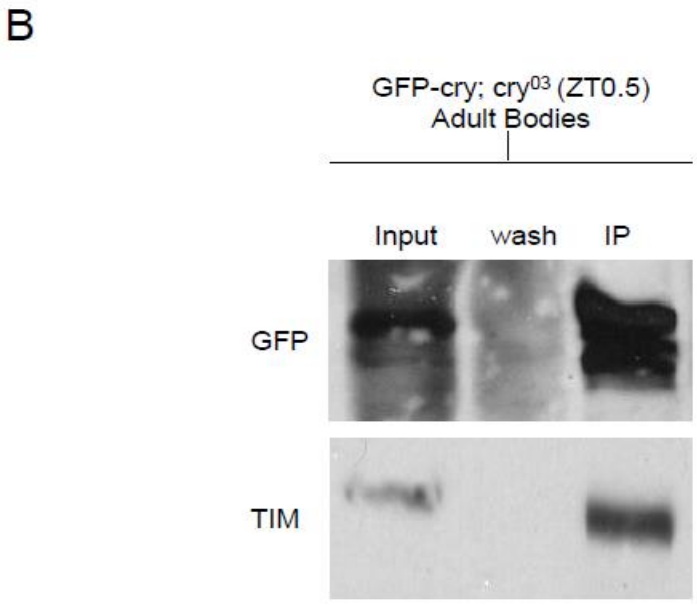

Figure 20 Continued

Light promotes CRY and TIM interaction in peripheral tissues

To determine whether GFP-CRY functions as a circadian photoreceptor and/or a transcriptional regulator in peripheral tissues from *Drosophila*, I performed co-immunoprecipitation assays to identify proteins that interact with CRY using GFP nanobodies to immunoprecipitate GFP-CRY complexes. Antibodies against CLK, PER, and TIM were used to probe Western blots containing adult MT extracts from GFP-*cry* transgenic flies and control GFP flies (data not shown) collected at ZT0.5 and 30 mins after lights would have turned on during day one in constant darkness, or Circadian Time 0.5 (CT0.5). These time points were selected to detect any light dependent CRY interactions with other clock proteins when transcriptional repression is expected to be high. Neither CLK nor PER was pulled down with GFP-CRY at either time point (data not shown), whereas TIM showed a light dependent interaction with GFP-CRY at ZT0.5 (Fig. 20*B*). These results demonstrate that light induces CRY-TIM interactions in fly bodies, but no interactions between CRY and PER or CLK occur. It is difficult to distinguish if lack of interaction between GFP-CRY and PER or CLK proteins is due to technical difficulties (e.g. transient or weak interactions) or if CRY is simply not acting as a transcriptional repressor in fly peripheral tissues.

Passive membrane properties of non-clock peripheral tissues are altered in CRY mutants

Previous studies demonstrate that lLN_vs mediate light-driven arousal behavior (Shang et al., 2008; Sheeba et al., 2010). Light stimulated arousal is dependent on CRY, which responds to light by initiating a rapid K^+ channel dependent increase in the firing rate of

lLN$_v$s and even non-clock neurons (Fogle et al., 2011). To investigate a role for CRY in controlling passive membrane properties in a non-excitable *Drosophila* peripheral tissue, I measured resting membrane potential (RMP) and input resistance (R_i) in larval salivary glands (Versalis et al., 1991). Although larval salivary glands express CRY (Fig. 21), this tissue lacks circadian clock function (data not shown).

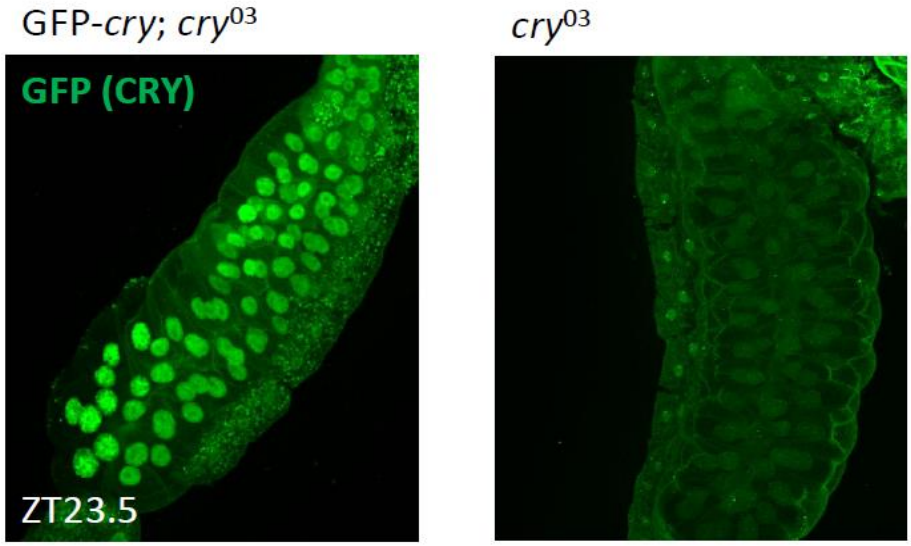

Figure 21: GFP-CRY is expressed in the larval salivary glands. Salivary glands dissected from w^{1118};GFP-*cry*;*cry*^{03} and w^{1118};+;*cry*^{03} L3 larvae, collected at the indicated time point during an LD cycle, were immunostained with GFP antisera and imaged by confocal microscopy.

Using wild-type, transgenic GFP-*cry*;*cry*^{03} and *cry*^{03}strains that had been entrained in LD cycles, I observed an RMP of similar magnitude in each genotype, suggesting CRY does not affect the RMP of larval salivary gland cells (Fig. 22*A*).

However, upon injection of hyper-polarizing current, the input resistance in *cry*^{03} salivary glands was significantly reduced compared to the wild-type and GFP-*cry*;*cry*^{03} rescue controls (Fig. 22*A*). Next, to determine if this impact on membrane physiology by CRY is light-dependent, I tested electrophysiological responses of these tissues right before lights off (when CRY is expected to be degraded) and on day one of constant darkness (at CT0.5) after LD entrainment (when CRY levels are expected to be high). I found that the RMP and R_i did not differ between wild-type and GFP-*cry*;*cry*^{03} rescue controls in either light condition (Fig. 22*B*). However, *cry*^{03} mutants still exhibited significantly reduced R_i, indicating that this CRY mediated effect on membrane resistance is independent of time of day or light (Fig. 22 *A and B*). To further validate a light-independent function for CRY in the larval salivary gland, both RMP and R_i were recorded from the same genotypes under dark conditions in response to high intensity white light pulse exposure (450 to 700 nm). Consistent with the results in the light during LD cycles, the R_i did not significantly decrease in the CRY/GFP-CRY expressing genotypes in response to an acute light pulse. Thus, CRY is required to maintain membrane physiology in non-clock containing larval salivary glands in a time of day and light-independent manner.

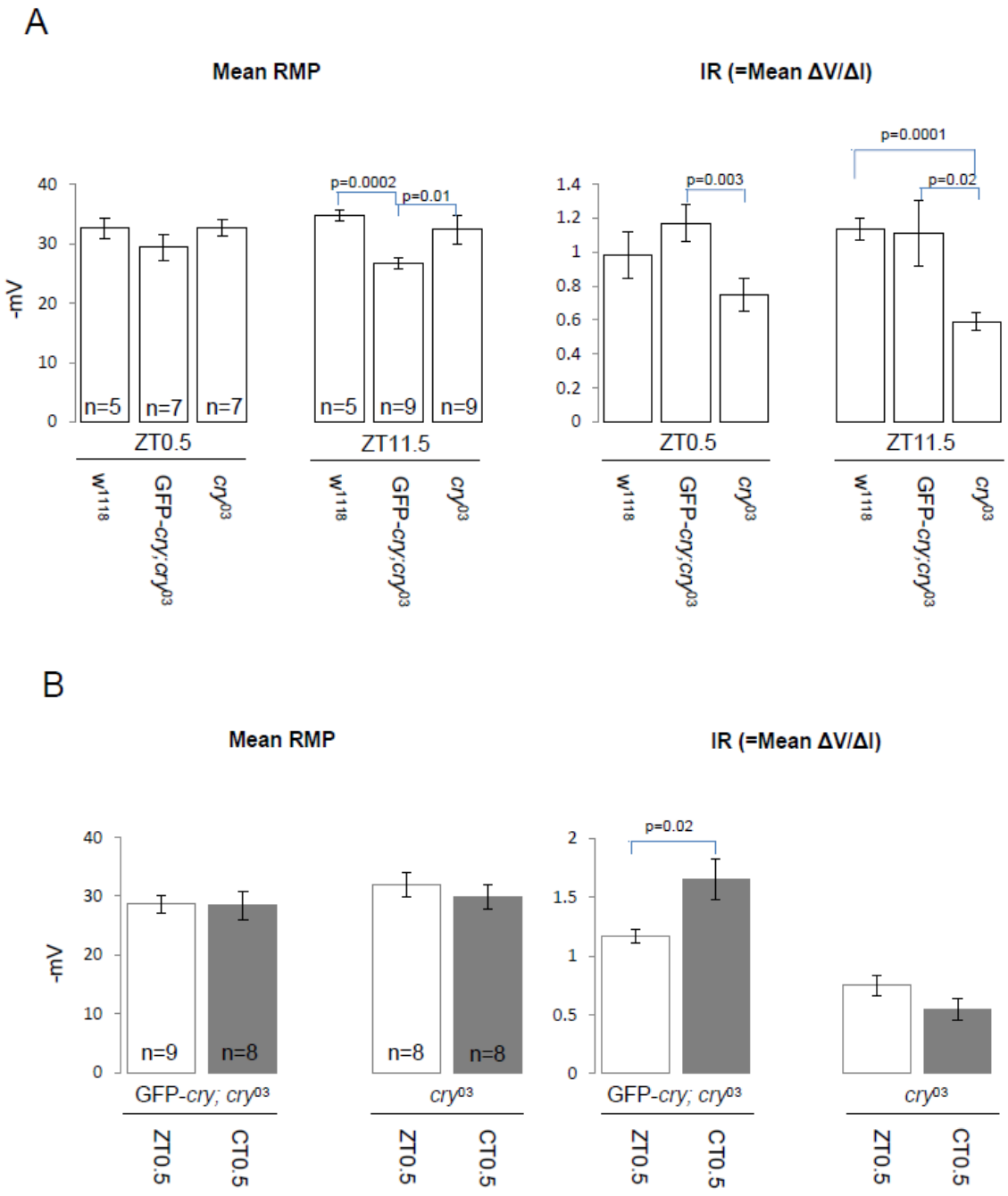

Figure 22: A and B. *Cry* mutants show a decrease in input resistance (R_i) of the larval salivary gland cells in a time of day (A) and light (B) independent manner. IR, Input Resistance; Mean ΔV, Mean change in voltage; ΔI, Change in current; error bars, standard error of the mean; ZT, Zeitgeber Time; and CT, Circadian Time. Other details are as described in the text and Methods.

CRY mediated differences in R_i are attenuated in K^+ channel mutants

Acute pharmacological block of K^+ channel currents eliminates the CRY mediated lLN_v light responses (Fogle et al., 2011). ETHER-A-GOGO (EAG) family K^+ channels regulate membrane resting potential and action potential repolarization, whereas SHAKER-type (SH) K^+ channels, which also co-assemble with HYPERKINETIC (HK), have very little effect on membrane resting potential, but regulate firing rate subject to rapid inactivation that contributes to cumulative inactivation (Peng and Wu, 2007). As K^+ channel signaling appears to be important for the CRY mediated neuronal responses, I tested whether EAG and SH K^+ channels, along with their co-assembled regulatory subunit HK, contributed to CRY mediated light-independent changes in R_i of larval salivary gland cells. RMP and R_i in salivary gland cells of *Hk* Kvß subunit (*Hk*^{1} and *Hk*^{2}), *Sh* (*Sh*^{5}) and *eag* (*eag* amorphic) K^+ channel mutants were recorded at ZT0.5 in an LD cycle. As previously observed, baseline RMP was comparable for all genotypes tested, with a small but significant, decrease in values for *Sh*^{5} and *eag* amorphic mutants (Fig. 23*A*). However, as observed for *cry*^{03} mutants, the membrane electrophysiological response to injected hyperpolarizing current in all of the K^+ channel mutant flies was significantly lower than GFP-*cry*;*cry*^{03} controls (Fig. 23*A*). Furthermore, to test if this attenuated R_i response in K^+ channel mutants was in fact acting through CRY, I generated transheterozygotes of different K^+ channel mutants and *cry*^{03}. Amazingly, these transheterozygous mutants showed a significantly lower R_i that was comparable to the R_i response observed for the individual homozygous mutants, but significantly lower than their respective heterozygous single mutant controls (Fig. 23*B*). This result suggests

that there is a strong genetic interaction between CRY and these K^+ channel subunits, which may act together to control membrane responses in larval salivary gland cells. In addition, mutants that eliminate any of these single components (i.e. *cry* or *Hk*) thus reducing R_i, can be rescued by salivary gland-restricted expression of their respective wild-type genes (Fig. 24), further demonstrating a cell-autonomous role for CRY and HK on larval salivary gland membrane responses.

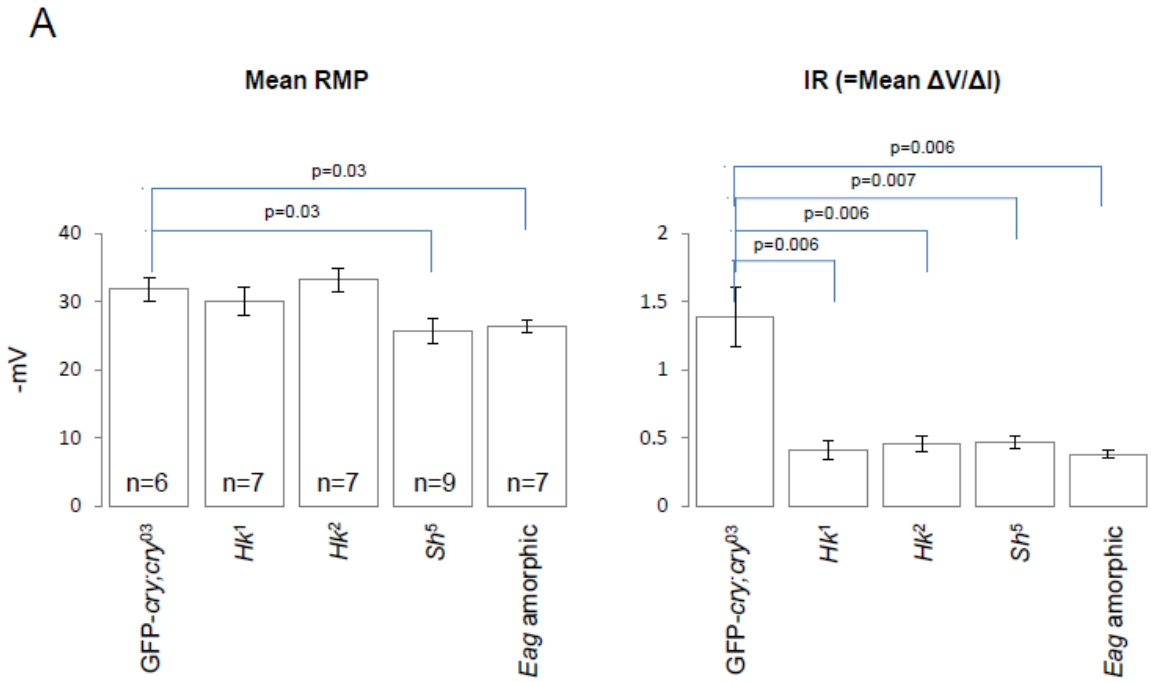

Figure 23: CRY mediates changes in R_i of salivary gland cells in collaboration with K^+ channel subunits. **A.** K^+ channel mutants show a decrease in R_i of the gland cells comparable to *cry*^{03}. B. CRY is required to bring about changes in membrane potential of the peripheral tissues through K^+ Channels. Other details are as described in text, Fig. 22 and Methods.

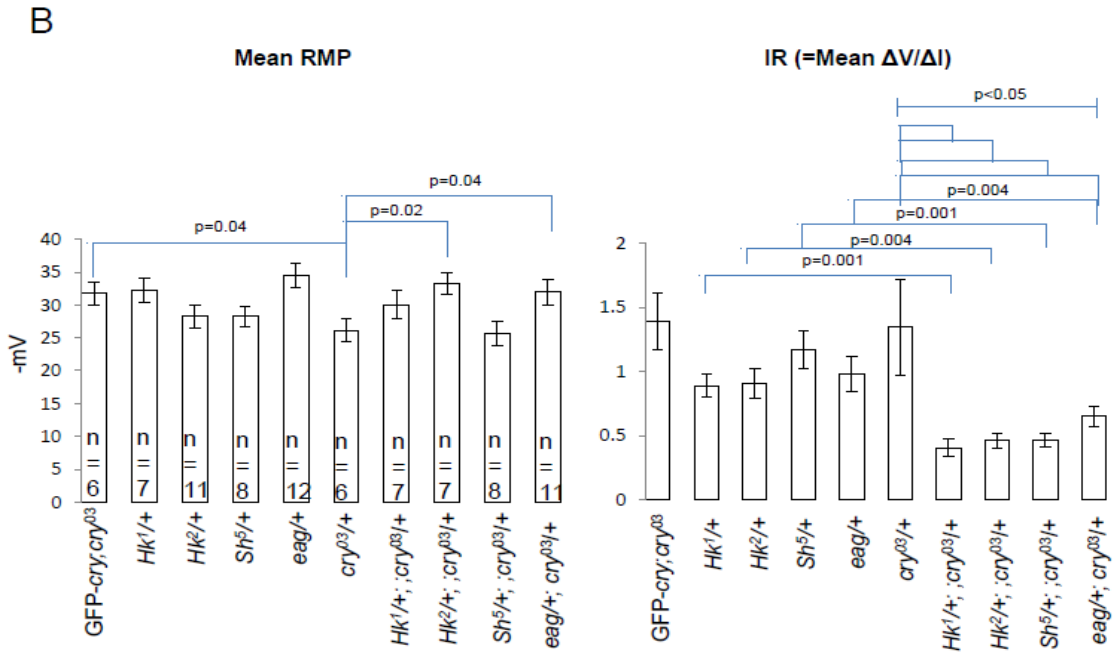

Figure 23 Continued

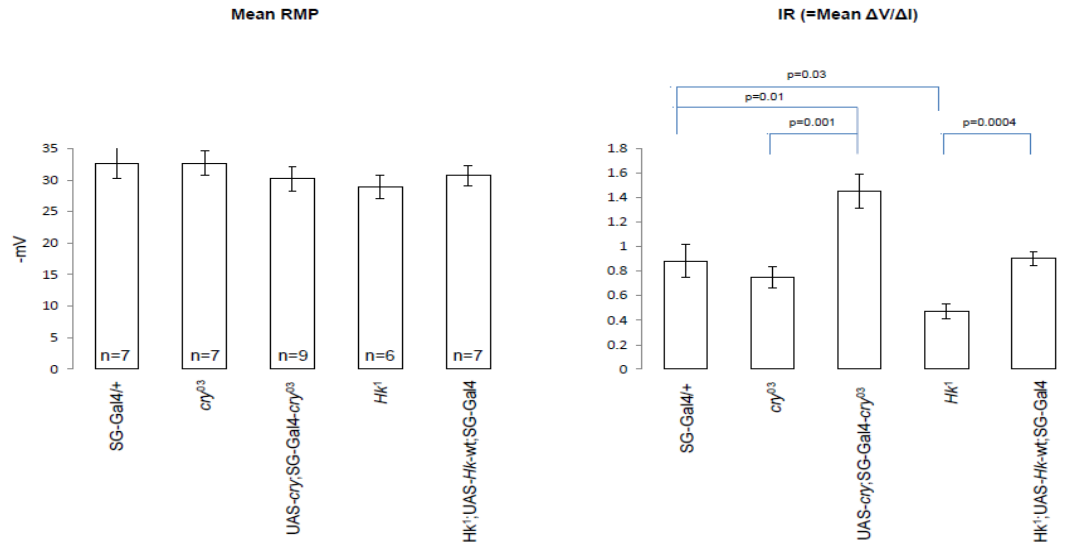

Figure 24: Salivary gland-restricted expression of the wild-type copy of *cry* and *Hk*, both rescue the null mutant phenotype in R_i suggesting a cell-autonomous role for CRY and HK in mediating the membrane responses. Other details are as described in text, Fig. 22 and Methods.

Conclusions

The fruit fly, *Drosophila melanogaster*, is a powerful system for elucidating the molecular mechanisms that underlie circadian rhythms. The circadian clock of *Drosophila*, like that of other animals, is exquisitely sensitive to changes in the environment that impart time-of-day cues, such as temperature changes and light. Specific wavelengths of light act directly on the clock, primarily through CRY, a blue-light photoreceptor. CRY activation causes rapid TIM degradation (Ceriani et al., 1999; Koh et al., 2006), which resets the clock on a daily basis at dawn and on an acute basis following a light pulse during the night hours. In the absence of *cry*, clocks in the LN_vs can still be entrained by photic input through the visual system (Helfrich-Forster et al., 2001; Ashmore and Sehgal, 2003).

Studies employing different strategies to characterize CRY expression pattern in the fly brain have produced variable results. However, these studies all show that CRY is expressed in multiple groups of pacemaker neurons (Egan et al., 1999; Emery et al., 2000; Zhao et al., 2003; Klarsfeld et al., 2004; Yoshii et al., and Benito et al., 2008). Therefore, to more sensitively characterize the expression and function of CRY in *Drosophila* peripheral tissues, an N-terminally tagged GFP-*cry* transgene was generated. I show that GFP-*cry* eliminates LL behavioral rhythms seen in cry^{03} mutants (Fig. 17), and reveals CRY protein expression in all fly brain neurons except some DN_1s and LN_ds, and all DN_2s, DN_3s and LPNs (Fig. 18). Lack of CRY expression in the DN_2s is supported by the absence of *cry*Gal4 driven labeling of these cells, and by the remarkable reversal of the phase of their PER cycling when they are forced to express

CRY (Klarsfeld et al., 2004). Consistent with previous studies, in the CRY-positive pacemaker neurons, CRY was similarly labeled in both the cytoplasm and nucleus, and accumulated to high levels when the flies were kept in constant darkness. The presence of CRY in the nucleus is consistent with the idea that CRY may play a role in the molecular clockwork under certain conditions, as well as with a role for CRY in photoreception. The synchronization of the clock by LD cycles implies that TIM is degraded every morning by sunrise. At that time, TIM is in the nucleus, and a direct interaction of CRY with TIM is possible only if CRY is also nuclear. DD staining also reveals that CRY accumulates in some axonal and dendritic projections and non-clock cells (Fig. 18). The presence of CRY in neurites provides another potential level of CRY function and regulation and suggests that it may interact with proteins other than TIM.

Peripheral clocks in MTs, antennae, legs, and wings maintain cell-autonomous molecular rhythms for days in cell culture (Hall, 2003; Bell-Pedersen et al., 2005; Shafer et al., 2006). Discovery of eye-independent light-entrainable peripheral oscillators, made it clear that there are extraocular photoreceptors in *Drosophila*. Indeed, these clocks, when isolated, can be entrained by light, indicating presence of CRY protein within these tissues themselves. Given the likely cell-autonomous nature and strong light-dependence of peripheral clocks in *Drosophila*, I expected that CRY expression and function must also be cell-autonomous. Consistent with this notion, *cry* mRNA is abundant and present in fly bodies as well as in many fly head tissues (Emery et al., 1998). To further address CRY expression in peripheral tissues, I carried out a detailed characterization of CRY expression in the MTs of *Drosophila*, using the GFP-*cry*

transgene, and show for the first time that CRY is expressed in a light-dependent manner in the peripheral tissue of adult flies with a noticeable enrichment in the nucleus (Fig. 18).

Study of the cry^{b} mutation has revealed that CRY is required for clock function in some peripheral oscillators (Krishnan et al., 2001; Levine et al., 2002). It is possible that CRY serves as a transcriptional repressor of CLK-CYC activity in some peripheral tissues (Collins et al., 2006), and thus plays a role similar to that of CRY in the mammalian circadian clock. Another study suggests that photoreception is not the only function of CRY in the clock neurons; CRY also appears to be involved in the maintenance of central clock function at extreme temperatures in pacemaker neurons (Dolezelova et al., 2007). Although CRY and PER seem to function together to repress CLK-BMAL activity in the mammalian system, my co-IP results suggest that CRY doesn't interact with PER and/or CLK proteins in *Drosophila* bodies. *Drosophila* CRY-PER interactions have been detected in yeast, but CRY and PER appear to interact only via TIM *in vivo* (Rosato et al., 2001). Furthermore, PER continues to repress CLK/CYC activity *in vivo* during the first half of the day, presumably after CRY has been degraded by light. Despite a lack of interaction between CRY and other clock proteins in fly bodies, CRY is necessary for circadian oscillator function in peripheral tissues.

I further demonstrate that entrainment of clock cells in the central brain and peripheral tissues, by short light pulses, is mediated by a common photoreceptive pathway that is disrupted by the cry^{03} mutation. This pathway induces rapid degradation of TIM in brain clock cells and in epithelial MT clock cells of transgenic rescued flies

exposed to light (Fig. 20*A*). In *cry*^{03} mutants, short pulses of light that disrupt the dark phase of the LD cycle fail to induce degradation of TIM in both types of cells (Fig. 20*A*) implying that in the periphery, CRY is absolutely required for light-dependent TIM degradation (Fig. 3) implying that in the periphery, CRY is absolutely required for light-dependent TIM degradation. Moreover, I show a direct CRY-TIM interaction in the fly body that is also light-dependent (Fig. 20*B*). This result further indicates that CRY mediates degradation of TIM induced by short light pulses in both clock cell types.

If CRY is not acting as a transcriptional repressor, then what is the function of CRY in the fly peripheral tissues? To address this question, I investigated whether CRY is involved in regulating membrane function. I used larval salivary glands, which lack a functional circadian clock and are amenable to electrophysiological recordings as our model tissue, and show that GFP-CRY is expressed in these cells with staining mainly in the nucleus (Fig. 21). Since most peripheral tissues are non-excitable in nature, I looked at the impact of CRY on passive membrane properties. Excitingly, I found a role for CRY in the regulation of cell membrane physiology in larval salivary gland cells, where membrane R_i in *cry*^{03} null mutants decreased significantly compared to the wild-type controls and GFP-*cry;cry*^{03} rescue flies (Fig. 22*A*). This decrease in R_i of *cry*^{03} null mutant cells implies that more current is required to alter the membrane changes in cells lacking CRY. Unexpectedly, CRY effects on the membrane properties of these non-excitable cells were also found to be light-independent (Fig. 22*B*), and potentially mediated by K^+ channels (Fig. 23*A*). Indeed, salivary gland cells of transheterozygous mutants for *cry* and K^+ channel subunits show decreased R_i similar to that of

homozygous *cry* or K^+ channel subunit mutants (Fig. 23*B*), supporting a role for these membrane ion channels in regulating passive membrane physiology through CRY. Additionally, the disruption of the CRY mediated membrane response in *cry* or *Hk* mutants is functionally rescued by salivary gland-restricted expression of their wild-type genes in the null backgrounds (Fig. 24). Thus, CRY, a multi-functional protein, seems to regulate ion channels and cell membrane physiological properties in a cell type-specific fashion. These findings for the first time not only define the expression profile of CRY in peripheral tissues, but also reveal that CRY protein is required for K^+ channel-dependent changes in membrane function that are light-independent, cell-autonomous and present in peripheral tissues devoid of a canonical circadian clock.

Methods

Fly strains

The following *Drosophila* strains were used in this study: w^{1118}, w^{1118}; Cyo/Sco;TM2/TM6B, w^{1118};*tim*Gal4, w^{1118};P{GMR16H06-GAL4}attP2 (BDSC), w^{1118};GFP-*cry*;cry^{03}, w^{1118};;cry^{03}, cry^{b}, UAS-*cry* (a gift from Patrick Emery), UAS-*Hk*RNAi, UAS-*Hk*-wt, *eag* amorphic mutant (a gift from Todd Holmes), Hk^{1}, Hk^{2}, and Sh^{5} (BDSC). Flies were reared on standard cornmeal/agar medium supplemented with yeast and kept in 12:12 LD cycles at 25°C. The GFP-*cry* transgene generated and cry^{03} strains were backcrossed seven times to w^{1118} to minimize effects due to differences in genetic background.

Generating the GFP-cry transgene

An N-terminal eGFP tagged *cryptochrome* transgene (GFP-*cry*) was constructed via recombineering. Phusion DNA polymerase (New England BioLabs) was used to amplify the eGFP-LoxP-kanamycin cassette from plasmid PL-452 N-eGFP (Addgene) using primer Cry-L (5′actgggattcgggagatttttgaagcccaaaagcagggaactcctcactgatgATGGTGAGCAAGGGCGAGGAG-3′), which contains 53 nts of *Cry* sequence upstream of the translation start (lowercase) and the first 21 nts of the GFP translated sequence (uppercase), and Cry-R (5′ tggaggcgcaatccatggcgaaaccaaatcacattcgcccctcgcgtggcACTAGTGGATCCCCTCGAGGGAC-3′), which contains 50 nts from *Cry* exon 1 (lowercase) and 23 nts from the 3′ end of the eGFP cassette (uppercase). This PCR reaction was ran at TM 54°C for 25 cycles, treated with DpnI enzyme and purified. This fragment was used to transform SW102 cells harboring the BAC clone CH322–118M12 (BAC-PAC Resources Center), which contains the *Cry* genomic region 20.636 kb, and recombinants containing the eGFP-LoxP-kanamycin cassette inserted into *Cry* were selected on plates containing kanamycin. The kanamycin gene was removed by inducing recombination at the LoxP sites (Venken et al., 2008, 2009), resulting in the chloramphenicol-resistant GFP-*Cry* p(ACMAN) clone. GFP-*Cry* was amplified in EPI 300 cells (Epicenter), and sequenced to confirm the N-terminal GFP-CRY fusion. The GFP-*Cry* transgene was inserted into attP40 on chromosome 2 via PhiC31-mediated transgenesis.

Drosophila activity monitoring and behavior analysis

One to three day old male flies were entrained for three days in 12:12 LD cycle and transferred to constant conditions of darkness (DD) or light (LL) for seven days at 25°C. To cause a phase shift, flies were subjected to a 15 min bright light pulse on day one of constant darkness either at CT15 or CT21. Locomotor activity was monitored using the *Drosophila* Activity Monitor (DAM) system (Trikinetics). Analyses of period, power and rhythm strength during DD was carried out using ClockLab (Actimetrics) software as previously described.

Immunohistochemistry

Antibody staining of larval CNSs, salivary glands; and adult fly brains and Malpighian tubules was carried out as previously described (Houl et al., 2008). Briefly, larval and adult tissues were dissected in 1XPBS and fixed with 3.7% formaldehyde in 1X PBS at room temperature (RT) for 15 mins. Samples were then washed and incubated with blocking solution containing 1X PBS, 5% BSA, 5% Goat serum (5% Donkey serum for primary antibodies raised in goat), 0.03% sodium deoxycholate, and 0.03% Triton-X100 at RT for 1 h followed by primary antibodies (overnight, ON at 4°C) in blocking solution. Primary antibodies and their dilutions used were as follows: guinea pig anti-CLK GP50 1:3,000 (Houl et al., 2008), goat anti-CLK dC-17 (Santa Cruz Biotechnology, Inc) 1:100, rabbit anti-GFP ab6556 (Abcam) 1:1000, rabbit anti-GFP ab290 (Abcam) 1:2000, guinea pig anti-CRY GP23 1:1000, pre-absorbed rabbit anti-PER (a gift from Michael Rosbash, Brandeis University) 1:15,000, and rat anti-TIM (a

gift from Amita Sehgal, University of Pennsylvania) 1:1000. For detection of primary antisera, the following secondary antibodies were used at a dilution of 1:200 (incubated ON at 4°C) in blocking solution: goat anti-rabbit Alexa 488 (Molecular Probes), donkey anti-rabbit Alexa 647 (Molecular Probes), goat anti-guinea pig Cy-3 (Jackson ImmunoResearch Laboratories, Inc.), goat anti-guinea pig Alexa 488 (Molecular Probes), donkey anti-guinea pig Alexa 488 (Molecular Probes), goat anti-rabbit Alexa647 (Molecular Probes), donkey anti-goat Alexa 488 (Molecular Probes) and goat anti-rat Cy-5 (Jackson ImmunoResearch Laboratories, Inc.). Brains were then mounted in Vectashield mounting medium (Vector Laboratories, CA) for imaging. Imaging using an Olympus FV1000 confocal microscope (Olympus America Inc., Waltham, MA) was carried out as previously described (Agrawal and Hardin, 2016). For each genotype and developmental stage, images were acquired using the same settings (power, gain, offset) at the same time. Entrained L3 larvae or one to five day old adults were used for dissection.

Western blot analysis

For preparing protein extract from adult fly heads, flies were entrained in a 12:12 LD cycle for at least three days and collected at ZT2 (Zeitgeber Time 2, where ZT0 is lights-on and ZT12 is lights-off), ZT6, ZT10, ZT14, ZT18 and ZT22 on day four of LD cycle. Lysis was performed in radioimmunoprecipitation assay (RIPA) buffer (20 mM Tris at pH 7.5, 150 mM NaCl, 1 mM EDTA, 0.05 mM EGTA, 10% glycerol, 1% Triton X-100, 0.4% sodium deoxycholate, 0.1% SDS [sodium dodecyl sulfate]) containing protease

inhibitor mixture (0.5 mM PMSF [phenylmethylsulfonyl fluoride], 10 µg/ml aprotinin, 10 µg/ml leupeptin, 2 µg/ml pepstatin A, 1 mM Na_3VO_4, and 1 mM NaF). This homogenate was sonicated 5-8 times for 10 s each, using a Microson ultrasonic cell disruptor at a setting of 4-5 and then centrifuged at 20,000 g for 10 mins. The supernatant was collected and protein concentration was determined by the Coomassie-based Bradford Assay. 300 ng of total protein for each genotype was loaded in each lane. Soluble protein extracts were separated on 5% polyacrylamide electrophoresis gels, transferred to supported nitrocellulose membranes (MSI, Westboro, MA) and incubated with ab6556 (Abcam) anti-GFP (1:1000) or anti-beta-ACTIN (1:5000; Sigma) antibodies. Goat anti-rabbit and anti-mouse conjugated to horseradish peroxidase were employed at a 1:2000 dilution (Jackson Immunoresearch) as secondary antibodies. Chemiluminescent detection was used to develop the reaction using ECL plus (Amersham) reagent.

Co-immunoprecipitation

For co-immunoprecipitation (co-IP) assays, protein extracts were prepared as described above. Briefly, frozen fly bodies collected at ZT0.5 and CT0.5 were homogenized and sonicated in RIPA buffer; centrifuged at 20,000 g for 10 mins, and the supernatant was collected as protein extract. GFP-CRY complexes were immunoprecipitated from protein extracts using GFP-nanobeads at 4°C/Over Night (ON) and then washing the beads three times with RIPA buffer. The immunoprecipitates were eluted by boiling the beads in 15 µl of 2X dilution buffer and then samples were run in parallel with 300 ng of

initial RIPA extracts (before binding to the nanobeads) as input. The resulting gel was used to prepare western blots, that were probed with GFP, CLK, PER, and TIM antibodies. Immunoblots were processed as described previously for Western blotting using GP50 anti-CLK (1:4000), pre-absorbed rabbit anti-PER, rat anti-TIM, or ab6556 anti-GFP (1:1000) antibodies.

Electrophysiology of larval passive membrane properties

The electrophysiology of salivary gland cells has a long history (Lundberg, 1955), in both vertebrates (Nishiyama and Peterson, 1974) and invertebrates (Wuttke and Berry, 1992). Larval salivary glands of *Drosophila* have been a model preparation for studies of membrane channels (Versalis et al., 1991) and were used in this study. Single-cell resting membrane potential (RMP) and input resistance (R_i) recordings were performed as previously described (Achee and Zoran, 1997). Briefly, shape electrode, current clamp recordings were carried out at the indicated ZT/CT time points on salivary glands dissected from L3 larvae of the appropriate genotype raised at 25^{o}C. Dissections were carried out as previously described using 1X PBS and recording in the dark were made possible with a red filter that allowed cut-off of less than 600 nm. The tissue was observed under 100X magnification that allowed individual cells to be resolved enough for penetration using a dissecting microscope (Olympus). Potential differences were recorded with glass electrodes (borosilicate; FHC) filled with 3 M KCl with tip resistance values of 8-20 MW. Current-clamp recordings of neuronal membrane potentials were amplified using a bridge-balanced electrometer (DP 301, Warner

Instruments), and recordings were digitized using a PowerLab A/D converter (ADInstruments). Neuronal input resistance and excitability were measured by injecting constant amplitude current pulses generated by a stimulator (Grass). Intracellular recording were performed in a petri-dish containing fly recording media (a mix of 50% Schneider's *Drosophila* medium [Caisson Labs] and 50% Diluting saline [NaCl 36 mmol, KCl 21 mmol, $MgCl_2$ 15 mmol, $CaCal_2$ 5 mmol, $NaHCO_3$ 4.8 mmol, NaH_2PO_4 2 mmol, Glucose 11.1 mmol, and Hepes 15 mmol; pH 6.5]; Blumenthal, 2001). A minimum of 3 cell recordings from at least six different animals were analyzed for each genotype per time point. The RMP and R_i values were measured using LabChart software (ADInstruments). Statistical significance with respect to pairwise comparison was calculated using Student's t-test using unequal variances, and multiple means were compared by one-way ANOVA followed by Student's t-test for post-hoc analysis.

CHAPTER V

SUMMARY AND DISCUSSION

Identification and analysis of candidate clock phosphatases

In animals ranging from *Drosophila* to humans, an autoregulatory feedback loop in gene expression drives the circadian timekeeping mechanism (Bell-Pedersen et al., 2005). Growing evidence suggests that normal progression through the feedback loop mechanism is dependent on integrating posttranslational regulatory pathways, most notably time-of-day-specific phosphorylation events that generate dynamic changes in clock protein stability, localization and/or activity (Edery et al., 1999; Harms et al., 2004; Mehra et al., 2009; Weber et al., 2011). However, the role these modifications play in regulating the circadian timekeeping mechanism is only partially understood for a few key clock components. Hence, my primary goal was to determine how dephosphorylation of clock components regulates rhythmic transcription within the autoregulatory feedback loop that keeps circadian time in flies.

To achieve this goal, I focused my efforts on identifying candidate phosphatases that regulate clock protein phosphorylation in *Drosophila*. Given that a core group of conserved clock proteins from animals are regulated via phosphorylation, what we learn about clock protein phosphorylation in *Drosophila* will likely be relevant to clock function in other organisms including mammals. My screen to identify clock phosphatases could therefore provide fundamental insight into our understanding of the contribution of phosphorylation events in the molecular clock mechanism. The candidate

phosphatases identified will help us determine how clock protein dephosphorylation controls transcriptional rhythms required for circadian timekeeping in flies. Moreover, the candidate phosphatases identified here could represent potential genetic links to clock associated disorders in humans and novel targets for the development of drugs to treat such disorders.

Clock cell-specific RNAi knockdown of ~100 phosphatases, representing all annotated *Drosophila* phosphatases or phosphatase regulators available at the time, identified a total of 22 candidates that disrupted circadian activity rhythms (Table 1). Three of the candidates identified were phosphatase inhibitors/ regulators or nucleotide/carbohydrate phosphatases rather than protein phosphatases, and thus were not pursued further. Several of the 19 candidates (n=8) were not validated upon testing independent genetic reagents (Table 2). However, these reagents consisted of additional P element inserts, where the P element insertion site may not interfere with gene expression; or strains that could be used for overexpression, which also may not impact the function of a protein that is already at saturating levels. Therefore, a lack of validation with P-element inserts and overexpression for these candidate clock phosphatases does not eliminate them from the list of viable candidates. However, for two candidate phosphatases, Ptp69D and CanA14F, loss of function mutants upon isogenization did not give rise to any alteration of activity rhythms (Table 2) and therefore they can be eliminated from the list of viable candidates. Additional loss or gain of function genetic reagents were not available for another five candidate

phosphatases, which can be characterized further when such reagents are available. For example, P element inserts are now available for *Gbs-70E* and CG3530.

Protein Phosphatase 1 (PP1) and Protein Phosphatase 2a (PP2a) had already been shown to function within the *Drosophila* clock when we started the screen (Sathyanarayanan et al., 2004; Fang et al., 2007). However, experiments showing dephosphorylation and stabilization of TIM by PP1 were carried out in S2 culture cells, and all the *in vivo* results were based on overexpression of the nuclear inhibitor of PP1 (NIPP1) (Fang et al., 2007). It is therefore possible that PP1 only indirectly targets TIM for dephosphorylation *in vivo*. Additionally, none of the PP2a subunits tested in Sathyanarayanan et al., 2004, were shown to affect the behavioral rhythms upon knock down. Andreazza et al., 2015, have now shown that the STRIPAK/PP2a phosphatase is involved in dephosphorylation of CLK. However, the phenotypes seen with PP2a knockdowns are using *Dicer2* that enhances the RNAi potency; a reagent that was not employed in my RNAi screen. Nonetheless, I have tested RNAi knockdown of different subunits for PP1 and PP2a including *Pp1-87B* (CG5650/GD35025), *flw* (CG2096/GD29622), *Pp1α-96A* (CG6593/KK105525), *Pp1-13C* (CG9156/KK107770), *tws* (CG6235/KK104167), *mts* (CG7109/GD41924) *wdb* (CG5643/KK101406), and *PP2A-B'* (CG7913/KK107057) in clock cells in my screen. However, only *Pp1α-96A* and *mts* fulfilled our criteria for altered period and/or % arrhythmicity in behavioral assays. None of the available *PP1α-96A* P element inserts or clock cell-specific *PP1α-96A* overexpression altered activity rhythms (Table 2). However, I wanted to test loss of *PP1α-96A* function and therefore used the CRISPR/Cas9 system to generate three *PP1α-*

96A deletion mutants (Fig. 9). Unfortunately, none of these mutants were homozygous viable as adults, and, heterozygotes did not display altered activity rhythms (Table 2). MTS was an important target of the screen, however, during the course of my screening and validation, STRIPAK/PP2a was found to dephosphorylate CLK by another group (Andreazza et al., 2015). Nevertheless, numerous viable candidate clock phosphatases still remain, and I have now shown that *Lar* provides novel insight into the function of PDF signaling among pacemaker neurons to control locomotor activity rhythms (Agrawal and Hardin, 2016).

Overall, I identified 19 protein phosphatases that may function within the *Drosophila* circadian clock. *Lar* and *mts* functions have now been characterized, and are shown to be important for dephosphorylation events regulating fly clocks (Agrawal and Hardin, 2016; Andreazza et al., 2015). *Ptp69D* and *CanA14F* loss of function mutants do not give rise to any alteration of activity rhythms upon isogenization and therefore are unlikely to directly dephosphorylate any core clock proteins. No loss of function mutants were available for the rest of the 15 candidates at present, and 5 of these candidates were not tested for validation at all in our study due to the lack of independent genetic reagents. One potential method for analyzing the remaining candidates is to use CRISPR technology (Gratz et al., 2013) to generate conditional mutants, which may avoid lethality associated with a complete loss of function. Further characterization of the remaining viable candidates may reveal novel features of the circadian timekeeping mechanism in *Drosophila* that are likely to be conserved in all animals including humans.

Identification and characterization of *Lar*

Further genetic validation of the candidate phosphatases identified a novel function for the RPTP LAR, which I show is required for the development of circadian pacemaker neuron processes that support rhythmic activity in constant darkness but not during light:dark cycles (Agrawal and Hardin, 2016). Although loss of LAR function disrupts clock output by eliminating PDF release into the dorsal brain, PDF expression persists in LN_v cell bodies and lLN_v projections. In contrast to flies that lack PDF, flies that lack *Lar* anticipate lights-on and lights-off transitions normally, which suggests that the remaining PDF expression mediates activity during light:dark cycles.

In *Drosophila*, sLN_vs control the M activity peak and LN_ds plus the PDF-negative fifth sLN_v control the E activity peak (Helfrich-Forster, 2014; Beckwith and Ceriani, 2015). Projections from the M (sLN_v) neurons and a subset of E (3 LN_ds plus fifth sLN_v) neurons, together with those from lLN_vs, terminate in the aMe (Helfrich-Forster et al., 2007; Helfrich-Forster, 2014), a structure that is well preserved in *Lar* mutants and RNAi knockdowns. Importantly, the lLN_vs play a major role in conveying light input from multiple cellular sources (e.g., retinal photoreceptors, Hofbauer-Buchner eyelets, and lLN_vs) to the circadian system (Helfrich- Forster et al., 2002 and 2007; Shang et al., and Sheeba et al., 2008; Fogle et al., 2011). PDF signaling by lLN_vs is known to phase advance (shorten the period) of M neurons and phase delay (lengthen the period) of E neurons (Wulbeck et al., 2008; Helfrich-Forster, 2014), suggesting that lLN_vs communicate with M and E neurons to define the pattern of diurnal activity. Consistent with this possibility, the M and E neurons that project into the aMe express

the PDF receptor (PDFR; Im et al., 2011; Helfrich-Forster, 2014), and are thus capable of responding to PDF. Our results, together with those from previous studies, suggest a model for how diurnal rhythms are regulated; lLN_vs receive light input, release PDF into the aMe, PDFR receptive E cells and M cells are phase delayed and phase advanced, respectively, thereby positioning the E activity peak at the lights-off transition and the M activity peak at the lights-on transition. Because the aMe houses the circadian pacemaker center in many insects (Homberg et al., 1991; Stengl and Homberg, 1994; Frisch et al., 1996; Helfrich-Forster et al., 1998 and 2005), it may play a conserved role in regulating diurnal activity rhythms. A simple experiment to test this model would employ disruption of the projections from lLN_vs into the aMe. If mutants that specifically disrupt lLN_v projections into the aMe are available, then they should abolish LD activity pattern.

Signaling by other neuropeptides and neurotransmitters may also be involved in mediating normal peaks of M and E activity in *Lar* mutant and RNAi knockdown flies (Beckwith and Ceriani, 2015). For instance, the two CRY positive LN_ds, the CRY positive fifth sLN_v, and the CRY-positive $DN1_a$ and $DN1_p$ neurons also express the short neuropeptide F (sNPF) neuropeptide (Johard et al., and Yoshii et al., 2009; Yao and Shafer, 2014). Since clock neurons are all present in the *Lar* mutant and RNAi knockdown flies, it is possible that sNPF activity in these neurons is important in regulating the diurnal activity pattern. Moreover, LN_d and DN_{1p} neurons expressing sNPF also send projections to the aMe. Therefore, it will be interesting to determine the expression pattern of sNPF in the *Lar* heterozygous mutant and determine whether its expression is intact in the relevant neurons and processes (i.e. CRY positive dorsal

neurons and their projections into the aMe) mediating the communication between dorsal and ventral pacemaker neurons to control diurnal rhythms. Also, there are P element transposon inserts available for sNPF that may be used to reveal if disruption of sNPF activity causes aberrant diurnal rhythms consistent with this hypothesis. Additionally, a more exciting possibility to test is to determine whether a rescue of PDF signaling from the dorsal brain into the aMe (i.e. via the $DN1_p$ projections that go down to the aMe) may be sufficient to rescue signaling between the dorsal and ventral set of neurons in the *Lar* transheterozygotes, and therefore restore the communication and hence synchrony. To test this hypothesis, we can drive expression of PDF using DN_{1p}Gal4 driver and test for rescue of arrhythmicity caused by *Lar* heterozygous and pdf^{01} mutants in constant darkness. These experiments will reveal novel mechanisms regulating diurnal rhythms.

LAR presumably functions to dephosphorylate substrates in sLN_vs that enable proper growth and targeting of dorsal projections. Previous work shows that *Lar* is required for segmental nerve b motoneuron growth cones to recognize and enter their correct target regions, suggesting that LAR regulates the phosphorylation state of intracellular target proteins critical for growth cone guidance (Krueger et al., 1996; Wills et al., 1999). It is likely that a dynamic balance of kinase and phosphatase activities at the leading edge of the growth cone endows it with the ability to integrate convergent signals and translate them into appropriate steering decisions. This suggests that *Lar* is a necessary component in a ligand-mediated mechanism that normally guides axons through their appropriate choice points during the development of sLN_v axon

architecture in the fly brain. Several LAR extracellular ligands, such as syndecan, dally-like protein, and laminin-nidogen complex have been identified that contribute to motor axon guidance and synaptogenesis in flies and/or mammals (O'Grady et al., 1998; Fox and Zinn, 2005; Johnson et al., 2006). Intracellular substrates of LAR include β-catenin and p130cas, which control neurite outgrowth and apoptosis, respectively, depending on their phosphorylation state (Kypta et al., 1996; Weng et al., 1999; Xu and Fisher, 2012). Whether any of these LAR ligands or substrates contributes to sLN_v dorsal projection development will require further investigation.

It is possible that *Lar* achieves its restricted specificity through the localization of its activating ligand Syndecan (Sdc). The transmembrane heparan sulfate proteoglycan *Sdc* is a ligand for the neuronal RPTP LAR and has been demonstrated to contribute to LAR's function in motor axon guidance (Fox et al., 2005). Interestingly, *Sdc* has also been shown to be one of the top targets in the Gene Ontology analysis of Mef2, a transcription factor in *Drosophila* (Sivachenko et al., 2013). Mef2 is rhythmically expressed in clock neurons, and altering Mef2 levels or activity disrupts circadian behavioral rhythms (Blanchard et al., 2010) and rhythms in the daily sLN_v fasciculation-defasciculation cycle (Sivachenko et al., 2013). ChIP-Chip analysis has identified numerous Mef2 target genes implicated in *Drosophila* nervous system development, axon guidance, and axonogenesis (Sivachenko et al., 2013). Hence, it is possible that *Sdc* is expressed in the fly brain regions that target LAR activity in pathways modulating the development of axonal processes from pacemaker neurons thus contributing to locomotor activity rhythms. To test this hypothesis, it would be important to determine

the SDC expression pattern in the fly brain. It will also be interesting to determine if RNAi knockdown of *Sdc* causes a similar phenotype as *Lar* RNAi knockdown flies. This information will help our understanding of how signal transduction pathways through LAR regulate the circadian neuronal architecture.

CRY expression and function in clock and non-clock cells

In *Drosophila*, rhythmic gene expression is synchronized to LD cycles by the blue light photoreceptor CRYPTOCHROME (CRY). Upon detection of light, CRY binds TIM and promotes its light-dependent degradation, thus entraining the molecular clockwork to LD cycles. CRY is also known to alter K^+ channel conductance in lLN_vs, thereby influencing neuronal excitability. In addition, CRY proteins have light-independent transcriptional functions in many animals and, like other canonical clock proteins, may have non-circadian roles. Despite this multi-functionality of CRY protein in different animals, CRY expression and function have been characterized only for the brain pacemaker neurons in the flies, thus it remains unclear which CRY functions extend to peripheral clock and non-clock tissues.

To define CRY function in peripheral clock and non-clock tissues, we generated a GFP-tagged-*cry* transgene that I have shown rescues all the known functions of endogenous CRY protein. Immunostaining with anti-GFP reveals the expected GFP-CRY expression pattern in the brain (Fig. 18), as well as neurons that have not been shown to be associated with the circadian clock. One cluster of ~12 non-clock containing neurons per brain hemisphere (Fig. 18) have projections that extend towards the central

complex where GFP-CRY is detected under constant dark conditions when CRY accumulates to high levels. The central complex is a structure in the insect brain that integrates sensory input and coordinates motor output. The same clusters of non-clock neurons were also revealed by different *cry*-gal4 lines and CRY antibody staining (Emery et al., 2000; Zhao et al., 2003; Klarsfeld et al., 2004; Yoshii et al., and Benito et al., 2008). The CRY positive non-clock neurons that project to the ellipsoid body resemble the large field neurons R4 (Renn et al., 1999). The R4m cells are presumed to receive afferent input from the optic foci and from fibers of widely branching neurons in the protocerebrum. Previous studies indicate that these neurons are involved in consolidation of long-term olfactory memory (Wu et al., 2007), but additional studies will be required to determine what role CRY may play in these cells. One possibility is to over-express *cry* in this central complex region using R4m specific Gal4 i.e. *c819*-Gal4 in a *cry* mutant background and measure differences in consolidation of long-term olfactory memory formation in comparison to *cry* mutants. If there is a significant effect of CRY in the memory formation, then this may identify the relevant molecule and hence the pathways important in mediating this behavior. Moreover, it will be interesting to see if light alters CRY levels in these non-clock cells thus affecting the associated behavior.

I also demonstrate that the entrainment of the central brain clock and peripheral clock by short light pulses is mediated by a common photoreceptive pathway, where GFP-CRY promotes light-dependent TIM degradation in peripheral clock tissues, which is disrupted by the cry^{03} mutation. My results suggest that CRY contributes in a cell-

autonomous manner to the PER/TIM molecular cycles. This presumably reflects photoreceptor-independent function for CRY in peripheral cells and tissues. It is not obvious why free-running clock oscillations are preserved in LNs but not in MTs of *cry*^{03} mutants. The lack of CRY may be compensated for by as yet unrevealed LN-specific clock components, by input from other structures in the central nervous system, or by the network that preserves synchronized molecular oscillations in the absence of CRY (Helfrich-Forster et al., 2001; Veleri et al., 2003 and 2007; Rieger et al., 2003; Yoshii et al., 2008). In contrast, MTs consist of non-innervated epithelium in which clock functions do not seem to be affected by the fly internal milieu. Thus, there may be more opportunities for redundant mechanisms to maintain free-running clocks in LNs than in MTs.

Using larval salivary glands, which lack a functional circadian clock and are amenable to electrophysiological recording, I found a role for CRY in the regulation of cell membrane physiology; membrane R_i in *cry*^{03} null mutant glands was lower than in wild-type and was rescued by the GFP-*cry* transgene. The impact of CRY on the R_i of these non-excitable cells is light-independent and mediated by K^+ channels. Having shown that CRY is important for maintaining PER/TIM molecular rhythms in adult peripheral tissues and membrane function in larval salivary glands, one interesting question that now arises is if CRY function in peripheral clock tissues is somehow required to maintain circadian oscillator function in different peripheral tissues. It is possible that CRY impacts the peripheral oscillators by getting feedback from membrane proteins and/or signaling molecules. This may be the reason why *cry*^{03} mutants show

loss of PER and TIM rhythms in adult MTs. In support of this possibility, it has been shown that rhythms in SCN neuron firing is required to maintain rhythms in PER2 expression (Granados-Fuentes et al., 2015) and that membrane hyperpolarization in SCN cultures, reversibly abolishes the rhythmic expression of PER1 (Lundkvist and Block, 2005). It will be important to see how changes in membrane responses impact the physiological function of different clock and non-clock peripheral tissues. For example, one can look at fluid secretion from adult MTs of flies (Dow et al., 1994), glue secretion from salivary glands and/or gene expression profile for digestive enzymes (as a proxy for salivary gland function) in *cry* mutants vs. the controls.

Light activation of *Drosophila* CRY also evokes conformational changes in the C-terminus of CRY that promotes interactions with TIM and the ubiquitin ligase component JETLAG (JET), which leads to the sequential degradation of TIM and CRY to effect circadian entrainment (Rosato et al., 2001; Busza et al., 2004; Koh et al., and Peschel et al., 2006; Peschel et al., 2009). However, light activated CRY mediates circadian entrainment and neuronal firing via different mechanisms based on their different activation thresholds and relative dependence on the C-terminus of CRY (Fogle et al., 2011). Moreover, light-induced CRY conformational changes that promote JET binding (thus causing circadian entrainment) occur in oxidized and reduced states of CRY, and are unaffected in CRY tryptophan mutants, that presumably are responsible for intra protein electron transfer reactions following light-evoked reduction of the FAD cofactor (Wang et al., 2012; Vaidya et al., 2013). Current evidence suggests that light induced membrane depolarization depends on the redox state of CRY, but not

conformational changes in the CRY C-terminal domain. In contrast, light-induced clock resetting depends on conformational changes in the CRY C-terminal domain, but may not depend on CRY redox state (Riganti et al., 2004; Ozturk et al., 2014; Fogle et al., 2015). Given these mechanistic differences, it would be interesting to see if redox state alters CRY dependent changes in salivary gland membrane physiology. Pharmacological treatments that specifically disrupt the CRY redox-sensitive flavin chromophore, such as the flavin-specific redox inhibitor diphenyleneiodonium (DPI) or the oxidizer H_2O_2, may abolish CRY mediated electrophysiological responses in salivary gland cells of wild-type flies. Likewise, it will be informative to test the membrane properties of salivary glands in superoxide dismutase (SOD) enzyme mutants that also lead to genetic disruption of the cellular redox environment.

CRY's homology with DNA photolyases leads to the suggestion that CRY was the original light sensitive molecule; primitive organisms could detect light and regulate gene expression with one molecule (CRY) to avoid damage by sunlight during light-sensitive processes such as DNA replication. Photoreception and transcriptional feedback loops are ubiquitous features of circadian pacemakers. Therefore, circadian rhythms may have begun when a DNA repair protein acquired the ability to auto-regulate expression in a light-and ultimately time-dependent manner. While ancestral CRY may have acted as both a light sensor and a transcriptional repressor, non-Drosophilid insects such as the monarch butterfly *Danaus plexippus* have two *cry* genes which either repress transcription or sense light. Thus, circadian clocks may well have their origins in rapid responses to light, and the anticipatory clock gene networks could

have subsequently been built around CRY, a light-responsive protein and a transcriptional repressor whose function has gradually become specialized. Nonetheless, recent discoveries including those described here implicate CRY proteins in fundamental cytoplasmic and plasma membrane regulatory roles. The multi-function CRY protein in insect peripheral tissues, which can be clock- and light-independent, raises questions as to what is the ancestral function of this protein, which ultimately gave rise to such diverse roles as a circadian photoreceptor in plants and a circadian transcriptional repressor in mammals. Thus, mCRYs could have evolved some distance away from their primordial photoreceptive functions into those that are more a part of the clockworks compared to other organisms, such as *Drosophila*.

Drosophila CRY in peripheral tissues, if not within the brain, could be a feedback loop component as well as a photoreceptor. In peripheral tissues (e.g. the eye) from other mammalian-like organisms, CRYs remain candidates for participating in the control of information flow from the environment into a centrally located circadian pacemaker. I therefore think that *Drosophila* CRY exemplifies the ancestral role of a photoreceptor acting as a light-dependent regulator of the circadian feedback loop, whereas mammalian CRYs have preserved a role within the circadian feedback loop but shed their direct photoreceptor function. I cannot, however, exclude the possibility that mammalian CRYs act as photoreceptors for other possible functions, circadian or otherwise, not detected in previous assays. Moreover, CRY mediated changes in larval salivary gland R_i, independent of light, adds further complexity in explaining the evolution of the functional properties for this molecule. It is possible that CRY function

in membrane properties at early developmental stages (i.e. the larvae) is yet not light sensitive, or that CRY has tissue specific functions to regulate the local physiology of that tissue. Based on my findings, I would speculate that many more roles for CRY as a regulator of cytoplasmic or membrane physiology might emerge, raising the question of when and where these functions arose? However, additional studies will be necessary to dissect the evolution of this protein's function and define the relevant signaling pathways.

Conclusions

A major objective of my research was to determine how dephosphorylation of core clock proteins impinges on rhythmic transcription within the autoregulatory feedback loop that keeps circadian time in *Drosophila melanogaster*. Specific post-translational modifications such as the phosphorylation of clock proteins carries timing information that controls circadian oscillations. Therefore, determining the role of protein phosphorylation was vital to understanding circadian timekeeping mechanisms. I approached this question by employing a genome-wide RNAi screen to identify candidate protein phosphatases that may advance our understanding of the molecular mechanism of *Drosophila* clocks.

Using genetic manipulations, immunohistochemistry, behavioral and biochemical tools, I have found a novel function for the RPTP *Lar* in the development of a circadian pacemaker neuron process that supports rhythmic activity in constant darkness but not during LD cycles. This finding, along with further analysis of other

candidate clock phosphatases, will help us unravel the mechanistic links between the core oscillator and the output pathways that are important for maintaining diurnal rhythms.

Lastly, I have demonstrated for the first time that CRY is not only essential in peripheral tissues to maintain PER and TIM molecular rhythms, but is also required for mediating K^+ channel-dependent changes in membrane responses. This effect is light-independent, cell-autonomous and is present in peripheral tissues devoid of a circadian clock. Future work is needed to answer several important questions. How does CRY support circadian oscillator function in peripheral tissues? How do CRY-dependent membrane properties in clock and non-clock tissues affect clock function and/or synchrony? What is the effect of eliminating CRY on salivary gland physiology? How did CRY evolve to perform such diverse functions in different tissues and different organisms? Results obtained from these studies should stimulate further interdisciplinary research in the fields of chronobiology, physiology and structural biology, and reveal mechanisms that are much awaited!

REFERENCES

Achee N, Zoran M (1997). Serotonin-induced modulation of excitability in an identified *Helisoma trivolvis* neuron. J Exp Biol 200:1537-48.

Agrawal P, Hardin PE (2016). The *Drosophila* receptor protein tyrosine phosphatase LAR is required for development of circadian pacemaker neuron processes that support rhythmic activity in constant darkness but not during Light/Dark cycles. J Neurosci 36:3860-3870.

Akten B, Jauch E, Genova GK, Kim EY, Edery I, Raabe T, Jackson FR (2003). A role for CK2 in the *Drosophila* circadian oscillator. Nat Neurosci 6:251-257.

Akten B, Tangredi MM, Jauch E, Roberts MA, Ng F, Raabe T, Jackson FR (2009). Ribosomal s6 kinase cooperates with casein kinase 2 to modulate the *Drosophila* circadian molecular oscillator. J Neurosci 29:466-475.

Andreazza S, Bouleau S, Martin B, Lamouroux A, Ponien P, Papin C, Chelot E, Jacquet E, Rouyer F (2015). Daytime CLOCK dephosphorylation is controlled by STRIPAK complexes in *Drosophila*. Cell Rep 11:1266-1279.

Andrew DJ, Henderson KD, Seshaiah P (2000). Salivary gland development in *Drosophila melanogaster*. Mech Dev 92:5-17.

Arble DM, Ramsey KM, Bass J, Turek FW (2010). Circadian disruption and metabolic disease: findings from animal models. Best Pract Res Clin Endocrinol Metab 24:785-800.

Ashmore LJ, Sehgal A (2003). A fly's eye view of circadian entrainment. J Biol Rhythms 18:206-16.

Bae K, Lee C, Hardin PE, Edery I (2000). dCLOCK is present in limiting amounts and likely mediates daily interactions between the dCLOCK-CYC transcription factor and the PER-TIM complex. J Neurosci 20:1746-53.

Bae K, Edery I (2006). Regulating a circadian clock's period, phase and amplitude by phosphorylation: insights from *Drosophila*. J Biochem 140:609-17.

Beckwith EJ, Ceriani MF (2015). Communication between circadian clusters: the key to a plastic network. FEBS Lett 589:3336-3342.

Bell-Pedersen D, Cassone VM, Earnest DJ, Golden SS, Hardin PE, Thomas TL, Zoran MJ (2005). Circadian rhythms from multiple oscillators: Lessons from diverse organisms. Nat Rev Genet 6:544-556.

Benito J, Zheng H, Hardin PE (2007). PDP1 epsilon functions downstream of the circadian oscillator to mediate behavioral rhythms. J Neurosci 27:2539-2547.

Benito J, Zheng H, Ng FS, Hardin PE (2007). Transcriptional feedback loop regulation, function, and ontogeny in *Drosophila*. Cold Spring Harb Symp Quant Biol 72:437-444.

Benito J, Houl JH, Roman GW, Hardin PE (2008). The blue-light photoreceptor CRYPTOCHROME is expressed in a subset of circadian oscillator neurons in the *Drosophila* CNS. J Biol Rhythms 23:296-307.

Berke B, Wittnam J, McNeill E, Van Vactor DL, Keshishian H (2013). Retrograde BMP signaling at the synapse: a permissive signal for synapse maturation and activity-dependent plasticity. J Neurosci 33:17937-17950.

Bixby JL (2001). Ligands and signaling through receptor-type tyrosine phosphatases. IUBMB Life 51:157-63.

Biyasheva A, Do TV, Lu Y, Vaskova M, Andres AJ (2001). Glue secretion in the *Drosophila* salivary gland: a model for steroid-regulated exocytosis. Dev Biol 231:234-51.

Blanchard FJ, Collins B, Cyran SA, Hancock DH, Taylor MV, Blau J (2010). The transcription factor Mef2 is required for normal circadian behavior in *Drosophila*. J Neurosci 30:5855-65.

Blumenthal EM (2001). Characterization of transepithelial potential oscillations in the *Drosophila* Malpighian tubule. J Exp Biol 20:3075-3084.

Buhr ED, Takahashi JS (2013). Molecular components of the Mammalian circadian clock. Handb Exp Pharmacol 217:3-27.

Busza A, Emery-Le M, Rosbash M, Emery P (2004). Roles of the two *Drosophila* CRYPTOCHROME structural domains in circadian photoreception. Science 304:1503-6.

Cao G, Nitabach MN (2008). Circadian control of membrane excitability in *Drosophila melanogaster* lateral ventral clock neurons. J Neurosci 28:6493-501.

Cardone L, Hirayama J, Giordano F, Tamaru T, Palvimo JJ, Sassone-Corsi P (2005). Circadian clock control by SUMOylation of BMAL1. Science 309:1390-4.

Cashmore AR (2003). Cryptochromes: enabling plants and animals to determine circadian time. Cell 114:537-43.

Cavanaugh DJ, Geratowski JD, Wooltorton JR, Spaethling JM, Hector CE, Zheng X, Johnson EC, Eberwine JH, Sehgal A (2014). Identification of a circadian output circuit for rest:activity rhythms in *Drosophila*. Cell 157:689-701.

Ceriani MF, Darlington TK, Staknis D, Más P, Petti AA, Weitz CJ, Kay SA (1999). Light-dependent sequestration of TIMELESS by CRYPTOCHROME. Science 285:553-6.

Chagnon MJ, Uetani N, Tremblay ML (2004). Functional significance of the LAR receptor protein tyrosine phosphatase family in development and diseases. Biochem Cell Biol 82:664-75.

Chen DY, Li MY, Wu SY, Lin YL, Tsai SP, Lai PL, Lin YT, Kuo JC, Meng TC, Chen GC (2012). The Bro1-domain-containing protein Myopic/HDPTP coordinates with Rab4 to regulate cell adhesion and migration. J Cell Sci 125:4841-52.

Chen F, Archambault V, Kar A, Lio P, D'Avino PP, Sinka R, Lilley K, Laue ED, Deak P, Capalbo L, Glover DM (2007). Multiple protein phosphatases are required for mitosis in *Drosophila*. Curr Biol 17:293-303.

Chiu JC, Vanselow JT, Kramer A, Edery I (2008). The phospho-occupancy of an atypical SLIMB-binding site on PERIOD that is phosphorylated by DOUBLETIME controls the pace of the clock. Genes Dev 22:1758-72.

Chiu JC, Ko HW, Edery I (2011). NEMO/NLK phosphorylates PERIOD to initiate a time-delay phosphorylation circuit that sets circadian clock speed. Cell 145:357-370.

Collins B, Mazzoni EO, Stanewsky R, Blau J (2006). *Drosophila* CRYPTOCHROME is a circadian transcriptional repressor. Curr Biol 16:441-9.

Collins B, Kane EA, Reeves DC, Akabas MH, Blau J (2012). Balance of activity between LN_vs and glutamatergic dorsal clock neurons promotes robust circadian rhythms in *Drosophila*. Neuron 74:706-718.

Cyran SA, Buchsbaum AM, Reddy KL, Lin MC, Glossop NRJ, Hardin PE, Young MW, Storti RV, Blau J (2003). vrille, Pdp1, and dClock form a second feedback loop in the *Drosophila* circadian clock. Cell 112:29-341.

De J, Varma V, Saha S, Sheeba V, Sharma VK (2013). Significance of activity peaks in fruit flies, *Drosophila melanogaster*, under seminatural conditions. Proc Natl Acad Sci U S A 110:8984-8989.

Depetris-Chauvin A, Fernández-Gamba A, Gorostiza EA, Herrero A, Castaño EM, Ceriani MF (2014). Mmp1 processing of the PDF neuropeptide regulates circadian structural plasticity of pacemaker neurons. PLoS Genet 10:e1004700.

Desai CJ, Krueger NX, Saito H, Zinn K (1997). Competition and cooperation among receptor tyrosine phosphatases control motoneuron growth cone guidance in *Drosophila*. Development 124:1941-1952.

Desai C, Purdy J (2003). The neural receptor protein tyrosine phosphatase DPTP69D is required during periods of axon outgrowth in *Drosophila*. Genetics 164:575-88.

Dietzl G, Chen D, Schnorrer F, Su KC, Barinova Y, Fellner M, Gasser B, Kinsey K, Oppel S, Scheiblauer S, Couto A, Marra V, Keleman K, Dickson BJ (2007). A genome-wide transgenic RNAi library for conditional gene inactivation in *Drosophila*. Nature 448:151-156.

Dinudom A, Fotia AB, Lefkowitz RJ, Young JA, Kumar S, Cook DI (2004). The kinase Grk2 regulates Nedd4/Nedd4-2-dependent control of epithelial Na^+ channels. Proc Natl Acad Sci U S A. 101:11886-90.

Dobbelaere J, Josué F, Suijkerbuijk S, Baum B, Tapon N, Raff J (2008). A genome-wide RNAi screen to dissect centriole duplication and centrosome maturation in *Drosophila*. PLoS Biol 6:e224.

Dolezelova E, Dolezel D, Hall JC (2007). Rhythm defects caused by newly engineered null mutations in *Drosophila's* cryptochrome gene. Genetics 177:329-45.

Doi M, Hirayama J, Sassone-Corsi P (2006). Circadian regulator CLOCK is a histone acetyltransferase. Cell 125:497-508.

Dow JA, Maddrell SH, Görtz A, Skaer NJ, Brogan S, Kaiser K (1994). The malpighian tubules of *Drosophila melanogaster*: a novel phenotype for studies of fluid secretion and its control. J Exp Biol 197:421-8.

Dunlap JC (1999). Molecular bases for circadian clocks. Cell 96:271-290.

Dunlap JC, Loros JJ, DeCoursey PJ (2004). Chronobiology: Biological Timekeeping; 4th edition. Sinauer Associates, Inc. Publishers, Sunderland, Massachusetts, U.S.A.

Ebisawa T, Fukuchi M, Murakami G, Chiba T, Tanaka K, Imamura T, Miyazono K (2001). Smurf1 interacts with transforming growth factor-beta type I receptor through Smad7 and induces receptor degradation. J Biol Chem 276:12477-80.

Edery I, Zwiebel LJ, Dembinska ME, Rosbash M (1994). Temporal phosphorylation of the *Drosophila* period protein. Proc Natl Acad Sci U S A 91:2260-4.

Edery I (1999). Role of posttranscriptional regulation in circadian clocks: Lessons from *Drosophila*. Chronobiology International 16:377-414.

Egan ES, Franklin TM, Hilderbrand-Chae MJ, McNeil GP, Roberts MA, Schroeder AJ, Zhang X, Jackson FR (1999). An extraretinally expressed insect cryptochrome with similarity to the blue light photoreceptors of mammals and plants. J Neurosci 19:3665-73.

Emery IF, Noveral JM, Jamison CF, Siwicki KK. Rhythms of *Drosophila* period gene expression in culture. Proc Natl Acad Sci U S A 94:4092-6.

Emery P, So WV, Kaneko M, Hall JC, Rosbash M (1998). CRY, a *Drosophila* clock and light-regulated cryptochrome, is a major contributor to circadian rhythm resetting and photosensitivity. Cell 95:669-79.

Emery P, Stanewsky R, Helfrich-Forster C, Emery-Le M, Hall JC, Rosbash M (2000). *Drosophila* CRY is a deep brain circadian photoreceptor. Neuron 26:493-504.

Etchegaray JP, Lee C, Wade PA, Reppert SM (2003). Rhythmic histone acetylation underlies transcription in the mammalian circadian clock. Nature 421:177-82.

Fang Y, Sathyanarayanan S, SehgalA (2007). Post-translational regulation of the *Drosophila* circadian clock requires protein phosphatase 1 (PP1). Genes Dev 21:1506-1518.

Fernandez MP, Berni J, Ceriani MF (2008). Circadian remodeling of neuronal circuits involved in rhythmic behavior. PLoS Biol 6:e69.

Fogle KJ, Parson KG, Dahm NA, Holmes TC (2011). CRYPTOCHROME is a blue-light sensor that regulates neuronal firing rate. Science 331:1409-1413.

Fogle KJ, Baik LS, Houl JH, Tran TT, Roberts L, Dahm NA, Cao Y, Zhou M, Holmes TC (2015). CRYPTOCHROME-mediated phototransduction by modulation of the potassium ion channel β-subunit redox sensor. Proc Natl Acad Sci U S A 112:2245-50.

Fox AN, Zinn K (2005). The heparan sulfate proteoglycan syndecan is an *in vivo* ligand for the *Drosophila* LAR receptor tyrosine phosphatase. Curr Biol 15:1701-1711.

Frisch B, Fleissner G, Brandes C, Hall JC (1996). Staining in the brain of *Pachymorpha sexguttata* mediated by an antibody against a *Drosophila* clock-gene product: labeling of cells with possible importance for the beetle's circadian rhythms. Cell Tissue Res 286:411-429.

Gallego M, Virshup DM (2007). Post-translational modifications regulate the ticking of the circadian clock. Nat Rev Mol Cell Biol 8:139-48.

Giebultowicz JM, Hege DM (1997). Circadian clock in Malpighian tubules. Nature 386:664.

Glossop NR, Lyons LC, Hardin PE (1999). Interlocked feedback loops within the *Drosophila* circadian oscillator. Science 286:766-8.

Glossop NR, Hardin PE (2002). Central and peripheral circadian oscillator mechanisms in flies and mammals. J Cell Sci 115:3369-3377.

Glossop NR, Houl JH, Zheng H, Ng FS, Dudek SM, Hardin PE (2003). VRILLE feeds back to control circadian transcription of Clock in the *Drosophila* circadian oscillator. Neuron 37:249-61.

Goodman CS (1996). Mechanisms and molecules that control growth cone guidance. Annu Rev Neurosci 19:341-77.

Granados-Fuentes D, Hermanstyne TO, Carrasquillo Y, Nerbonne JM, Herzog ED (2015). IA channels encoded by Kv1.4 and Kv4.2 regulate circadian period of PER2 expression in the Suprachiasmatic Nucleus. J Biol Rhythms 30:396-407.

Gratz SJ, Cummings AM, Nguyen JN, Hamm DC, Donohue LK, Harrison MM, Wildonger J, O'Connor-Giles KM (2013). Genome engineering of *Drosophila* with the CRISPR RNA-guided Cas9 nuclease. Genetics 194:1029-35.

Grima B, Lamouroux A, Chélot E, Papin C, Limbourg-Bouchon B, Rouyer F (2002). The F-box protein slimb controls the levels of clock proteins period and timeless. Nature 420:178-82.

Hall JC (2003). Genetics and molecular biology of rhythms in *Drosophila* and other insects. Adv Genet 48:1-280.

Hamblen MJ, White NE, Emery PT, Kaiser K, Hall JC (1998). Molecular and behavioral analysis of four period mutants in *Drosophila melanogaster* encompassing extreme short, novel long, and unorthodox arrhythmic types. Genetics 149:165-78.

Hardin PE, Hall JC, Rosbash M (1990). Feedback of the *Drosophila* period gene-product on circadian cycling of its mRNA levels. Nature 343:536-540.

Hardin PE (2005). The circadian timekeeping system of *Drosophila*. Current Biology 15:R714-R722.

Hardin PE (2011). Molecular genetic analysis of circadian timekeeping in *Drosophila*. Adv Genet 74:141-173.

Hardin PE, Panda S (2013). Circadian timekeeping and output mechanisms in animals. Curr Opin Neurobiol 23:724-731.

Hariharan IK, Chuang PT, Rubin GM (1991). Cloning and characterization of a receptor-class phosphotyrosine phosphatase gene expressed on central nervous system axons in *Drosophila melanogaster*. Proc Natl Acad Sci U S A 88:11266-70.

Harms E, Kivimae S, Young MW, Saez L (2004). Posttranscriptional and posttranslational regulation of clock genes. J Biol Rhythms 19:361-73.

Harrisingh MC, Wu Y, Lnenicka GA, Nitabach MN (2007). Intracellular Ca^{2+} regulates free-running circadian clock oscillation *in vivo*. J Neurosci 27:12489-12499.

Helfrich-Forster C (1997). Development of pigment-dispersing hormone immunoreactive neurons in the nervous system of *Drosophila melanogaster*. J Comp Neurol 380:335-354.

Helfrich-Forster C, Stengl M, Homberg U (1998). Organization of the circadian system in insects. Chronobiol Int 15:567-594.

Helfrich-Forster C, Winter C, Hofbauer A, Hall JC, Stanewsky R (2001). The circadian clock of fruit flies is blind after elimination of all known photoreceptors. Neuron 30:249-61.

Helfrich-Forster C, Edwards T, Yasuyama K, Wisotzki B, Schneuwly S, Stanewsky R, Meinertzhagen IA, Hofbauer A (2002). The extraretinal eyelet of *Drosophila*: development, ultrastructure, and putative circadian function. J Neurosci 22:9255-66.

Helfrich-Forster C (2003). The neuroarchitecture of the circadian clock in the brain of *Drosophila melanogaster*. Microsc Res Tech 62:94-102.

Helfrich-Forster C (2005). Organization of endogenous clocks in insects. Biochem Soc Trans 33:957-961.

Helfrich-Forster C, Shafer OT, Wülbeck C, Grieshaber E, Rieger D, Taghert P (2007). Development and morphology of the clock-gene-expressing lateral neurons of *Drosophila melanogaster*. J Comp Neurol 500:47-70.

Helfrich-Forster C (2014). From neurogenetic studies in the fly brain to a concept in circadian biology. J Neurogenet 28:329-347.

Hirayama J, Sahar S, Grimaldi B, Tamaru T, Takamatsu K, Nakahata Y, Sassone-Corsi P (2007). CLOCK-mediated acetylation of BMAL1 controls circadian function. Nature 450:1086-90.

Homberg U, Wurden S, Dircksen H, Rao KR (1991). Comparative anatomy of pigment-dispersing hormone immunoreactive neurons in the brain of orthopteriod insects. Cell Tissue Res 266:343-357.

Houl JH, Ng F, Taylor P, Hardin PE (2008). CLOCK expression identifies developing circadian oscillator neurons in the brains of *Drosophila* embryos. BMC Neurosci 9:119.

Hyun S, Lee Y, Hong ST, Bang S, Paik D, Kang J, Shin J, Lee J, Jeon K, Hwang S, Bae E, Kim J (2005). *Drosophila* GPCR Han is a receptor for the circadian clock neuropeptide PDF. Neuron 48:267-278.

Im SH, Li W, Taghert PH (2011). PDFR and CRY signaling converge in a subset of clock neurons to modulate the amplitude and phase of circadian behavior in *Drosophila*. PLoS One 6:e18974.

Ishikawa T, Matsumoto A, Kato T Jr, Togashi S, Ryo H, Ikenaga M, Todo T, Ueda R, Tanimura T (1999). DCRY is a *Drosophila* photoreceptor protein implicated in light entrainment of circadian rhythm. Genes Cells 4:57-65.

Ivanchenko M, Stanewsky R, Giebultowicz JM (2001). Circadian photoreception in *Drosophila*: functions of cryptochrome in peripheral and central clocks. J Biol Rhythms 16:205-15.

Janssens V, Goris J (2001). Protein phosphatase 2A: a highly regulated family of serine/threonine phosphatases implicated in cell growth and signaling. Biochem J 353:417-39.

Jeon M, Nguyen H, Bahri S, Zinn K (2008). Redundancy and compensation in axon guidance: genetic analysis of the *Drosophila* Ptp10D/Ptp4E receptor tyrosine phosphatase subfamily. Neural Dev 31;3:3.

Jhaveri D, Saharan S, Sen A, Rodrigues V (2004). Positioning sensory terminals in the olfactory lobe of *Drosophila* by Robo signaling. Development 131:1903-1912.

Johard HA, Yoishii T, Dircksen H, Cusumano P, Rouyer F, Helfrich-Forster C, Nassel DR (2009). Peptidergic clock neurons in *Drosophila*: ion transport peptide and short neuropeptide F in subsets of dorsal and ventral lateral neurons. J Comp Neurol 516:59-73.

Johnson KG, Tenney AP, Ghose A, Duckworth AM, Higashi ME, Parfitt K, Marcu O, Heslip TR, Marsh JL, Schwarz TL, Flanagan JG, Van Vactor D (2006). The HSPGs Syndecan and Dallylike bind the receptor phosphatase LAR and exert distinct effects on synaptic development. Neuron 49:517-531.

Kaasik K, Kivimae S, Allen JJ, Chalkley RJ, Huang Y, Baer K, Kissel H, Burlingame AL, Shokat KM, Ptáček LJ, Fu YH (2013). Glucose sensor O-GlcNAcylation coordinates with phosphorylation to regulate circadian clock. Cell Metab 17:291-302.

Katada S, Sassone-Corsi P (2010). The histone methyltransferase MLL1 permits the oscillation of circadian gene expression. Nat Struct Mol Biol 17:1414-21.

Kaufmann N, DeProto J, Ranjan R, Wan H, Van Vactor D (2002). *Drosophila* liprin-alpha and the receptor phosphatase *Dlar* control synapse morphogenesis. Neuron 34:27-38.

Kerekes É, Kókai E, Páldy FS, Dombrádi V (2014). Functional analysis of the glycogen binding subunit CG9238/Gbs-70E of protein phosphatase 1 in *Drosophila melanogaster*. Insect Biochem Mol Biol 49:70-9.

Kim EY, and Edery I (2006). Balance between DBT/CKI epsilon kinase and protein phosphatase activities regulate phosphorylation and stability of *Drosophila* CLOCK protein. Proc Natl Acad Sci U S A 103:6178-6183.

Kim EY, Ko HW, Yu WJ, Hardin PE, Edery I (2007). A DOUBLETIME kinase binding domain on the *Drosophila* PERIOD protein is essential for its hyperphosphorylation, transcriptional repression, and circadian clock function. Mol Cell Biol 27:5014-5028.

Kivimae S, Saez L, Young MW (2008). Activating PER repressor through a DBT-directed phosphorylation switch. PLoS Biol 6:e183.

Klarsfeld A, Malpel S, Michard-Vanhée C, Picot M, Chélot E, Rouyer F (2004). Novel features of cryptochrome-mediated photoreception in the brain circadian clock of *Drosophila*. J Neurosci 24:1468-77.

Kloss B, Price JL, Saez L, Blau J, Rothenfluh A, Wesley CS, Young MW (1998). The *Drosophila* clock gene double-time encodes a protein closely related to human casein kinase I epsilon. Cell 94:97-107.

Kloss B, Rothenfluh A, Young MW, Saez L (2001). Phosphorylation of period is influenced by cycling physical associations of double-time, period, and timeless in the *Drosophila* clock. Neuron 30:699 -706.

Ko CH, Takahashi JS (2006). Molecular components of the mammalian circadian clock. Hum Mol Genet 15:R271-7.

Ko HW, Jiang J, Edery I (2002). Role for Slimb in the degradation of *Drosophila* Period protein phosphorylated by Doubletime. Nature 420:673-8.

Ko HW, Kim EY, Chiu J, Vanselow JT, Kramer A, Edery I (2010). A hierarchical phosphorylation cascade that regulates the timing of PERIOD nuclear entry reveals novel roles for proline-directed kinases and GSK-3beta/SGG in circadian clocks. J Neurosci 30:12664-75.

Koh K, Zheng X, Sehgal A (2006). JETLAG resets the *Drosophila* circadian clock by promoting light-induced degradation of TIMELESS. Science 312:1809-12.

Krishnan B, Dryer SE, Hardin PE (1999). Circadian rhythms in olfactory responses of *Drosophila melanogaster*. Nature 400:375-378.

Krishnan B, Levine JD, Lynch MK, Dowse HB, Funes P, Hall JC, Hardin PE, Dryer SE (2001). A new role for cryptochrome in a *Drosophila* circadian oscillator. Nature 411:313-7.

Krueger NX, Van Vactor D, Wan HI, Gelbart WM, Goodman CS, Saito H (1996). The transmembrane tyrosine phosphatase DLAR controls motor axon guidance in *Drosophila*. Cell 84:611-622.

Kypta RM, Su H, Reichardt LF (1996). Association between a transmembrane protein tyrosine phosphatase and the cadherin-catenin complex. J Cell Biol 134:1519-1529.

Laposky AD, Bass J, Kohsaka A, Turek FW (2008). Sleep and circadian rhythms: key components in the regulation of energy metabolism. FEBS Lett 582:142-51.

Lear BC, Merrill CE, Lin JM, Schroeder A, Zhang L, Allada R (2005). A G protein-coupled receptor, groom-of-PDF, is required for PDF neuron action in circadian behavior. Neuron 48:221-227.

Lee CG, Parikh V, Itsukaichi T, Bae K, Edery I (1996). Resetting the *Drosophila* clock by photic regulation of PER and a PER-TIM complex. Science 271:1740-1744.

Lee E, Jeong EH, Jeong HJ, Yildirim E, Vanselow JT, Ng F, Liu Y, Mahesh G, Kramer A, Hardin PE, Edery I, Kim EY (2014). Phosphorylation of a central clock transcription factor is required for thermal but not photic entrainment. PLoS Genet 10:e1004545.

Lee J, Lee Y, Lee MJ, Park E, Kang SH, Chung CH, Lee KH, Kim K (2008). Dual modification of BMAL1 by SUMO2/3 and ubiquitin promotes circadian activation of the CLOCK/BMAL1 complex. Mol Cell Biol 28:6056-65.

Levine JD, Funes P, Dowse HB, Hall JC (2002). Advanced analysis of a cryptochrome mutation's effects on the robustness and phase of molecular cycles in isolated peripheral tissues of *Drosophila*. BMC Neurosci 15;3:5.

Lim C, Allada R (2013). Emerging roles for post-transcriptional regulation in circadian clocks. Nat Neurosci 16:1544-50.

Lin F, Song W, Meyer-Bernstein E, Naidoo N, and Sehgal A (2001). Photic signaling by cryptochrome in the *Drosophila* circadian clock. Mol Cell Biol 21:7287-7294.

Lin JM, Kilman VL, Keegan K, Paddock B, Emery-Le M, Rosbash M, Allada R (2002). A role for casein kinase 2 alpha in the *Drosophila* circadian clock. Nature 420:816-820.

Lin Y, Stormo GD, Taghert PH (2004). The neuropeptide pigment dispersing factor coordinates pacemaker interactions in the *Drosophila* circadian system. J Neurosci 24:7951-7957.

Liu T, Mahesh G, Houl JH, Hardin PE (2015). Circadian activators are expressed days before they initiate clock function in late pacemaker neurons from *Drosophila*. J Neurosci 35:8662-8671.

Lundberg A (1955). The electrophysiology of the submaxillary gland of the cat. Acta Physiol Scand 35:1-25.

Mahesh G, Jeong E, Ng FS, Liu Y, Gunawardhana K, Houl JH, Yildirim E, Amunugama R, Jones R, Allen DL, Edery I, Kim EY, Hardin PE (2014). Phosphorylation of the transcription activator CLOCK regulates progression through a ~ 24-h feedback loop to influence the circadian period in *Drosophila*. J Biol Chem 289:19681-93.

Maier B, Wendt S, Vanselow JT, Wallach T, Reischl S, Oehmke S, Schlosser A, Kramer A (2009). A large-scale functional RNAi screen reveals a role for CK2 in the mammalian circadian clock. Genes Dev 23:708-718.

Martinek S, Inonog S, Manoukian AS, Young MW (2001). A role for the segment polarity gene shaggy/GSK-3 in the *Drosophila* circadian clock. Cell 105:769-779.

Mazzoni EO, Desplan C, Blau J (2005). Circadian pacemaker neurons transmit and modulate visual information to control a rapid behavioral response. Neuron 45:293-300.

McGuire SE, Le PT, Osborn AJ, Matsumoto K, Davis RL (2003). Spatiotemporal rescue of memory dysfunction in *Drosophila*. Science 302:1765-1768.

Mehra A, Baker CL, Loros JJ, Dunlap JC (2009). Post-translational modifications in circadian rhythms. Trends Biochem Sci 34:483-90.

Menet JS, Hardin PE (2014). Circadian clocks: the tissue is the issue. Curr Biol 24:R25-R27.

Mertens I, Vandingenen A, Johnson EC, Shafer OT, Li W, Trigg JS, De Loof A, Schoofs L, Taghert PH (2005). PDF receptor signaling in *Drosophila* contributes to both circadian and geotactic behaviors. Neuron 48:213-219.

Mizoguchi T, Putterill J, Ohkoshi Y (2006). Kinase and phosphatase: The cog and spring of the circadian clock. Int Rev Cytol 250:47-72.

Mohawk JA, Green CB, Takahashi JS (2012). Central and peripheral circadian clocks in mammals. Annu Rev Neurosci 35:445-62.

Muskus MJ, Preuss F, Fan JY, Bjes ES, Price JL (2007). *Drosophila* DBT lacking protein kinase activity produces long-period and arrhythmic circadian behavioral and molecular rhythms. Mol Cell Biol 27:8049-8064.

Nakai Y, Horiuchi J, Tsuda M, Takeo S, Akahori S, Matsuo T, Kume K, Aigaki T (2011). Calcineurin and its regulator sra/DSCR1 are essential for sleep in *Drosophila*. J Neurosci 31:12759-66.

Nawathean P, Rosbash M (2004). The doubletime and CKII kinases collaborate to potentiate *Drosophila* PER transcriptional repressor activity. Mol Cell 13:213-223.

Nawathean P, Stoleru D, Rosbash M (2007). A small conserved domain of *Drosophila* PERIOD is important for circadian phosphorylation, nuclear localization, and transcriptional repressor activity. Mol Cell Biol 27:5002-13.

Nishiyama A, Petersen OH (1974). Membrane potential and resistance measurement in acinar cells from salivary glands in vitro: effect of acetylcholine. J Physiol 242:173-88.

Nitabach MN, Taghert PH (2008). Organization of the *Drosophila* circadian control circuit. Curr Biol 18:R84-R93.

O'Grady P, Thai TC, Saito H (1998). The laminin-nidogen complex is a ligand for a specific splice isoform of the transmembrane protein tyrosine phosphatase LAR. J Cell Biol 141:1675-1684.

Ozturk N, Selby CP, Zhong D, Sancar A (2014). Mechanism of photosignaling by *Drosophila* cryptochrome: role of the redox status of the flavin chromophore. J Biol Chem 289:4634-42.

Park JH, Helfrich-Forster C, Lee G, Liu L, Rosbash M, Hall JC (2000). Differential regulation of circadian pacemaker output by separate clock genes in *Drosophila*. Proc Natl Acad Sci U S A 97:3608-3613.

Partch CL, Green CB, Takahashi JS (2014). Molecular architecture of the mammalian circadian clock. Trends Cell Biol 24:90-99.

Peng IF, and Wu CF (2007). Differential contributions of Shaker and Shab K^+ currents to neuronal firing patterns in *Drosophila*. J Neurophysiol 97:780-94.

Peng Y, Stoleru D, Levine JD, Hall JC, Rosbash M (2003). *Drosophila* free running rhythms require intercellular communication. PLoS Biol 1:E13.

Peschel N, Veleri S, Stanewsky R (2006). Veela defines a molecular link between Cryptochrome and Timeless in the light-input pathway to *Drosophila's* circadian clock. Proc Natl Acad Sci U S A 103:17313-8.

Peschel N, Chen KF, Szabo G, Stanewsky R (2009). Light-dependent interactions between the *Drosophila* circadian clock factors cryptochrome, jetlag, and timeless. Curr Biol 19:241-7.

Peschel N, Helfrich-Forster C (2011). Setting the clock–by nature: circadian rhythm in the fruitfly *Drosophila melanogaster*. FEBS Lett 585:1435-1442.

Pfeiffenberger C, Lear BC, Keegan KP, Allada R (2010). Sleep and circadian behavior monitoring in *Drosophila*. In: *Drosophila* neurobiology: a laboratory manual (Zhang B, Freeman MR, Waddell S, eds), pp 483-504. New York: Cold Spring Harbor.

Plautz JD, Kaneko M, Hall JC, Kay SA (1997). Independent photoreceptive circadian clocks throughout *Drosophila*. Science 278:1632-5.

Preitner N, Damiola F, Molina LL, Zakany J, Duboule D, Albrecht U, Schibler U (2002). The orphan nuclear receptor REV-ERB alpha controls circadian transcription within the positive limb of the mammalian circadian oscillator. Cell 110:251-260.

Price JL, Dembinska ME, Young MW, Rosbash M (1995). Suppression of PERIOD protein abundance and circadian cycling by the *Drosophila* clock mutation timeless. EMBO J 14:4044-9.

Price JL, Blau J, Rothenfluh A, Abodeely M, Kloss B, Young MW (1998). double-time is a novel *Drosophila* clock gene that regulates PERIOD protein accumulation. Cell 94:83-95.

Ren X, Sun J, Housden BE, Hu Y, Roesel C, Lin S, Liu LP, Yang Z, Mao D, Sun L, Wu Q, Ji JY, Xi J, Mohr SE, Xu J, Perrimon N, Ni JQ (2013). Optimized gene editing technology for *Drosophila melanogaster* using germ line-specific Cas9. Proc Natl Acad Sci U S A 110: 19012-19017.

Renn SC, Park JH, Rosbash M, Hall JC, Taghert PH (1999). A *pdf* neuropeptide gene mutation and ablation of PDF neurons each cause severe abnormalities of behavioral circadian rhythms in *Drosophila*. Cell 99:791-802.

Reppert SM, and Weaver DR (2002). Coordination of circadian timing in mammals. Nature 418:935-941.

Rieger D, Stanewsky R, Helfrich-Forster C (2003). Cryptochrome, compound eyes, Hofbauer-Buchner eyelets, and ocelli play different roles in the entrainment and masking pathway of the locomotor activity rhythm in the fruit fly *Drosophila melanogaster*. J Biol Rhythms 18: 377-391.

Riganti C, Gazzano E, Polimeni M, Costamagna C, Bosia A, Ghigo D (2004). Diphenyleneiodonium inhibits the cell redox metabolism and induces oxidative stress. J Biol Chem 279:47726-31.

Ripperger JA, Schibler U (2006). Rhythmic CLOCK-BMAL1 binding to multiple E-box motifs drives circadian Dbp transcription and chromatin transitions. Nat Genet 38:369-74.

Romanenko VG, Nakamoto T, Catalán MA, Gonzalez-Begne M, Schwartz GJ, Jaramillo Y, Sepúlveda FV, Figueroa CD, Melvin JE (2008). Clcn2 encodes the hyperpolarization-

activated chloride channel in the ducts of mouse salivary glands. Am J Physiol Gastrointest Liver Physiol 295:G1058-67.

Rosato E, Codd V, Mazzotta G, Piccin A, Zordan M, Costa R, Kyriacou CP (2001). Light-dependent interaction between *Drosophila* CRY and the clock protein PER mediated by the carboxy terminus of CRY. Curr Biol 11:909-17.

Sami F, Smet-Nocca C, Khan M, Landrieu I, Lippens G, Brautigan DL (2011). Molecular basis for an ancient partnership between prolyl isomerase Pin1 and phosphatase inhibitor-2. Biochemistry 50:6567-78.

Sathyanarayanan S, Zheng X, Xiao R, Sehgal A (2004). Posttranslational regulation of *Drosophila* PERIOD protein by protein phosphatase 2A. Cell 116:603-615.

Schertel C, Huang D, Björklund M, Bischof J, Yin D, Li R, Wu Y, Zeng R, Wu J, Taipale J, Song H, Basler K (2013). Systematic screening of a *Drosophila* ORF library *in vivo* uncovers Wnt/Wg pathway components. Dev Cell 25:207-19.

Schibler U (1998). Circadian rhythms - New cogwheels in the clockworks. Nature 393:620-621.

Seeger M, Tear G, Ferres-Marco D, Goodman CS (1993). Mutations affecting growth cone guidance in *Drosophila*: genes necessary for guidance toward or away from the midline. Neuron 10:409-426.

Sehgal A, Rothenfluhhilfiker A, Hunterensor M, Chen YF, Myers MP, Young MW (1995). Rhythmic expression of timeless - a basis for promoting circadian cycles in period gene autoregulation. Science 270:808-810.

Shafer OT, Helfrich-Forster C, Renn SC, Taghert PH (2006). Reevaluation of *Drosophila melanogaster's* neuronal circadian pacemakers reveals new neuronal classes. J Comp Neurol 498:180-93.

Shafer OT, Yao Z (2014). Pigment-dispersing factor signaling and circadian rhythms in insect locomotor activity. Curr Opin Insect Sci 1:73-80.

Shang Y, Griffith LC, Rosbash M (2008). Light-arousal and circadian photoreception circuits intersect at the large PDF cells of the *Drosophila* brain. Proc Natl Acad Sci U S A 105:19587-19594.

Sheeba V, Fogle KJ, Kaneko M, Rashid S, Chou YT, Sharma VK, Holmes TC (2008). Large ventral lateral neurons modulate arousal and sleep in *Drosophila*. Curr Biol 18:1537-1545.

Sheeba V, Fogle KJ, Holmes TC (2010). Persistence of morning anticipation behavior and high amplitude morning startle response following functional loss of small ventral lateral neurons in *Drosophila*. PLoS One 5:e11628.

Sivachenko A, Li Y, Abruzzi KC, Rosbash M (2013). The transcription factor Mef2 links the *Drosophila* core clock to Fas2, neuronal morphology, and circadian behavior. Neuron 79:281-92.

Sopko R, Foos M, Vinayagam A, Zhai B, Binari R, Hu Y, Randklev S, Perkins LA, Gygi SP, Perrimon N (2014). Combining genetic perturbations and proteomics to examine kinase-phosphatase networks in *Drosophila* embryos. Dev Cell 31:114-27.

Stanewsky R, Kaneko M, Emery P, Beretta B, Wager-Smith K, Kay SA, Rosbash M, Hall JC (1998). The *cry*^{b} mutation identifies cryptochrome as a circadian photoreceptor in *Drosophila*. Cell 95:681-92.

Stengl M, Homberg U (1994). Pigment-dispersing hormone-immunoreactive neurons in the cockroach *Leucophaea maderae* share properties with circadian pacemaker neurons. J Comp Physiol A 175:203-213.

Streuli M, Krueger NX, Tsai AY, Saito H (1989). A family of receptor-linked protein tyrosine phosphatases in humans and *Drosophila*. Proc Natl Acad Sci U S A 86:8698-8702.

Stroschein-Stevenson SL, Foley E, O'Farrell PH, Johnson AD (2006). Identification of *Drosophila* gene products required for phagocytosis of *Candida albicans*. PLoS Biol 4:e4.

Sun L, Yu MC, Kong L, Zhuang ZH, Hu JH, Ge BX (2008). Molecular identification and functional characterization of a *Drosophila* dual-specificity phosphatase DMKP-4 which is involved in PGN-induced activation of the JNK pathway. Cell Signal 20:1329-37.

Suri V, Qian Z, Hall JC, Rosbash M (1998). Evidence that the TIM light response is relevant to light-induced phase shifts in *Drosophila melanogaster*. Neuron 21:225-34.

Szabo A, Papin C, Zorn D, Ponien P, Weber F, Raabe T, Rouyer F (2013). The CK2 kinase stabilizes CLOCK and represses its activity in the *Drosophila* circadian oscillator. PLoS Biol 11:e1001645.

Szular J, Sehadova H, Gentile C, Szabo G, Chou WH, Britt SG, Stanewsky R (2012). Rhodopsin 5- and Rhodopsin 6-mediated clock synchronization in *Drosophila melanogaster* is independent of retinal phospholipase C-β signaling. J Biol Rhythms 27:25-36.

Tayler TD, Robichaux MB, Garrity PA (2004). Compartmentalization of visual centers in the *Drosophila* brain requires slit and Robo proteins. Development 131:5935-5945.

Taylor P, Hardin PE (2008). Rhythmic E-box binding by CLK-CYC controls daily cycles in *per* and *tim* transcription and chromatin modifications. Mol Cel Biol 28:4642-4652.

Tian SS, Tsoulfas P, Zinn K (1991). Three receptor-linked protein-tyrosine phosphatases are selectively expressed on central nervous system axons in the *Drosophila* embryo. Cell 67:675-85.

Turek FW, Dugovic C, Zee PC (2001). Current understanding of the circadian clock and the clinical implications for neurological disorders. Arch Neurol 58:1781-1787.

Ueda HR, Hagiwara M, Kitano H (2001). Robust oscillations within the interlocked feedback model of *Drosophila* circadian rhythm. J Theor Biol 210:401-6.

Vaidya AT, Top D, Manahan CC, Tokuda JM, Zhang S, Pollack L, Young MW, Crane BR (2013). Flavin reduction activates *Drosophila* cryptochrome. Proc Natl Acad Sci U S A 110:20455-60.

Veleri S, Brandes C, Helfrich-Forster C, Hall JC, Stanewsky R (2003). A self-sustaining, light-entrainable circadian oscillator in the *Drosophila* brain. Curr Biol 13:1758-1767.

Veleri S, Rieger D, Helfrich-Forster C, Stanewsky R (2007). Hofbauer-Buchner eyelet affects circadian photosensitivity and coordinates TIM and PER expression in *Drosophila* clock neurons. J Biol Rhythms 22:29-42.

Venken KJ, Kasprowicz J, Kuenen S, Yan J, Hassan BA, Verstreken P (2008). Recombineering-mediated tagging of *Drosophila* genomic constructs for *in vivo* localization and acute protein inactivation. Nucleic Acids Res 36(18):e114.

Venken KJ, Carlson JW, Schulze KL, Pan H, He Y, Spokony R, Wan KH, Koriabine M, de Jong PJ, White KP, Bellen HJ, Hoskins RA (2009). Versatile P[acman] BAC libraries for transgenesis studies in *Drosophila melanogaster*. Nat Methods 6:431-4.

Verselis VK, Bennett MV, Bargiello TA (1991). A voltage-dependent gap junction in *Drosophila melanogaster*. Biophys J 59:114-26.

Walton KM, Dixon JE (1993). Protein tyrosine phosphatases. Annu Rev Biochem 62:101-20.

Wang TA, Yu YV, Govindaiah G, Ye X, Artinian L, Coleman TP, Sweedler JV, Cox CL, Gillette MU (2012). Circadian rhythm of redox state regulates excitability in suprachiasmatic nucleus neurons. Science 337:839-42.

Weber F, Zorn D, Rademacher C, Hung HC (2011). Post-translational timing mechanisms of the *Drosophila* circadian clock. FEBS Lett 585:1443-9.

Weng LP, Wang X, YuQ (1999). Transmembrane tyrosine phosphatase LAR induces apoptosis by dephosphorylating and destabilizing p130 Cas. Genes Cells 4:185-196.

Wheeler DA, Hamblen-Coyle MJ, Dushay MS, Hall JC (1993). Behavior in light-dark cycles of *Drosophila* mutants that are arrhythmic, blind, or both. J Biol Rhythms 8:67-94.

Wills Z, Bateman J, Korey CA, Comer A, Van Vactor D (1999). The tyrosine kinase Abl and its substrate enabled collaborate with the receptor phosphatase *Dlar* to control motor axon guidance. Neuron 22:301-312.

Wu CL, Xia S, Fu TF, Wang H, Chen YH, Leong D, Chiang AS, Tully T (2007). Specific requirement of NMDA receptors for long-term memory consolidation in *Drosophila* ellipsoid body. Nat Neurosci 10:1578-86.

Wulbeck C, Grieshaber E, Helfrich-Forster C (2008). Pigment-dispersing factor (PDF) has different effects on *Drosophila's* circadian clocks in the accessory medulla and in the dorsal brain. J Biol Rhythms 23:409-424.

Wuttke WA, Berry MS (1992). Modulation of inwardly rectifying Na ($^{+}$)-K^{+} channels by serotonin and cyclic nucleotides in salivary gland cells of the leech, *Haementeria*. J Membr Biol 127:57-68.

Xu Y, Fisher GJ (2012). Receptor type protein tyrosine phosphatases (RPTPs): roles in signal transduction and human disease. J Cell Commun Signal 6:125-138.

Yang Z, Emerson M, Su HS, Sehgal A (1998). Response of the timeless protein to light correlates with behavioral entrainment and suggests a nonvisual pathway for circadian photoreception. Neuron 21:215-23.

Yang ZH, Sehgal A (2001). Role of molecular oscillations in generating behavioral rhythms in *Drosophila*. Neuron 29:453-467.

Yao Z, Shafer OT (2014). The *Drosophila* circadian clock is a variably coupled network of multiple peptidergic units. Science 343:1516-20.

Yoshii T, Todo T, Wulbeck C, Stanewsky R, Helfrich-Forster C (2008). Cryptochrome is present in the compound eyes and a subset of *Drosophila's* clock neurons. J Comp Neurol 508:952-66.

Yoshii T, Ahmad M, Helfrich-Forster C (2009). Cryptochrome mediates light-dependent magnetosensitivity of *Drosophila's* circadian clock. PLoS Biol. 2009 Apr 7;7(4):e1000086.

Yoshii T, Rieger D, Helfrich-Forster C (2012). Two clocks in the brain: an update of the morning and evening oscillator model in *Drosophila*. Prog Brain Res 199:59-82.

Yu W, Zheng H, Houl JH, Dauwalder B, Hardin PE (2006). PER-dependent rhythms in CLK phosphorylation and E-box binding regulate circadian transcription. Gene Dev 20:723-733.

Yu WJ, Zheng H, Price JL, Hardin PE (2009). DOUBLETIME plays a non-catalytic role to mediate CLOCK phosphorylation and repress CLOCK-dependent transcription within the *Drosophila* circadian clock. Mol Cel Biol 29:1452-1458.

Yu W, Houl JH, Hardin PE (2011). NEMO kinase contributes to core period determination by slowing the pace of the *Drosophila* circadian oscillator. Curr Biol 21:756-761.

Zeng HK, Qian ZW, Myers MP, Rosbash M (1996). A light-entrainment mechanism for the *Drosophila* circadian clock. Nature 380:129-135.

Zhang ZY (1998). Protein-tyrosine phosphatases: biological function, structural characteristics, and mechanism of catalysis. Crit Rev Biochem Mol Biol 33:1-52.

Zhao J, Kilman VL, Keegan KP, Peng Y, Emery P, Rosbash M, Allada R (2003). *Drosophila* clock can generate ectopic circadian clocks. Cell 113:755-66.

APPENDIX

The GFP-*cry* transgene can also be used to identify CRY interacting proteins that mediate CRY-dependent neuronal activity and phase resetting in the fly peripheral tissues. Identifying proteins associated with CRY will define mechanisms that mediate light-dependent phase shifting. In addition, it will enhance our understanding of how CRY activates neuronal activity and behavior via environmental stimulation and will reveal mechanisms underlying arousal. I carried out a pilot experiment to identify CRY interacting proteins via mass-spectrometry of purified GFP-CRY complexes from fly heads using GFP-nanobodies (Fig. 25). Analysis shows that GFP-CRY is highly enriched (i.e. > 600 peptides detected representing > 80% coverage), and that TIM and JET (proteins expected to interact after light exposure) can be successfully pulled down specifically in the light treated sample (positive controls). My preliminary results have identified several CRY interacting proteins (Table 8) that function in multiple cellular processes including ubiquitin/proteasome pathways, redox signaling and signal transduction pathways. Further work using GFP-CRY as a tool for mass spectrometric analysis will identify novel proteins that mediate CRY-dependent phase shifting and/or neuronal activity in response to light.

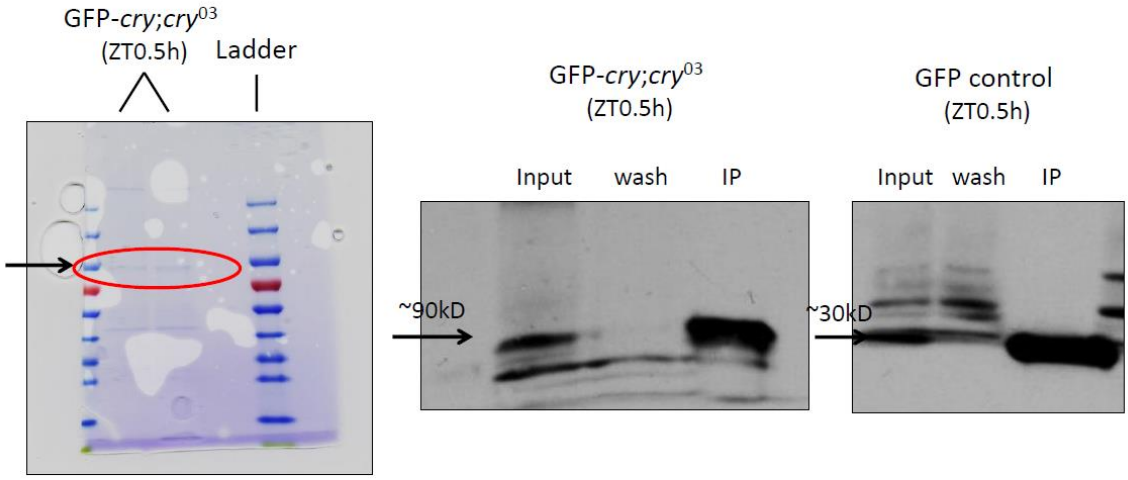

Figure 25: GFP-*cry*;*cry*^{03} transgenic flies as a tool for mass spectrometric analysis. GFP-CRY complexes were successfully purified from the heads (~5ml) of GFP-*cry*;*cry*^{03} flies entrained to a 12h light:12h dark (LD) cycle using anti-GFP nanobody coated beads. Purified samples were submitted to MS Bioworks for LC/MS/MS analysis. Other details are as described in text and Methods.

Table 8: Key hits identified upon mass spectrometric analysis of GFP-CRY complexes. Other details are as described in text and Methods.

Key examples of CRY interacting proteins	**Spectral counts in light treated sample**	**Spectral counts in dark sample**	**Spectral counts in control GFP sample**
CRY	643	661	6
TIM	26	-	0
JET	5	-	0
TRPL	18	13	0
CG4587	6	-	0
UBCD4	5	6	0
Total Interactors	172	220	

Methods

Briefly, to identify novel CRY interacting proteins, young (1-2 day old) w^{1118};GFP-*cry*;cry^{03} flies were entrained to 12h light:12h dark (LD) cycle. ~5 ml fly heads were collected either after a 30 min light pulse applied at dawn or kept in the dark 30 min after 'subjective' dawn in case of controls. GFP-CRY complexes in the fly head extracts were purified using anti-GFP nanobody coated beads and the purified samples were then sent to MS Bioworks for LC/MS/MS analysis. Results were analyzed to identify proteins that were significantly elevated/present in the light pulsed animals as compared to the non-pulsed controls using the criteria specified by MS Bioworks.